DISLOCATIONS AND STRENGTH IN THIN FILMS: SIMULATIONS AND MODELING

A Dissertation

Presented to the Faculty of the Graduate School

of Cornell University

In Partial Fulfillment of the Requirements for the Degree of

Doctor of Philosophy

by

Ray Stuart Fertig

February 2010

DISLOCATIONS AND STRENGTH IN THIN FILMS: SIMULATIONS AND MODELING

Ray Stuart Fertig, Ph. D.

Cornell University 2010

Single-crystal films were simulated using three-dimensional discrete dislocation dynamics simulations, where an initial distribution of dislocation loops was allowed to move naturally in response to successive applied strains. The types of interactions that stopped threading dislocations (threads) were identified and the relative fraction of threads stopped in each interaction was determined. An inhomogeneous stress field in the film evolved as the dislocation structure evolved. Threads were observed to interact primarily in regions of low stress. The simulations were used as a virtual test bed for understanding dislocation behavior in thin films. The intuition gained from the simulations led to the construction of three models, which are discussed in detail. First, a model was developed to determine the capture cross-section of a thread, such that if another thread was within its capture cross-section the two threads would interact. Second, a statistical model was constructed to evaluate the effect of stress inhomogeneity on the local concentration of threads. Finally, results from the simulations and analytical models were used to construct a model of strain hardening in thin films based on fundamental behavior of dislocations in thin films.

BIOGRAPHICAL SKETCH

Ray was born in Wheatland, WY to Ray Jr. and Catherine. He grew up in Cheyenne, WY with his three younger brothers, all four of his grandparents, and many aunts, uncles, and cousins. Ray graduated from Cheyenne East High School in 1997 and enrolled at the University of Wyoming, where he received a B.S. in Mechanical Engineering and Mathematics in 2001. Having spent eleven months as an intern for Rockwell Collins, he began to better understand the type of work he really enjoyed, namely, developing new modeling methods to solve problems. To test the research waters, he pursued and received a M.S. in Mechanical Engineering at the University of Wyoming in 2003. After presenting and writing up his thesis work on the relationship between microstructure and elastic properties of polymer-clay nanocomposites, the verdict was in: research was a fit!

In the course of his M.S. work, Ray's curiosity drew him in a slightly different direction. While he was seeking to answer the question of *how* the unique properties of nanocomposites could be explained from structure-property relationships of constituents, a nagging question refused to be dismissed: *Why* does any material have the properties that it does? The answer to this question lay in physics. But with the intent to be a bridge between engineering and physics, Ray decided to become a materials scientist. He enrolled at Cornell University in 2003 as the "modeling guy" for the Baker group. A portion of his work at Cornell is contained in this dissertation. (His work analyzing tantalum films is not included.) During his time in Ithaca, Ray enjoyed the company of wonderful friends, Ithaca's picturesque landscapes, and hunting New York's whitetails.

While pursuing his Ph.D. at Cornell, Ray had the opportunity to travel. In 2005 he went to work with Dr. Huajian Gao at the Max Planck Institut für Metallforshung

in Stuttgart, Germany for about a month. Here he examined the feasibility of incorporating dislocation core spreading into a dislocation dynamics code. In the summer of 2007, he was a Computational Science Graduate Intern at Lawrence Livermore National Laboratory in Livermore, CA. Here he worked with Tom Arsenlis to determine (a) the effects of dislocation core size on the strength of dislocation interactions and (b) if a closed-form solution existed to describe the stress field of a dislocation with a non-compact core intersecting a free surface in an elastic half-space.

Currently, Ray is back in Wyoming with his wife Jessica, where they are expecting their first child, Daniel Ray. They enjoy spending time with family and in the big outdoors of the Rocky Mountains. Ray is employed at Firehole Technologies, where he is developing physics-based multiscale modeling techniques for use with composite structural modeling tools.

To Dad and Mom for the years of encouragement and wisdom, and to my wife Jessica for the promise of a wonderful future

ACKNOWLEDGMENTS

There are so many people to thank for their support during a Ph.D. First, I would like to thank my advisor, Shefford Baker, who was not only a mentor but also a friend. He has taught me the importance of precision in my work, the effort required to communicate clearly, and an overall framework for thinking about research. But perhaps most importantly, his encouragement to think critically about everything ranging from specific research tasks to group presentations to world economics to local politics, pushed me to do better research and will drive my thinking in many other areas for the rest of my life.

I would also like to thank my committee members, Stephen Sass, Herbert Hui, and Richard Hennig, who replaced Prof. Sass after his retirement.

I would like to thank the members of the Baker Research Group for their help, critique, and conversation (we theorists need to interact with people once in a while to avoid insanity). Special thanks to Prita Pant who got me started with dislocation dynamics and was always a great sounding board for new ideas. Thanks to Rob Knepper, Dave Nowak, and Aaron Vodnick for the many enlightening discussions, both technical and non-technical. Thanks to Margie Pang, Catherine Oertel, and Eve Donnely for perspectives on research not in my area of expertise.

Financial support from the National Science Foundation (DMR-0311848) is gratefully acknowledged. I would also like to thank the Cornell Center for Advanced Computing for the computer resources and technical support given to perform the simulations reported in this dissertation.

No one can live in a place for five years without a community of friends. My years in Ithaca were pleasant, thanks in no small part to my friends in the Cornell Graduate Christian Fellowship (GCF) and at Christ Chapel. In fact, my memories of

Ithaca are marked most by the friends I made there. Although I can't list them all, I would like to single several out. Thanks to Steve Kirby for his friendship and refreshing blue-collar attitude, which made me feel at home away from home. Thanks to Steve Hicks, Geoff Recktenwald, and David Roundy for the thousands of deep conversations ranging from quantum physics to relationships to theology, and everywhere in between. Thanks to Chris and Heather for their passion to create friendships and for opening their home so often to bring many together. Thanks to Steve Felker for his counsel and spiritual mentoring and to Josh Bridwell for demonstrating faith in the midst of suffering.

I want to thank my parents, Ray and Catherine. Their support has been invaluable. Their counsel has always been wise and supportive. I appreciate their willingness to let me walk on a path that wasn't theirs, but still giving me the tools to walk down it. I appreciate their example as role models and for the stability that it always gave me.

Finally, I must thank my Creator, Lord, and Savior Jesus Christ. He has blessed me immensely in my time at Cornell, both with endurance and with success. Through it I have come to know him better and he has strengthened my faith. I have no accomplishment apart from him. *Sola Dei Gloria*.

TABLE OF CONTENTS

LIST OF FIGURES

LIST OF TABLES

LIST OF ABBREVIATIONS

DD	Dislocation dynamics
DDD	Discrete dislocation dynamics
MD	Molecular dynamics
NATM	Non-annihilating thread-misfit interaction
NATT	Non-annihilating thread-thread interaction
TEM	Transmission electron microscope
TM	Thread-misfit interaction
TMA	Thread-misfit annihilation interaction
TT	Thread-thread interaction
TTA	Thread-thread annihilation

CHAPTER 1
INTRODUCTION

It is sometimes said that the turbulent flow of fluids is the most difficult problem remaining in classical physics. Not so. Work hardening is worse. – A. H. Cottrell[1]

1.1 Motivation

Metals are strong. To the majority of world's population, this statement seems so trivial that it does not merit further inquiry. But why are metals strong? What makes one metal stronger than another? Why do variations in heat treatment or cold working affect metal strength? Any undergraduate engineering course in the mechanical properties of materials will yield a basic answer to why metals are strong or, more accurately, why they resist permanent deformation. Permanent deformation is caused either by vacancy diffusion or dislocation motion; thus, metals are strong because diffusion or dislocation motion in them is difficult. For the purposes of this thesis, we consider only deformation at temperatures and strain rates such that dislocations are the dominant mechanism controlling plasticity.

During the last century the theory of dislocations has advanced greatly such that it is now a mature field with several classic texts, e.g. *Theory of Crystal Dislocations* by Nabarro [2] and *Theory of Dislocations* by Hirth and Lothe [3]. Nevertheless, despite the immense knowledge about dislocations, the link between the behavior of individual dislocations and the macroscopic behavior of a material is still unknown. That is, a theory of strain hardening stemming from fundamental dislocation behavior

does not yet exist. L. M. Brown, a pioneer in the field of dislocation theory, notes the difficulty of constructing a microscopic strain hardening theory "*...but when it comes to explaining the plastic behaviour of metals, particularly work hardening, one gets lost in a mass of detail and controversy.*" [4] Thus, although we can measure macroscopic properties and behavior, we do not really understand the strength of crystalline materials from a microscopic perspective.

In recent decades, increasing miniaturization of products and the introduction of microelectronics has caused many metals and other crystalline materials to be used in thin film form. The mechanical behavior of thin films is different from the behavior of bulk materials, which introduces significant challenges to designing products that utilize thin films. The yield strengths of films are an order of magnitude larger than bulk yield stresses [5]. The strain hardening rates are much higher than bulk materials [6]. And plastic recovery on unloading, which leads to a Bauschinger effect, is much more pronounced [7]. High stresses degrade reliability in devices that utilize films by contributing to mechanical failure in the form of fracture [8], delamination [9], and stress voiding [10]. Thus, understanding the origin of high stresses in films is critical to maximizing device or product reliability.

Unfortunately, in thin films, like in bulk materials, understanding the link between microscopic dislocation behavior and macroscopic mechanical behavior remains an elusive goal. Dislocation behavior in thin films can be further complicated by the presence of surfaces and interfaces, which give rise to image stresses [11, 12]. However, the quasi-two-dimensional nature of films makes them ideal for study because dislocation motion in the dimension normal to the film can be constrained [13, 14]. This limitation on dislocation in the third dimension leads to a much smaller set of possible dislocation configurations. Many specific *facts* are known about dislocations in thin films and thin film stresses. For example, the stress fields of

dislocations are well known [3]. Many of the types of dislocation interactions that occur in thin films have been studied [15] and the stresses required to break these interactions are or can be determined. X-ray microdiffraction studies have shown that strong stress inhomogeneities exist in thin films [16]. Stresses and strain hardening rates in a variety of films has been measured (e.g. [7, 17]). However, none of these facts has led to a model linking dislocation behavior to film strength. The goal of this thesis is to begin to develop a framework for understanding dislocation motion in thin films from which to construct such a model.

In order to set the stage for the research in this thesis, it is important to consider how a dislocation relaxes film stress. For our purposes, we will presume that a dislocation loop exists in a passivated film and that the stress in the film is sufficiently high to cause the loop to expand. As the loop expands it deposits a segment of dislocation along the top and bottom interfaces. Figure 1.1 shows half of a loop that has expanded and illustrates the two different components of a dislocation in a film. The interfacial dislocation segments are called misfit dislocations (misfits). The portion of the dislocation that moves through the film is called a threading dislocation (thread). As the threads move through the film, the stress in the film is relaxed. When all threads in the film have stopped moving, the film stops relaxing. Thus, for dislocation-mediated plasticity, the film strength is entirely determined by the answer to the question: what stops threads?

We can be more specific yet about this key to understanding film strength. Consider a thread moving through a film. The relationship of the motion of the thread to the plastic strain rate $\dot{\varepsilon}_P$ in the film is given by the simple relationship

$$\dot{\varepsilon}_P = -C_1 \rho_T b v_T , \tag{1.1}$$

where C_1 constant related to the geometry of the slip system and the film orientation, ρ_T is the density of threads, b is the Burgers vector, and v_T is the thread velocity. The

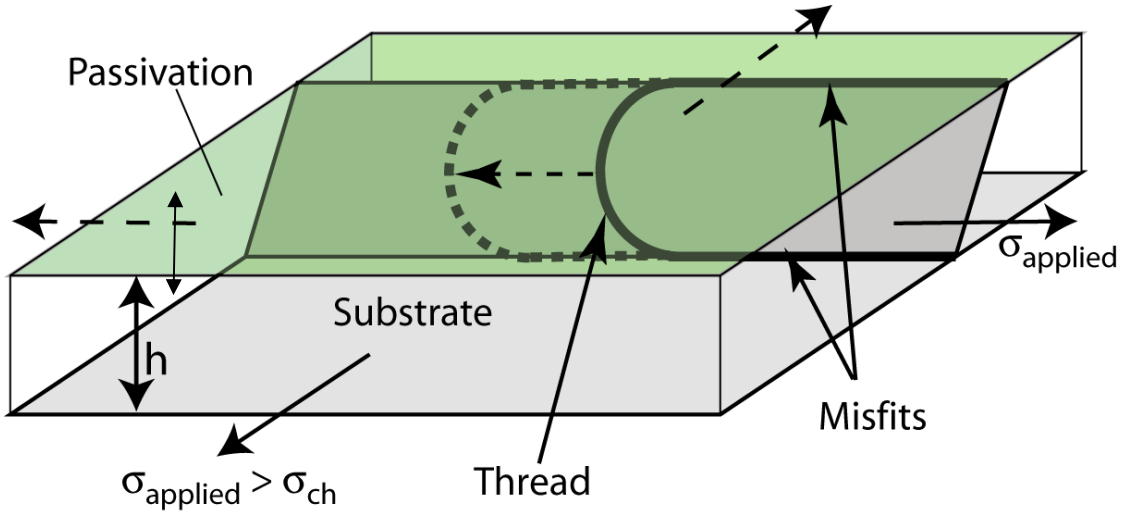

Figure 1.1 One half of a dislocation loop propagating through a film. The threading portion (thread) of the dislocation moves through and deposits an interfacial portion of the dislocation, called a misfit dislocation (misfit).

velocity of the thread is related to the resolved shear stress on the thread and the temperature. The remaining term ρ_T, which varies with time, is not easily defined. Thus, the impediment to linking dislocation motion and macroscopic film relaxation is the difficulty of determining how the thread density evolves with time, dislocation density, stress, etc. The chapters in this thesis detail computational and analytical efforts to understand what stops threads and why, so that the evolution of threading dislocation density in the film, and ultimately film strength and strain hardening, can be modeled.

1.2 Structure of this thesis

This thesis is organized into seven chapters. This chapter provides the framework to understand the purpose and scope of the reported research. Chapter 2 was published in Progress in Materials Science [18]; Chapters 3-5 are manuscripts in preparation to be submitted at the time of acceptance of this thesis by the special committee; and Chapter 6 has been accepted as a TMS conference proceeding. As such, each chapter contains its own introduction and set of references, so there is some repetition from chapter to chapter.

Chapter 2 contains a review of efforts to model dislocations in thin films, including results from analytical models, two-dimensional simulations, and three-dimensional simulations of dislocations in thin films. This review highlights the rather novel approach taken in this dissertation to the use of dislocation dynamics simulations. While three-dimensional simulations are a necessary tool for accurate understanding of dislocation behavior in thin films, another value of such simulations, apart from quantitative results, is the ability to train our intuition regarding dislocation motion. *In situ* observation of dislocations is only possible using a transmission

electron microscope, but this usually requires boundary conditions and sample preparation methods much different from those of films. Three dimensional simulations allow simultaneous access to stresses and dislocation configurations as they evolve and with arbitrarily small resolution. Thus, by using the simulations to understand the dislocation configurations that arise during film relaxation, it is possible to construct plausible film relaxation models based on details of microstructural phenomena.

Chapter 3 details the results of a set of large-scale three-dimensional dislocation dynamics simulations. Many of the features that we know occur in real films were observed: dislocation interactions, high stresses, inhomogeneous stresses, and high strain hardening rates. But most importantly the results provided insight into the relationship between mean stress, stress inhomogeneity, and dislocation interactions. Threads were found to be concentrated in regions of low stress and their capture cross-section is much larger in these regions than in regions of high stress.

Motivated by the results in Chapter 3, Chapter 4 presents an analytical investigation of the capture cross-section of a thread. Specifically, the area of the region inside which two threads with opposite Burgers vectors would annihilate was calculated for a range of film stresses and thicknesses. The results of this investigation showed that the size of the capture cross-section is very sensitive to the film stress a and that this relationship explains much of the dislocation behavior observed in the dislocation dynamics simulations.

Chapter 5 is also motivated by the results given in Chapter 3. Chapter 5 details a statistical model to predict the effect of inhomogeneous film stresses on thread concentration. This model revealed that low stress regions in the film did serve to concentrate the threads, as suggested by the dislocation dynamics simulations, and that this effect was substantial.

In Chapter 6 the results from Chapters 3-5 are used to construct an analytical model for film strength based on Eq. (1.1). This is the first model ever proposed for film strength that is based on the motion and interaction of individual dislocations. A side-by-side comparison of the predictions of this model with the results of the dislocation dynamics simulations reveals that the analytical model captures relaxation behavior remarkably well, particularly given coarseness of the assumptions involved. This model is the capstone of this research because it describes the crucial link between the wide range of dislocation behaviors and macroscopic film stresses, a link has been a mystery for the past four decades.

Finally, we conclude in Chapter 7 that a construction of a strain hardening model from fundamental dislocation behavior is possible and review some of the remaining issues to be addressed in the future to refine the model proposed in Chapter 6.

REFERENCES

[1] Cottrell AH. Commentary: A brief view of work hardening. In: Nabarro FRN, Duesbery MS, editors. Dislocations in Solids, vol. 11. Amsterdam: Elsevier, 2002. p.vii.

[2] Nabarro FRN. Theory of Crystal Dislocations. New York: Dover Publications, 1987.

[3] Hirth JP, Lothe J. Theory of Dislocations. New York: John Wiley and Sons, Inc., 1982.

[4] Brown LM. A brief rejoinder. In: Nabarro FRN, Duesbery MS, editors. Dislocations in Solids, vol. 11. Amsterdam: Elsevier, 2002. p.xliii.

[5] Baker SP. Plastic deformation and strength of materials in small dimensions. Mater. Sci. Eng. A 2001;319-321:16.

[6] von Blanckenhagen B, Arzt E, Gumbsch P. Discrete dislocation simulation of plastic deformation in metal thin films. Acta Mater. 2004;52:773.

[7] Baker SP, Keller-Flaig RM, Shu JB. Bauschinger effect and anomalous thermomechanical deformation induced by oxygen in passivated thin Cu films on substrates. Acta Mater. 2003;51:3019.

[8] Espinosa HD, Prorok BC, Fischer M. A methodology for determining mechanical properties of freestanding thin films and MEMS materials. J. Mech. Phys. Solids 2003;51:47.

[9] Pang MZ, Baker SP. Quantitative measurements of subcritical debonding of Cu films from glass substrates. J. Mater. Res. 2005;20:2420.

[10] Weiss D, Gao H, Arzt E. Constrained diffusional creep in thin copper films. Dislocations and Deformation Mechanisms in Thin Films and Small Structures Symposium, 17-19 April 2001. San Franciso, CA, USA: Mater. Res. Soc, 2001. p.1.

[11] Hartmaier A, Fivel MC, Canova GR, Gumbsch P. Image stresses in a free-standing thin film. Model. Simul. Mater. Sci. Eng. 1999;7:781.

[12] Liu XH, Schwarz KW. Modelling of dislocations intersecting a free surface. Model. Simul. Mater. Sci. Eng. 2005:1233.

[13] Freund LB. The Stability of a Dislocation Threading a Strained Layer on a Substrate. J. Appl. Mech. 1987;54:553.

[14] Nix WD. Mechanical properties of thin films. Metall. Trans. A 1989;20:2217.

[15] Pant P, Schwarz KW, Baker SP. Dislocation interactions in thin FCC metal films. Acta Mater. 2003;51:3243.

[16] Phillips MA, Spolenak R, Tamura N, Brown WL, MacDowell AA, Celestre RS, Padmore HA, Batterman BW, Arzt E, Patel JR. X-ray microdiffraction: local stress distributions in polycrystalline and epitaxial thin films. Microelec. Engr. 2004;75:117.

[17] Keller R-M, Baker SP, Arzt E. Stress-temperature behavior of unpassivated thin copper films. Acta Mater. 1999;47:415.

[18] Fertig RS, Baker SP. Simulation of dislocations and strength in thin films: A review. Prog. Mater. Sci. 2009;54:874.

CHAPTER 2
SIMULATION OF DISLOCATIONS AND STRENGTH IN THIN FILMS: A REVIEW[1]

Ray S. Fertig and Shefford P. Baker

Department of Materials Science and Engineering, Cornell University, Ithaca, NY 14853

ABSTRACT- Crystalline thin films have mechanical properties that cannot be predicted based on bulk scaling laws. Owing to their importance in technology, a great deal of effort has gone into modeling and simulation of the behaviors of dislocations in thin films. In this review, the successes and failures of modeling dislocations in thin films via analytical techniques, two dimensional dislocation dynamics simulations, and three dimensional discrete dislocation dynamics (DDD) simulations are discussed. Brief discussions of phase field models and level set methods are also included. The unique importance of three-dimensional DDD simulations is highlighted, as these simulations allow study of realistic dislocation behavior that is otherwise difficult or impossible to observe. The utility of three-dimensional DDD in discovering the mechanisms that control deformation in films is demonstrated, and first steps towards construction of a strain hardening model based on those mechanisms are described.

2.1. Introduction and background

Crystalline thin films are indispensable elements in a wide range of nanofabricated devices. Polycrystalline metal films are used as electrical conductors and resistors,

[1] Reprinted from Progress in Materials Science, 54(6), Ray S. Fertig and Shefford P. Baker, Simulation of dislocations and strength in thin films: A review, pp. 874-908

magnetic layers, optical reflectors and absorbers, chemical passivations and catalysts, and structural elements. Single crystal semiconductor films are used for their electrical properties. In such films, very high stresses may arise due to differential thermal expansion between film and substrate, an epitaxial relationship of film to substrate, or microstructural evolution in a film attached to a substrate. These stresses may in turn lead to failure by a variety of mechanisms, including excessive elastic or plastic deformation, stress voiding, fracture, or delamination. Thus, considerable effort has been invested in understanding the mechanical behavior of films on substrates.

This behavior is typically studied experimentally by determining the stress in a film as a function of temperature using either substrate curvature (*e.g.* [1, 2]), or x-ray diffraction methods (*e.g.* [3]). Such data, however, are *not* generally well understood. It is well known from experiments that thin films exhibit significantly different mechanical behavior than their bulk counterparts [4-11]. As an example, Figure 2.1 shows the mechanical behavior of a passivated 1 μm thick Cu film on a Si substrate determined during thermal cycling between room temperature and 600 ˚C using a substrate curvature method [2]. The strains in the film arise from differential thermal expansion with the substrate. The strain is assumed to be zero at the point where the stresses are zero on cooling. This film has a stable microstructure and repeated cycles trace the same hysteresis. Also shown are results of a simulation of this experiment based on empirical creep and plasticity equations [12] developed to describe steady-state deformation in bulk Cu. This simulation uses physical data for bulk Cu and the measured microstructural characteristics of the film [13]. It approximates the behavior of a bulk specimen which has the same microstructure as the film and is subjected to the same strain-temperature history. The measured stress-strain hysteresis is clearly very different from that predicted by the simulation.

While unlike the bulk material, the stress-strain behavior of the film in Fig. 2.1 shows a form that is common to many passivated metal films on substrates and much work

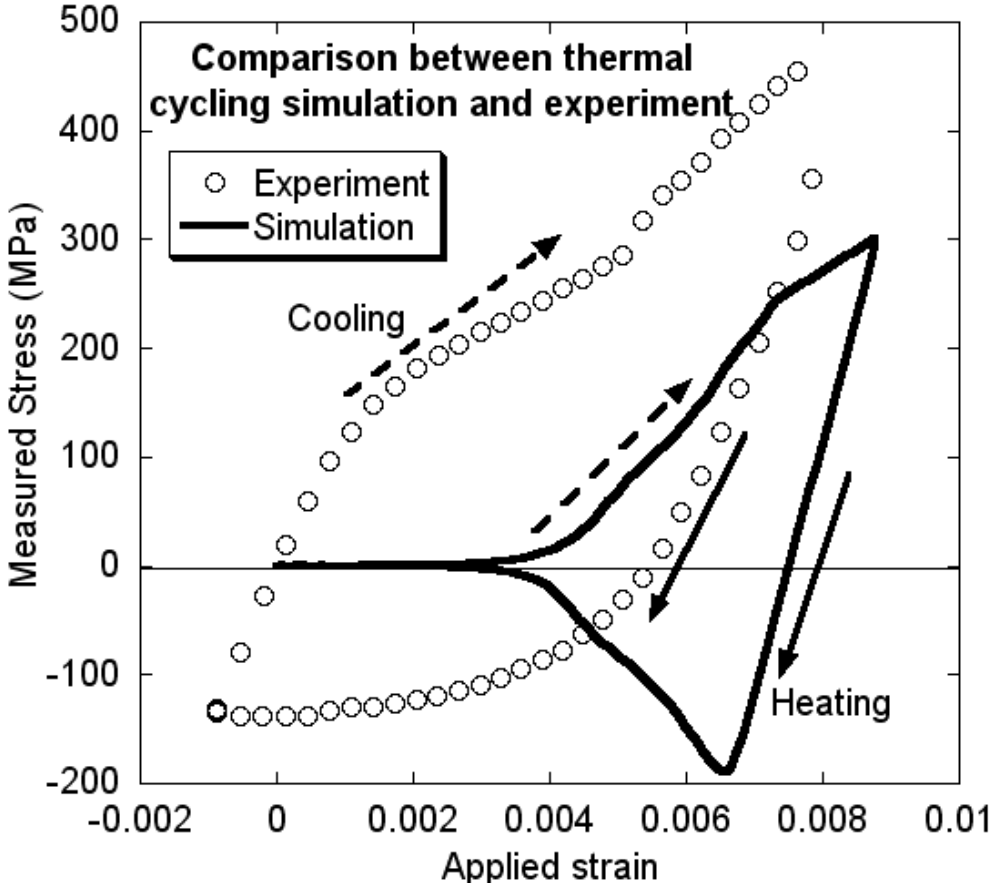

Figure 2.1. Simulated (solid line) and experimental (open circles) stress-strain curves obtained from thermal cycling of 1 μm thick, passivated Cu films Si substrates. Strains arise from differential thermal expansion between film and substrate and were set to zero at the point where the (average) film stress is zero during cooling. Experimental stresses were measured using a substrate curvature method [2]. Stresses in the simulation were calculated using empirical deformation equations developed for bulk materials [12] but incorporating the microstructural characteristics of the film (as in [13]). The measured and predicted behaviors are very different, highlighting the fact that films behave very differently from bulk materials.

has been devoted to understanding the differences between the measured behavior of films and expectations based on empirical scaling laws developed for bulk materials [1, 2, 14-19]. The main deviations, evident in Fig. 2.1, are high stresses at both low and high temperature, strong Bauschinger effects, and high strain hardening rates.

A key observation, at least for the purposes of this review, is that all of these deviations appear to depend on dislocation mechanisms [2, 13, 20]. Thus, the first step in understanding these behaviors is to describe how dislocations move and interact in films. As in bulk, dislocation loops may originate at sources within grains or as half loops expanding in from grain boundaries or interfaces. Regardless of where it originates, a dislocation loop (or half loop) moving into a film grows until it is stopped by the film/substrate and film/passivation (if any) interface(s), a grain boundary, or other dislocations. Neglecting grain boundaries and dislocation-dislocation interactions for the moment, continued dislocation motion will be as illustrated in Figure 2.2. A segment that runs through the thickness of the film, called a threading dislocation (or "thread"), moves through the film [21] and creates either a surface step in the case of a free surface, or a misfit dislocation (or "misfit"), in the case where the film intersects a substrate or passivation layer. Much work has been done to understand the deviations from bulk behavior shown in Fig.1 in light of the constrained dislocation motion shown in Fig. 2.2. We make this case for each of the categories of deviations described above as follows:

High strength at low temperature: At low temperatures, where dislocation motion is *expected* to be the dominant deformation mechanism, it is well known that thin films can support flow stresses that exceed the yield strength of bulk metals by more than an order of magnitude [3, 5, 6, 22, 23]. Even with the fine grain size and the orientation of the film accounted for, the simulation in Fig. 2.1 fails to predict the strength of the film. This immediately raises the question of what mechanisms inhibit dislocation motion in thin films. Since the thread is the mobile dislocation segment, this translates

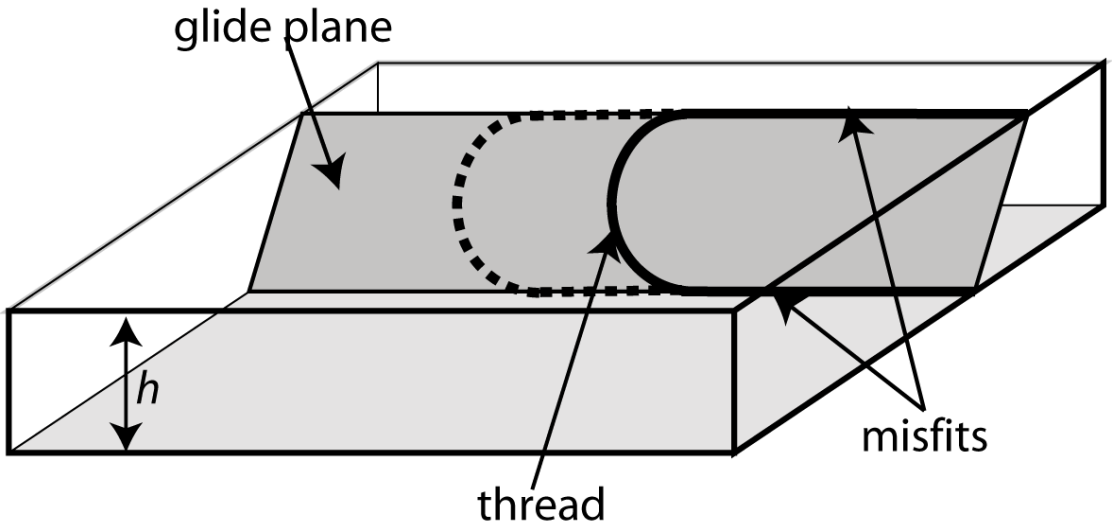

Figure 2.2. A threading dislocation (thread) deposits misfit dislocations (misfits) as it moves through a film of thickness h. The dislocation can only advance (dotted line) when the strain energy reduction due to motion of the dislocation is greater than the energy cost of the additional misfit length

directly to the basic question: what stops threads? The answer, at least for pure films, is: a thickness (dimensional) constraint, other dislocations, and grain boundaries. Each of these features can act to stop threads, but, as we shall see, none is alone sufficient to account for the stresses measured in films.

We first consider the dimensional constraint. A thread moving through a film of thickness h relaxes the elastic strain in the nearby film but leaves misfits behind it (Fig. 2.2). For this to occur, the reduction in strain energy due to thread motion must equal or exceed the increase in energy due to insertion of misfit dislocation line length. For a fixed misfit strain, the strain energy varies linearly with thickness, while the misfit dislocation energy varies as $\ln(h)$ [5], leading to a critical thickness for dislocation motion [5, 24, 25]. Conversely, for a fixed thickness, this energy balance leads to a critical stress for dislocation motion that we, following Nix [26], refer to as the channeling stress. This dimensional constraint has been shown to be insufficient to account for the magnitude of the experimentally observed stresses in real films [2, 4, 15, 23].

Of course, a thread moving under a global stress greater than the channeling stress can be stopped by interacting with other dislocations. As shown in Figure 2.3, this may occur when thread motion is blocked by misfits on an intersecting slip plane (Fig. 2.3a), by threads on an intersecting slip plane (Fig. 2.3b), by misfits on parallel planes, which lower the local stress below the channeling stress (Fig. 2.3c), or by threads on parallel planes which cause a thread-thread dipole to be formed (Fig. 2.3c). It is well known that dislocation interactions can give rise to not only high stresses but also to high strain hardening rates in bulk materials. It might be tempting to think that, if the strengths of the dislocation interactions shown in Fig. 2.3 could be catalogued, a predictive model for film strength could be developed. However, despite the fact that dislocation interactions in thin films have been a focus of study in the past two

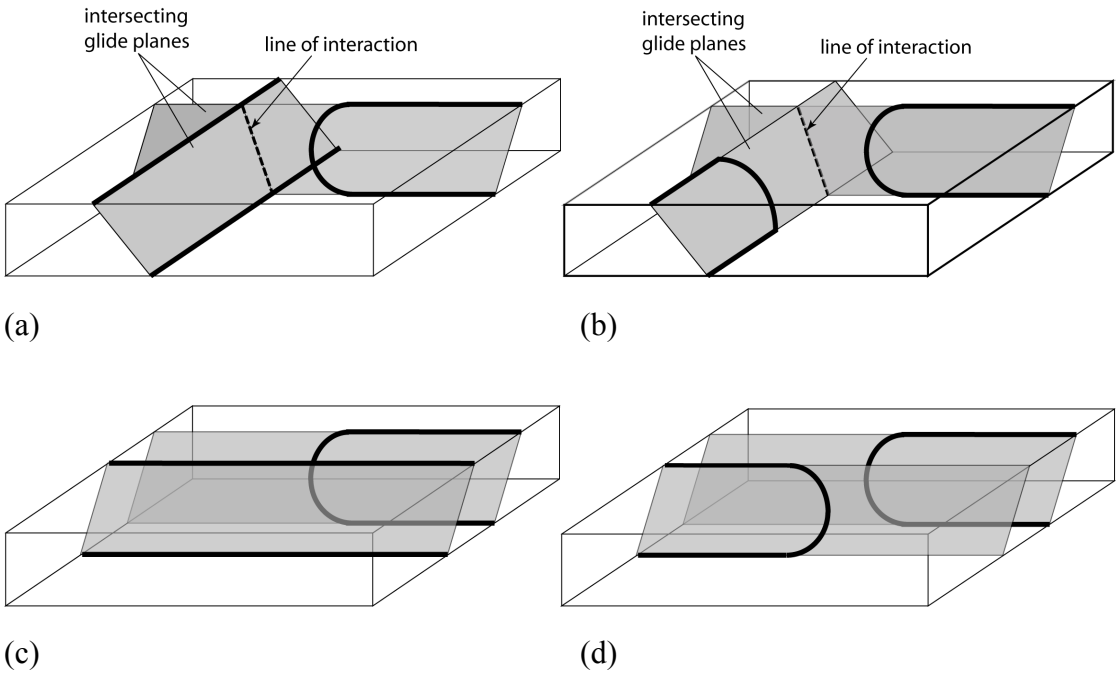

Figure 2.3. Types of dislocation interactions in films: (a) intersecting thread-misfit interaction, (b) intersecting thread-thread interaction, (c) parallel thread-misfit interaction, and (d) parallel thread-thread interaction (after Pant et al. [29]).

decades (*e.g.* [27-29]), a predictive model for strain hardening in thin films remains elusive.

Finally, threads can be stopped or hindered at grain boundaries, as in Figure 2.4. Interactions of dislocations with grain boundaries can be quite complicated. While the dislocation may be simply blocked (Fig. 2.4), it may also be absorbed into the boundary, or retransmitted on either side of the boundary [30, 31]. While much work has been done to understand the behavior of dislocations at grain boundaries in model systems [30-35], applications to films have typically either simply assumed that the dislocation is either blocked or fully absorbed [36-38]. Relatively little work has been done specific to films on this topic but phenomenological models based on a Hall-Petch type mechanism have been developed [2, 4], and this mechanism has also been shown to be insufficient to account for observed film stresses.

High strength at high temperature: The simulation in Fig. 2.1 predicts that stresses should be relaxed to zero above about 400˚C by diffusional flow. In contrast, passivated films support high stresses at elevated temperatures. Since typical metallizations have columnar grain structures (all grain boundaries perpendicular to the plane of the film), diffusion between grain boundaries and interfaces is required to relax stresses. Stresses cannot be relaxed by diffusion along grain boundaries alone in such a structure. Thus, in virtually all modeling to date, high stresses at high temperatures are accounted for by assuming that diffusion along interfaces is negligible in the tested temperature range [2, 13, 17, 18, 39]. While there is no reason, *a priori,* to assume this should be true in all of the tested systems, stresses are nonetheless high at high temperatures, suggesting that plastic deformation is controlled by dislocation processes, even at those temperatures [13]. As a result, it may be possible to attribute thermomechanical behavior over a range of temperatures to dislocation-based mechanisms.

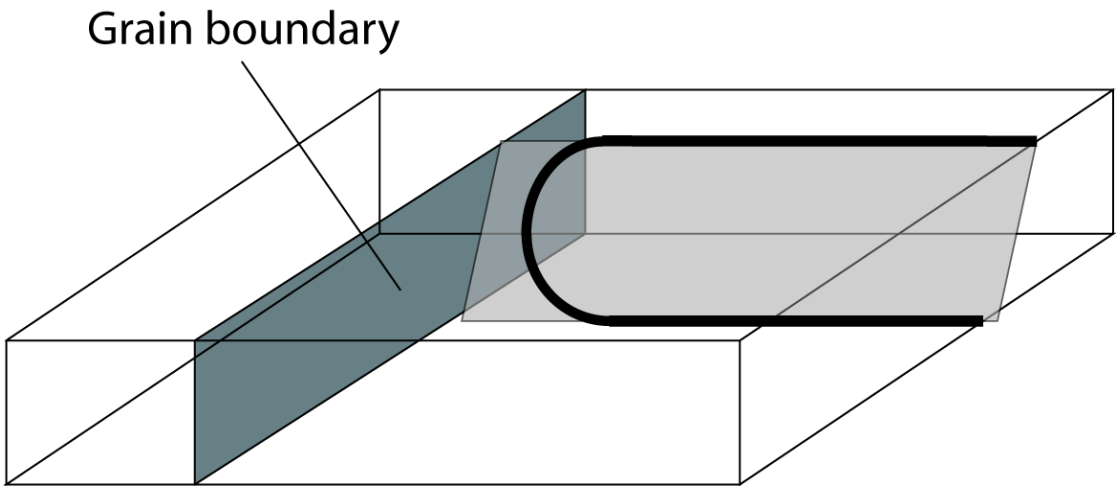

Figure 2.4. Schematic of a thread blocked by a grain boundary. Depending on the stress and the orientations of the neighboring grains and the boundary, the dislocation may remain blocked, be absorbed into the boundary, or be retransmitted on either side of the boundary.

Large Bauschinger effect: In the simulation shown in Fig. 2.1, the stresses during initial unloading (heating) follow the thermoelastic slope until the compressive stress and temperature are both high enough to initiate plastic flow. The experimental data, however, deviate from this slope much earlier in the unloading process. This behavior is similar to the well-known Bauschinger effect in bulk materials. However, the effect is much stronger in films. That the data lie above the thermoelastic line (*i.e.* towards more tensile stresses) indicates that the plastic strains are compressive, even though the applied stress is still tensile. This phenomenon has been dubbed "negative yielding" [19, 40-43], and can be seen in published thermomechanical data from many passivated films (*e.g.* [1, 3, 4, 13, 19, 40]). This behavior has been attributed to threads moving "backwards," against the applied stress, so as to reduce misfit dislocation line length when the stress is reduced below the channeling stress [40] or in response to the stress field of a dislocation pileup at a grain boundary [37]. To understand how much strain is recovered at what stress levels, it is again necessary to understand the interactions that stop threads. In this case interest is in the strength of those interactions on *un*loading.

High strain hardening rates: Finally, in addition to supporting high stresses, films also show high strain hardening rates. Von Blanckenhagen *et al*. [37] collected data from several research groups and showed that strain hardening rates increase exponentially with decreasing film thickness. Strain hardening rates depend strongly on the nature of the film interfaces (free surface or interface with a substrate or passivation) [44]. Of course, the elastic modulus provides an upper limit to the strain hardening rate that is invariant with film thickness, and is achieved in very thin films having interfaces that are impenetrable to dislocations [45]. Thus, strain hardening rates in thin films can be very high and depend strongly on the constraints on dislocation motion.

The evidence suggests that high strength at high and low temperatures, large Bauschinger effects, and high strain hardening rates in thin films all depend on dislocation-based mechanisms. Clearly, a detailed understanding of how dislocations move and interact would shed a great deal of light on the deviations between bulk scaling laws and the thermomechanical behavior of thin metal films, as illustrated in Fig. 2.1. In addition, we note that another class of problems, plastic relaxation of epitaxial semiconductor films, is well described in terms of constraints on the motion of threading dislocations [46-48] and would benefit similarly from a detailed mechanistic understanding of dislocation behavior. To understand the mechanical behavior of both metal and crystalline semiconductor films, a great deal of "bottom-up" dislocation modeling and simulation work has been done using analytical [5, 10, 24-27, 49, 50], dislocation dynamics [28, 29, 51-54], and atomistic methods [55]. In such methods, the goal is to develop descriptions of macroscopic film behavior by accounting for the more-or-less realistic motion and interactions (*e.g.* annihilation and junction formation) of individual dislocations. Alternatively, "top-down" models, such as those of Sedlacek *et al*. [56-58] that consider dislocation interactions only through their average effect on dislocation motion, are also useful for studying the behavior of thin films, but such top-down modeling efforts are not the focus of this review.

The goal of this review is to highlight the results of bottom-up modeling and simulations of dislocations in thin films with a focus on 3-D dislocation dynamics (DD) simulations. Toward this end, we first review analytical models of dislocation behaviors in films. While limited to straight infinitely long dislocations, or dislocation segments of well-defined shape, such models have been used to accurately characterize the thickness constraint (Fig. 2.2) and as an initial approach to certain types of dislocation interaction problems. Next, we look at 2-D dislocation dynamics simulations. Such simulations cannot answer the critical question of what stops threads, but provide a detailed overview of how parallel dislocations (Fig 3c) can

interact and move. We then turn to the 3-D simulations that are the focus of this review.

3-D DD simulations are very powerful for two reasons. First, since dislocations modeled using 3-D simulations can adopt realistic arbitrarily-curved configurations in response to the local stress state, the configurations and strengths of individual dislocation interactions can be studied in detail. Second, since large numbers of dislocations can be simulated, it is possible to generate realistic dislocation structures and to identify the features of those structures that determine strength. Rather than *assume* what dislocation configurations will dominate in determining film strength, 3D-DD simulations can be used to *find out*. This exploratory approach has proven to be very effective. However, we will argue that the main value of such simulations is that the results can be used to develop new concepts and new empirical scaling laws for describing thin film behavior. By using the simulations to study dislocation motion, interactions, and configurations, as well as the details of the stress field that develops, it is possible to develop simple empirical scaling laws for films that have a much higher degree of predictive accuracy than the bulk-based models of the past. For completeness, we also describe two relatively new DD simulation methods: phase field and level set. Finally, we discuss some of the main contributions and limitations of DD simulations in thin films, as well as prospects for future work.

2.2. Analytical models

Analytical models for dislocation behavior are typically limited to descriptions of simple configurations since only straight dislocations or segments with fixed curvature in a plane can be modeled with closed-form solutions [59], and since only small numbers of dislocations can be modeled unless they are in regular arrays. In contrast, in real 3-D materials, dislocations adopt complex 3-D shapes, react with each other in

complex ways, and multiply rapidly with plastic strain. In thin films, however, the thickness constraint creates a quasi 2-D structure in which the possible dislocations configurations are limited. As described in Section 2.1 above (Fig's 2.2-2.4), this structure can be described in terms of threads moving and interacting in an environment of (relatively) stationary misfits. This constrained geometry is amenable to analytical modeling in the sense that one can propose and analyze configurations that might play a dominant role in determining film strength. In this spirit, analytical models have been formulated to address the channeling stress (Fig. 2.2) [5, 25], dislocation interactions (Fig. 2.3) [26, 27, 49, 60], and interactions between threads and grain boundaries (Fig. 2.4) [61, 62].

The analytical models for the channeling stress are self-consistent [10] and accurately predict the onset of dislocation motion for a variety of materials [24]. In fact, these models are routinely used to "calibrate" simulations. However, analytical models of threads interacting with other dislocations and grain boundaries require highly idealized simplifications and are difficult to verify experimentally. As discussed below, recent simulations (e.g. [29]) suggest that analytical models predict neither the morphology nor the strength of thread stopping mechanisms accurately. Nonetheless, these analytical models have played an important role in conceptualizing strengthening mechanisms in thin films and in providing order-of-magnitude estimates of their effects. In this section, we briefly describe analytical models of the channeling stress as well as efforts to analytically model dislocation-dislocation interactions and dislocation-grain boundary interactions. The interaction models, although not accurate, are useful for later comparison to dislocation dynamics simulations, as they show why dislocation dynamics simulations are such a powerful tool for modeling thin films.

2.2.1 Channeling stress

The idea of a thickness-dependent channeling strain was first developed by Frank and van der Merwe [63, 64], who demonstrated that a misfit dislocation can form in an epitaxial layer only when the strain energy reduction that results is greater than or equal to the energy increase due to the presence of the dislocation. They further postulated that this critical misfit strain should decrease with increasing film thickness.

Following the work of Frank and van der Merwe, Matthews and Blakeslee [65, 66] developed a model to describe the relationship between misfit strain and threading dislocation motion. In their model, a thread moves as shown in Fig. 2.2. The force on the thread due to line tension is balanced with the force arising from the misfit strain to determine when the thread would propagate and extend the misfit dislocations. According to this model, the channeling strain, ε_{ch}, at which thread motion would occur in an unpassivated isotropic film of thickness h attached to a substrate with identical elastic properties is (from [65])

$$\varepsilon_{ch} = \frac{b}{8\pi h}\frac{\left(1-\nu\cos^2\alpha\right)}{(1+\nu)\cos\lambda}\left(\ln\frac{h}{b}\right), \tag{2.1}$$

where α is the angle between the sense vector and Burgers vector of the misfit, λ the angle between the slip direction and the slip plane normal, b the magnitude of the Burgers vector, and ν the Poisson ratio. The key finding here is that the minimum strain required for thread motion is inversely proportional to the film thickness; a result that has been verified experimentally (*e.g.* [2, 23]).

Using a similar approach, Freund [25] showed that for $h >> b$, the Matthews-Blakeslee model is equivalent to using an energy balance. In the Freund model, the reduction in strain energy from motion of a thread is balanced with the increase in energy due to the addition of misfit dislocation line length to calculate the channeling

strain for a particular film thickness. The ε_{ch} values calculated using this method are nearly identical to those calculated using Eq. (2.1).

Various researchers have added to the basic Matthews-Blakeslee and Freund channeling models with refinements to account for phenomena found in real films. Nix used the energy formulation in various forms to account for elastic anisotropy (*e.g.* differences in the biaxial modulus M between, say, (001)- and (111)-oriented films) [5], and the effect of elastic mismatch between the film and substrate on the channeling strain [5, 26]. Baker *et al.* [67] and Gao *et al*. [68] showed that if a dislocation core spreads out into the film/substrate interface, as has been observed in films deposited on amorphous substrates (*e.g.* [69]), the channeling strain can be substantially less than predicted by Eq. (2.1). This is because a spread-out core has lower energy than the core of a perfect Volterra dislocation. Recently, Douin *et al.* [50] have examined the effect propagating a thread that is composed of two Shockley partial dislocations in films of different orientations. They showed that for some orientations and loadings the propagation of a set of partials was qualitatively different from the propagation of a perfect dislocation. Notably, some loadings favored propagation of only one partial, leaving behind a growing stacking fault.

2.2.2 Dislocation interactions

While the channeling stress represents a fundamental component of film strength, the stresses observed in real films are much higher [2, 5]. Furthermore, this simple dimensional constraint cannot account for strain hardening. Thus, in order to more accurately model film strength, several attempts have been made to generate analytical models of interactions between threads and other dislocations. Freund developed an analytical solution for the effect of a thread being blocked by a misfit intersecting its path [27, 49]. He proposed a configuration in which the stress field of the misfit causes

the effective thickness of the channel in which a thread could move to decrease from h to h^*, increasing the stress required to drive the thread past the misfit. A schematic of this type of blocking configuration is shown in Figure 2.5. Freund showed the calculated blocking effect in an unpassivated film to be substantial: the applied biaxial strain required to propagate a thread past a misfit was calculated to be $\sim 2\varepsilon_{ch}$. Later calculations by Nix predicted a similar strengthening effect in passivated films [26]. Nix also calculated the effect on a thread of an infinite array of intersecting misfits on the same slip system [26] and showed that this configuration could produce very high strength and strain hardening rates.

Analytical models of thread-misfit interactions provide an order-of-magnitude estimate of interaction strength and demonstrate the importance of local stress interactions in controlling thread motion in a film. However, the assumed critical configurations are not correct, as has been shown in numerous discrete dislocation dynamics simulations [28, 29, 70, 71]. In analytical models of thread/misfit interactions, the misfit is assumed to be rigid and infinitely long while the thread is assumed to propagate self-similarly, such that its shape does not change during the interaction [27]. However, both experiment [72, 73] and simulations [28, 29, 70, 71, 74-76] have shown that the (changing) shape of the thread and the motion of the misfit are important in determining interaction strength. Analytical models cannot model these effects and cannot be expected to be quantitatively accurate; indeed they significantly overestimate the strength of these interactions [28, 70, 77].

Analytical models have also been proposed to evaluate the effect of misfit dislocations lying parallel to a moving thread, as shown in Fig. 2.3c. One effect is obvious *a priori*: if a fixed strain is applied and an array of misfits is introduced that relaxes that strain, any thread on the same slip system as the misfits will feel a lower driving force for motion than if the array was not present. Thus, the applied *global* strain must be increased to achieve the same *local* stress as would be the case in a

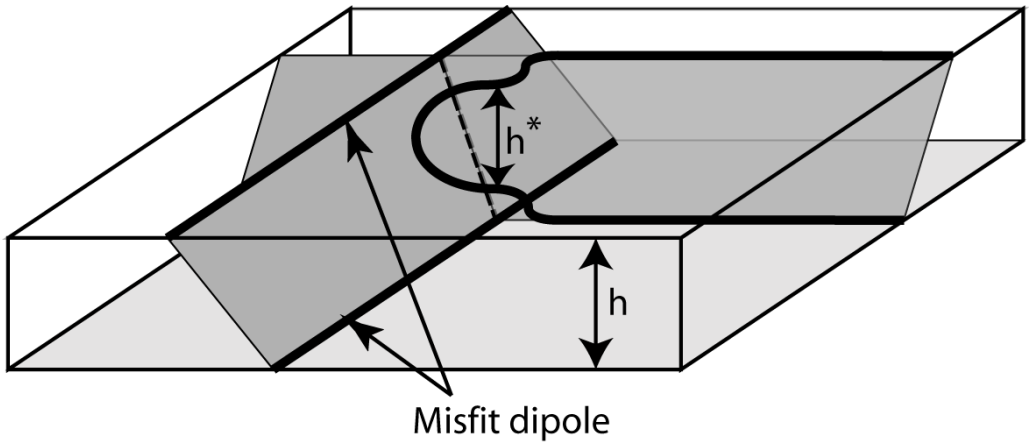

Figure 2.5. Schematic of a misfit dipole blocking a threading dislocation (after Freund [60] and Nix [25]). The stress field of the misfits decreases the "channel" thickness that the thread must pass through, which increases the driving stress required to move the thread.

misfit-free film with the same applied strain. Freund showed that *how* an array of infinite misfits evolves can influence the relaxed configuration of the array, and thusthe residual strain (or stress) [78]. If misfits are deposited simultaneously, the relaxation can be greater than if misfits are deposited sequentially because misfits deposited after some initial misfit structure has been established feel not only the applied stress but also the stress from the misfits that have already been deposited. In fact, any model of film stress that only incorporates dislocations through a film-averaged strain cannot capture the stress-strain behavior of the film because the stress on any particular thread is the *local* stress, not necessarily the film-averaged stress. Weihnacht and Bruckner [79] also examined this effect by calculating the stress required to drive a misfit dislocation into a preexisting array of misfits at an interface.

2.2.3 Dislocation-grain boundary interactions

As in bulk materials, grain boundaries are an important impediment to dislocation motion in films, but interactions between dislocations and grain boundaries are too complex to completely model analytically, so analytical modeling efforts have focused on generating descriptive models of the relationship between film stress and grain size [22, 61]. The functional form of this relationship is still disputed. Thompson presented an analytical model in which a thread blocked by an impenetrable grain boundary is treated in the same way as a misfit blocked by an interface [22]. This model is identical to the channeling model discussed above, except that the constraining dimension is the grain size instead of the thickness. Not surprisingly, film stresses were calculated to be inversely proportional to the grain size d. Other studies [61] have used a Hall-Petch description, which predicts that film stress should be inversely proportional to the square root of the grain size. In a typical interpretation of Hall-Petch behavior (*e.g.* [7]), dislocations are assumed to pile up at a grain boundary until

a critical stress is exerted on the boundary by the lead dislocation in the pileup, at which point that dislocation is transmitted, or a new dislocation is nucleated, in the adjacent grain. The size of the pileup is taken to be proportional to the grain size. This model implicitly assumes that dislocations are repeatedly nucleated from a single dislocation source, which has yet to be confirmed experimentally as a dominant form of nucleation in thin films.

Experimental results have not yet resolved this dispute. Venkatraman and Bravman reported flow stresses proportional to d^{-1} in aluminum films, in agreement with the Thompson model, while Keller *et al.* [2] found that their own data for Cu films, as well as the Al film data of Venkatraman and Bravman were better described by a Hall-Petch $d^{-1/2}$ description. Friedman and Chrzan [61] and Friedman [62] developed an analytical model of dislocation pileups in multilayers and showed that generally the Hall-Petch description provides the correct functional form, but that the scaling exponent could vary depending on the elastic mismatch between layers and the orientation of the slip planes.

Given the complexity of dislocation-grain boundary interactions, it is not surprising that a realistic picture of the effects of grain boundaries on thin film strength has not yet been provided by analytical modeling. The grain boundary contribution to film strength depends on the grain size, orientation and grain boundary structure, as has been robustly demonstrated for nanocrystalline materials, *i.e.* bulk materials with nanometer-scale grain sizes [80]. Thus, detailed atomistic simulations, which are beyond the scope of this review, are the best tool for studying this problem because they can capture the effect of grain boundary structure on an intersecting dislocation. These effects must be accounted for in order to accurately model dislocation-grain boundary interactions.

2.2.4 Summary of analytical models

The analytical work summarized above has helped our understanding of the relationship between dislocation behavior and film strength. Analytical models of the channeling stress have been shown to be accurate and are now widely used to calculate the minimum stresses required for dislocation motion (*e.g.* [81]). Models of dislocation interactions provide conceptual insight and order-of-magnitude estimates, but cannot be considered quantitative or predictive for two reasons: First, because analytical solutions have considered only infinitely long, straight dislocations, they cannot address changes in dislocation shape or the formation of junctions as dislocations move and interact. Second, analytical solutions only consider limited, idealized configurations, such as a thread traveling through an infinite array of periodic misfits. In real films, the spacing between misfits is statistically distributed, the types of interactions that stop the threads in any film will be diverse, and the stresses are neither homogeneous nor periodic. Analytical models of the effects of grain boundaries do not even attempt to capture details of local interactions, only global scaling behavior, and even there, there is much debate over the appropriate scaling of film strength with grain size in thin films.

Thus, from the current analytical calculations of channeling stress, interaction strength, and grain boundary strengthening it is impossible even to predict the *average* film stress. Accurate studies of stresses in thin films must permit a realistic dislocation structure to evolve naturally. This provides the motivation for the dislocation dynamics work presented below.

2.3. Two dimensional dislocations dynamics simulations

The simplest means of modeling a statistical distribution of dislocations that move through a naturally evolving stress field are two-dimensional dislocation dynamics simulations [77-90]. In 2D simulations, infinitely long parallel dislocations move in response to applied stresses and the stress fields of the other dislocations in the problem. One simply sums up the forces on each dislocation, and then moves each dislocation at a rate that is determined by a mobility law. The configuration is updated accordingly and the process is iterated. A complete method was presented by van der Giessen and Needleman [82]. In this method, the displacement fields of dislocations in an infinite elastic medium are superimposed on displacement fields that correct for the appropriate boundary conditions.

A 2D simulation has several advantages compared with analytical methods: Dislocations can move and interact in a complex way; new dislocations can be nucleated by specifying "sources" at each of which a pair of dislocations are added to the problem whenever the stress at that location exceeds the strength of the source; and annihilation can be incorporated by removing dislocations of opposite Burgers vectors when they come within a specified distance of each other. Thus, a dislocation structure can evolve naturally. In addition, since exact image solutions can be superimposed on the elastic field solution for an infinite medium, careful scrutiny of the effect on film stress of free surfaces and elastic mismatch between film and substrate/passivation is possible. Finally, since each dislocation is represented by only a single point and because of the closed-form solution of the dislocation displacements, simulations with large numbers of dislocations are feasible.

2D simulations have been used to obtain a range of insights into film behavior. A series of systematic studies were conducted by Nicola *et al.* [83-86], using the Van der Giessen and Needleman method [82]. Initial simulations [83-85, 87] modeled

unpassivated Al films on Si substrates. Three slip systems oriented 60° from each other, as shown in Figure 2.6, where the dislocations on each system are of pure edge character, were used. Possible active slip planes were spaced 100*b* apart and dislocation sources were seeded randomly on these planes. The sources were locations in the film that were assigned some nucleation strength τ_{nuc}, corresponding to a prescribed Gaussian distribution. When the resolved stress at a source exceeded τ_{nuc}, a dipole was generated. Each dislocation was moved with a velocity proportional to the force acting on it. Annihilation was assumed to occur if two dislocations with opposite Burgers vectors were within 6*b* of each other. A periodic unit cell 2 μm wide was used to mimic a film with infinite planar dimensions. Films with thicknesses ranging from 125 nm to 2000 nm were simulated, with the source density held constant for all thicknesses.

The results of these single crystal simulations suggested that two different mechanisms contribute to the thickness-dependent strength in thin films. First, a region with high stress gradients and high dislocation density was observed near the film-substrate interface, as shown in Figure 2.7. The stress gradients were roughly the same for three different film thicknesses. Thus, Nicola *et al.* modeled this situation by considering a film of thickness *h* with a boundary layer with thickness h_L. By using the rule of mixtures, the film stress σ_f must be

$$\sigma_f = \sigma_b + \frac{h_L}{h}\left(\sigma_L - \sigma_b\right), \tag{2.2}$$

where σ_b and σ_L are the average stresses outside and inside the boundary layer, respectively. The 2D simulations showed that there exists a threshold thickness above which σ_b, σ_L, and h_L are independent of thickness. This result is important because it predicts a 1/*h* dependence of the *flow stress*, which has been robustly demonstrated experimentally (*e.g.* [2, 23]). This experimental result had previously been compared with channeling stress models, which predict only the *onset* of yielding.

Figure 2.6. Slip system configuration typically used in 2D DD simulations in films. Although this configuration does not represent a real slip system configuration, it allows simulation of multiple slip systems.

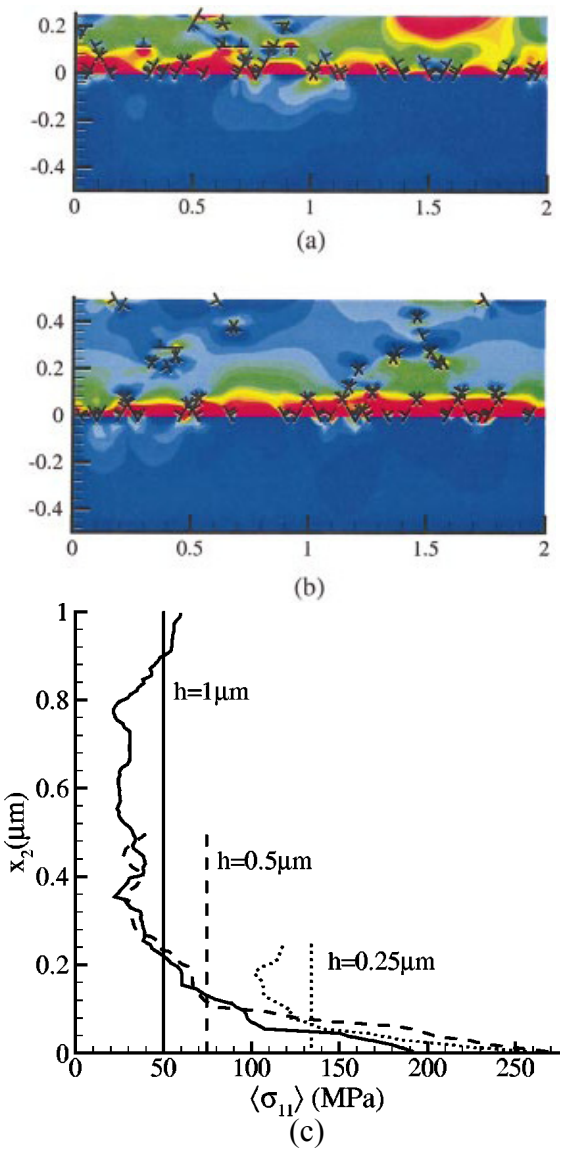

Figure 2.7. 2D DD simulation results showing in-plane film stresses (color) and dislocation locations for (a) 250 nm and (b) 500 nm films, and (c) average in-plane film stresses at different positions through the thickness for 1000 (solid), 500 (dashed), and 250 (dotted lines) nm thick films. Straight lines indicate the film stress σ_f. A boundary layer with high stress gradient and dislocation density forms near the interface and leads to an inverse thickness dependence of σ_f. (From Nicola et al. [84]). Reprinted with permission from Nicola L, Van der Giessen E, Needleman A. Discrete dislocation analysis of size effects in thin films. J Appl. Phys. 93, 5920 (2003). Copyright 2003, American Institute of Physics.

In films thinner than the threshold thickness, a second strengthening mechanism was identified: a backstress arising from interfacial dislocation pileups prevents a source from operating, resulting in a marked increase in σ_b compared with films above the threshold thickness. In accord with Eq. 2.2, this results in a higher film stress at a given strain and was thus observed as an increase in strain hardening rate (after initial plastic deformation to establish pileups). Interestingly, this second strengthening mechanism does not follow a $1/h$ dependence, or indeed any Hall-Petch type dependence on thickness [87]. Deviations from a $1/h$ dependence of film strength with decreasing h have also been reported experimentally (*e.g.* [2]).

Nicola *et al.* extended their simulations to study polycrystalline thin films [87] with both thickness and grain size ranging from 250 nm to 1000 nm. In this case, the periodic unit cell consisted of eight grains with boundaries that were impenetrable to dislocations. The grains had identical elastic properties but rotated slip systems (Fig 6). As in their single crystal film simulations, these films exhibited an interface boundary layer with a high stress gradient and a bulk region with roughly constant stress through the thickness. Interestingly, the polycrystal films showed an additional boundary layer at the surface of the unpassivated film. The interface and surface boundary layers were both about 150 nm thick, roughly invariant with film thickness or grain size. However, the average stresses in these layers increased with decreasing grain size; *i.e.* the stress gradients are invariant with thickness but not with grain size. These results indicate a complex coupling between film stress, film thickness, and grain size, and suggest, in contrast with the analytical models described in section 2.3, that the functional form of a Hall-Petch equation is inadequate to describe this relationship.

Hartmaier *et al*. [88, 89] also modeled polycrystalline films with varying thicknesses using a similar 2D approach. They incorporated dislocation climb to simulate the buildup of diffusion wedges at grain boundaries [39]. The grain size in

these simulations was a factor of three larger than the thickness. These simulations showed a transition from plasticity dominated by dislocation glide to plasticity dominated by diffusional processes as film thickness decreased below 140 nm. The flow stress was simply proportional to the inverse of the film thickness in both regimes.

The 2D simulations discussed above provide insights into the functional relationship between flow stresses and film parameters such as thickness, grain size, and dislocation density. In particular these simulations have provided models for the $1/h$ dependence of the flow stress, and a change in the thickness dependence of strength below some critical thickness, both of which have been observed experimentally. Furthermore, they suggest that a complex interplay between film thickness and grain size may lead to non-Hall-Petch-like behavior, possibly making the debate over whether the grain size exponent is -1 or -1/2 (discussed in Section 2.2) moot.

However, a 2D model cannot capture realistic motion of dislocations in thin films even qualitatively. Rather than threads moving through the channel of the film interacting with other threads and misfits (*e.g.* Fig's 2.2-2.5), in this formulation one must imagine that source-sized loop ends move unimpeded laterally over large distances to create straight dislocations parallel to the interfaces in the interior of the film which then move about. As in the analytical solutions described in Section 2.2, dislocation curvature and shape change are not accounted for. Junctions cannot form. The two-dimensional nature of the problem also limits the realism of the slip systems that can be used. The configuration shown in Fig. 2.6 is commonly used, but does not represent any real orientation in the modeled systems. It is simply a means to provide multiple slip systems in the 2D geometry.

Furthermore, these simulations contain *ad hoc* assumptions that remain unverified but upon which the results depend. First is the use of dislocation sources to nucleate

dislocations. Regardless of how the source strengths or locations are prescribed, the *type* of source is assumed. For glide dislocations, Frank-Read sources are envisioned. For dislocations that climb into the film, surface nucleation is prescribed. Second, simulations of polycrystalline films assume grain boundaries and interfaces to be impenetrable, whereas dislocations may be blocked, absorbed, reflected, or transmitted at real grain boundaries [30, 31] or interfaces [55, 67, 68, 90]. Assuming that dislocations are generated by repeated source activation and blocked by grain boundaries and interfaces automatically gives rise to pileup behavior. Neither Frank-Read sources nor pileups have been widely observed in thin films.

How serious deficiencies due to the 2D geometry and *ad hoc* assumptions may be is a matter of speculation. There is very little experimental evidence that can be used to support or deny conclusions based on these simulations. However, as discussed below, 3D simulations can be used to address the geometry issues (at the expense of dramatically increased computational demands). The *ad hoc* assumptions, however, are common to both 2D and 3D DD simulations, and will be revisited below.

2.4. Three-dimensional dislocation dynamics simulations

Unlike 2D simulations, 3D simulations can capture the fundamental aspects of dislocation motion in films: motion of threads and the interactions that stop them. In addition, 3D simulations allow dislocations to adopt arbitrary shapes consistent with their line tension and local stress environment. The most developed and widely used 3D simulation technique is discrete dislocation dynamics (DDD). All DDD codes operate on similar basic principles. First, as the name implies, a line representing a dislocation is discretized. Then, the forces on the discretized dislocation are calculated. The velocity of each point on the dislocation is then determined by

applying a mobility law and the position is updated according to a time step. Finally, the dislocation is rediscretized and the process is repeated.

The first 3D DDD code was developed by Kubin and Devincre [91, 92]. In this code, a dislocation is represented as a connected series of edge and screw segments. Since this initial work, there has been much interest in this technique and various groups have generated and refined a number of different DDD codes (e.g. [28, 51, 93-100]. Some DDD codes have been used to simulate dislocations in thin films. These are listed in Table 1, which includes a summary of their salient features, as well as some important applications. The first column, *Simulation Code*, gives the title of the code if it has one, or the name of the primary developers. The second column, *Code Ref.*, gives the references where detailed descriptions of the codes can be found. In the following, we discuss the distinguishing characteristics as well as some important results of each code.

Three discretization schemes have been used: edge-screw, straight line, and tracking points. The *Discretization* column in Table 2.1 lists the scheme used by each code. In the edge-screw scheme, dislocations are discretized into pure edge and pure screw segments (Figure 2.8). This method is used because of its simplicity, particularly for simulating anisotropic materials. In the straight-line scheme, dislocations are discretized into straight lines and each segment moves as a straight line. This method is attractive because of its similarity to finite element methods. In the tracking point scheme, the dislocation is marked by tracking points. In contrast to the straight line discretization scheme, the portion of the dislocation *between* tracking points is not constrained to be linear during motion. The choice of discretization scheme is largely a matter of preference, since no benchmarking tests comparing the accuracy or calculation time have been performed to date. However, straight-line and tracking point discretization techniques most closely approximate the shape of a curved dislocation and are likely more accurate for generally curved dislocations.

Table 2.1. Summary of three-dimensional dislocation dynamics codes used for dislocation dynamics simulation in thin films and some of their key features and application.

Simulation Code	Code Ref.	Discretization	Core Treatment	FEM Coupling	Channeling Stress	Dislocation Interactions	Large-scale Film Simulations
PARANOID	**[51, 126]**	**Tracking points**	**Modified Brown [51]**	**[105]**	**[28]**	**[28, 29, 70-72, 74]**	**[52-54, 81, 111]**
K-F (Kukta-Freund)	**[77, 127]**	**Straight line**	**Brown [102]**	**None**	**[127]**	**[77]**	**None**
K-D (Kubin-Devincre)	**[91]**	**Edge-screw**	**Brown [102]**	**[108]**	**[107] w/anisotropic line tension [108] w/o line tension [106]**	**[107]**	**None**
W (Weygand-Friedman-van der Giessen-Needleman)	**[128]**	**Straight line**	**Brown [102]**	**[128]**	**Free-standing film (no misfits) [95, 128]**	**None**	**None**
micro3d (Zbib, Rhee, Hirth)	**[98, 129]**	**Straight line**	**Simple dislocation bend using NN pts→ analytical solution**	**[129]**	**[76, 109]**	**[76, 109]**	**None**
VGA (von Blanckenhagen-Gumbsch-Arzt)	**[36, 97]**	**Tracking points**	**Modified Brown [51]**	**None**	**[36]**	**None**	**[36, 37, 97]**
ParaDiS	**[100, 130]**	**Straight line segments**	**non-singular core [104]**	**[131]**	**None**	**None**	**None**

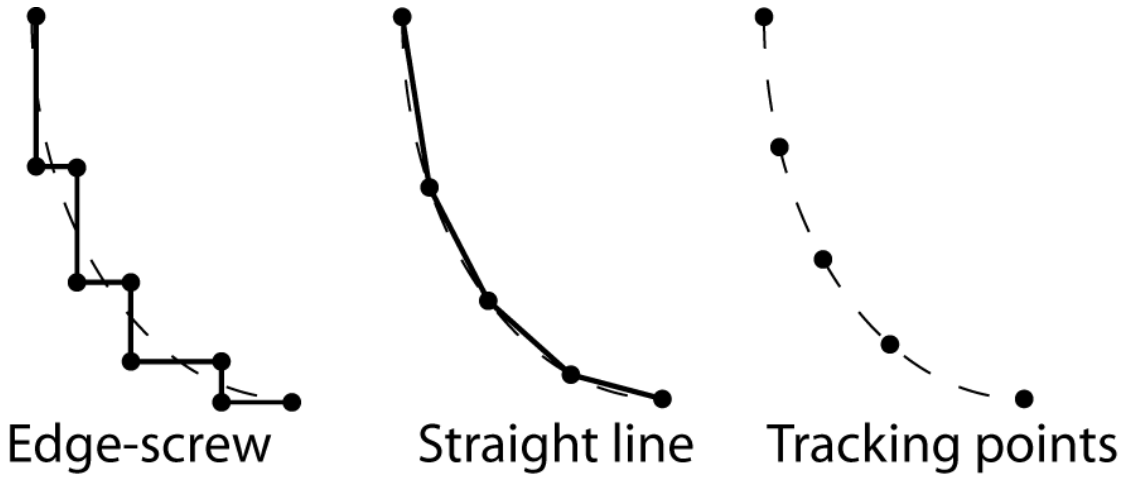

Figure 2.8. Comparison of dislocation discretization schemes: edge-screw, straight line, and tracking points.

Following the discretization step, the forces on the dislocations are calculated. The forces on the dislocations arise from applied stresses, the stress fields of other dislocations, and the so-called self-stress due to curvature. The force F_i due to the applied stresses and stress fields of other dislocations far from the point of interest is simply calculated using the Peach-Koehler formulation [59],

$$\frac{F_i}{L} = \varepsilon_{ijk}\xi_k b_m \sigma_{mj}, \tag{2.3}$$

where ε_{ijk} is the permutation tensor, ξ_i is the sense vector of the dislocation, b_i is the Burgers vector, σ_{ij} is the stress on the dislocation, and repeated indices are summed. The contribution of the self-stress depends on how the finite core of the dislocation is dealt with, which is discussed below.

Once the force on the dislocations is determined, the discretized dislocations are moved according to a mobility law. All of the simulations reported here assume a viscous law to describe the dislocation velocity v such as [59, 78]

$$v = v_0\left(\frac{\tau_{RSS}}{\mu}\right)^m \exp\left[-Q_0 / kT\right], \tag{2.5}$$

where τ_{RSS} is the total resolved shear stress on the dislocation [101], Q_0 an activation energy, k the Boltzmann constant, μ the shear modulus, v_0 a material constant, and m a constant. Typically, m is taken to be unity, so that under isothermal conditions the velocity is proportional to the force on the dislocation.

Because linear elastic solutions for the stress fields of a Volterra dislocation vary as $1/r$, where r is the distance from the dislocation core, the stresses diverge near the core. Therefore, calculating the force on a segment or node in a DDD simulation due to immediately adjacent segments—the self-stress—is impossible without some approximation to deal with this singularity. The methods used by each of the simulations for calculating the self-stresses are given in the *Core Treatment* column of Table 1. Three basic approaches have been taken: perform some variant of an

operation known as Brown core-splitting [102], use an analytical solution for an arc of fixed radius [103], or use equations for a non-singular core [100, 104]. Brown core splitting [102] is used in the majority of dislocation codes used to model thin films. In this approximation, an arc is passed through the point of interest and the nearest neighbor points on the dislocation line. The arc is displaced by some distance $+\delta$ and again by $-\delta$ and the self-stress on the point of interest is taken as the average of the stress from the two arcs. Schwarz [51] modified this approach such that the arc included more than just the nearest neighbor points, making calculation of the self-stress computationally stable for arbitrarily small segment sizes. Approximating the self-stress by passing an arc of fixed radius through the point of interest and using an analytical solution to calculate the self-stress has been used in the Micro3D code [103]. Simulations using a non-singular core approximation have not yet been extensively used for simulating dislocations in films. It should be noted that that regardless of the approximation technique, the goal is to resolve a numerical problem that arises from the use of linear elasticity and thus the core splitting distance or core smearing width does not necessarily represent the width of a real dislocation core.

Finally, image effects on dislocations can be important due to the proximity of surfaces and interfaces in films. Approaches to this problem range from ignoring image effects in symmetric layers to using mirror images of the dislocations on the opposite side of an interface or surface to overlaying a finite element mesh to correctly enforce the traction boundary conditions. Schwarz has shown that unless films are extremely thin, it is reasonable to neglect image forces in free-standing and passivated films because the image forces from the two interfaces roughly cancel out [105]. He has also shown that a good approximation for modeling an unpassivated film is to model it as half of a passivated film [28]. For the codes that do use a finite element overlay, the references containing the details of this implementation are shown in the fourth column of Table 1, *FEM Coupling*.

In the following subsections we detail the successes of DDD simulations in simulating channeling stress, dislocation interactions, and large scale simulations.

2.4.1 Simulations of channeling stress/strain

The dependence of the channeling stress on film thickness is one of the fundamental size effects observed in thin films. This effect is elegantly captured by Eq. 2.1. Virtually all groups conducting DDD simulations of thin films have used the channeling stress as a benchmark for their simulations. All the codes are able to correctly simulate the thickness-dependent channeling stress, with the exception that Hartmaier *et al.* [106] used the line tension to fit an edge-screw discretization length. The references containing this benchmarking for each of the dislocation dynamics codes described above are shown in Table 1 in the column labeled *Channeling Stress*. Ideally, agreement between the simulations and analytical solution implies that thread motion is being accurately modeled over a range of length scales in the simulation. In fact, simulation parameters are sometimes tuned so that this agreement takes place. For example Gomez-Garcia *et al.* [107] used the analytical solution of the channeling stress to select a dislocation discretization and time step that allowed their edge-screw dislocation discretization to accurately model size effects in films.

Three-dimensional DDD simulations have also been used to shed new light on the channeling stress and its effects on film strength. Groh *et al*. [108] studied the effect of elastic anisotropy on the channeling stress. They simulated Cu on Cu, Cu on Au, and Cu on Ni using dislocation dynamics coupled with a finite element analysis to account for image stresses at the interface and the free surface. After demonstrating agreement with Eq. 2.1 using isotropic elastic constants, they showed that using anisotropic elastic constants can increase the channeling stress above the stress predicted by the Matthews-Blakeslee criterion for an isotropic material by a factor of about two. For

these calculations, they used anisotropic elasticity with isotropic line tension calculations. When anisotropic line tension calculations were also added, the channeling stress increased by an additional 20%. Their simulations also revealed that films on stiffer substrates have higher channeling stresses than films on more compliant substrates.

Simulations of the channeling stress do not suffer from either simplified geometries or *ad hoc* assumptions. They provide both a means of verifying 3D codes and an area in which dislocation behavior can be unambiguously studied using DDD simulations.

2.4.2 Dislocation interactions

The channeling stress may accurately predict the *onset* of the motion of a *single* dislocation, but it does not address strain hardening. Strain hardening is the result of dislocations interacting with each other. As described in the Introduction, in thin films one can envision a thread moving through the "channel" of the film thickness interacting with other threads (Fig. 2.3b and d) and with misfits (Fig. 2.3a and d)—at least for single crystal or large-grained films. We define the strength of an interaction to be the applied biaxial stress or strain required to cause a thread to break free of the interaction and continue moving through an otherwise dislocation-free film. The flow stress in such a film is therefore determined by the strength of dislocation interactions, and it is appealing to think that a model might be constructed in which the strengths of the interactions are combined to determine the strength of the film. To do this, we must first understand the strengths of the possible thread-misfit and thread-thread interactions.

In the first subsection below, we discuss simulations of interactions between threads and misfits. The next subsection addresses simulations of interactions between

two threading dislocations. What becomes clear from these results is that threads can be stopped by a variety of interactions; some are strong and some are weak. The observed strength of a film lies in between the strengths of these interactions, but we argue that the strengths of particular interactions cannot be combined in a simple way to predict film strength.

2.4.2.1 Thread-misfit interactions

Broadly speaking, thread-misfit interactions can be classified into interactions between a thread and misfits lying either on an intersecting slip plane (Fig. 2.3a) or on a parallel slip plane (Fig. 2.3b). Interactions between threads and misfits lying on intersecting slip planes have been the most studied dislocation interaction—mostly because a moving thread must interact with every misfit in its path, leading to the expectation that this interaction must be quite common, but probably also owing to the ability to make a direct comparison to the analytical solution calculated by Freund [25].

Using PARANOID, Schwarz and Tersoff were the first to simulate the interaction between a thread and a misfit lying in its path [28]. A thread moving in a (001) fcc film was simulated and interactions with intersecting misfits having four different Burgers vectors were considered. The misfits were rigid in this simulation, but the thread was allowed to adapt its shape based on the resolved shear stresses on the thread. The strength of the interactions with all four misfits was about 1.15 $\varepsilon_{ch,}$ much less than Freund's analytical prediction [27] of about 2.0 ε_{ch}. Other simulations that considered a thread moving past a rigid misfit were those of Gomez-Garcia *et al.* [107], who found blocking strengths similar to those of Schwarz and Tersoff, and Kukta and Freund [77], who found an interaction greater than that of Schwarz and Tersoff but about 50% less than Freund's analytical value [27]. These simulations all

showed that changes in the *configuration* of the thread as it interacted with the misfit greatly affected the strength of the interaction. In particular, threads were able to find lower energy configurations than the fixed shape assumed in the analytical solution.

An additional level of complexity is realized if the intersecting misfit dislocation is allowed to move in response to an approaching thread. Schwarz studied epitaxial unpassivated films in which the misfits were free to move into the substrate [70] as did Kukta and Freund [77]. Pant *et al.* [29] later simulated passivated films in which misfits were confined to, but could move around in, the film. Thread-misfit interactions in these simulations were also weak relative to Freund's prediction [27], but rather than simple blocking, a range of behaviors was observed. When the misfit can move into the substrate, this reduces the interaction strength. But whether the misfit can move in the substrate or not, if it can move it will tend to align with the line of intersection of the slip planes of the thread and misfit so as to lower the energy of the interaction. This can result in an attractive interaction without reaction (referred to by Schwarz as "bound states" [70]) or the formation of junctions [29] or thread-misfit annihilation reactions [29, 53, 54] which occur when part of a thread annihilates with a part of the misfit.

The thread-misfit annihilation is an example of the type of insight that can be gained from 3-D dislocation dynamics simulations. Examples of the configuration changes that can occur due to this interaction are shown in Figure 2.9 for 800 and 80 nm films from the simulations of Pant *et al.* [29]. As the thread approaches the misfits in these simulations, the misfits lift up off the interface to annihilate with the thread along the line of intersection of their slip planes. If the applied strain is sufficiently high, the thread can pass the misfits but, due to the annihilation, the trailing misfits behind the thread and the intersecting misfits will be connected as shown in the top images in Fig. 2.9. The subsequent images (from top to bottom) show that if the applied strain on the film is reduced, the thread reconnects with the misfits to form

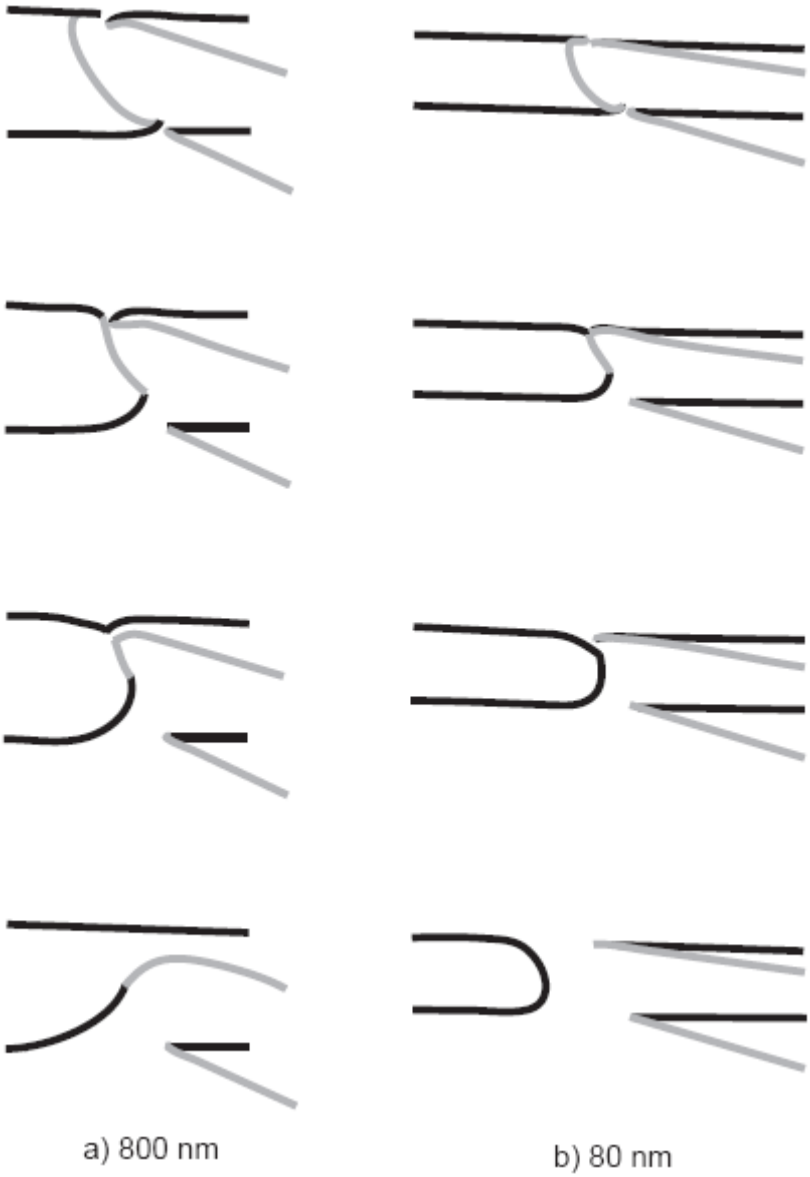

Figure 2.9. Evolution of thread-misfit annihilation interactions in films (a) 800 nm thick and (b) 80 nm thick. The same interaction takes on different configurations due to increased constraints on dislocation motion in the thinner film. (from Pant et al. [29]). Reprinted from Acta Mater., 51, Pant P, Schwarz KW, Baker SP, Dislocation interactions in thin FCC metal films, 3243, Copyright (2003), with permission from Elsevier.

new dislocation structures. In the case of the 800 nm film, the thread now exists on two different slip planes. In the 80 nm film, the thread has changed slip planes. In both cases, at least one misfit changes slip planes at a right angle for these (100) films generating a "corner misfit" [72].

The thread-misfit annihilation turns out to be surprisingly important. Experiments have shown that this interaction occurs frequently [72], making this one example of DDD simulations informing experimental work. Thread-misfit annihilation reactions are also common in large scale DDD simulations containing many dislocations [29, 53, 54] where, because this interaction can permanently change the both the configuration of the misfit and the slip plane of the thread, it has a significant influence on the final dislocation configuration.

The simulations by Pant *et al.* [29] represent the most comprehensive single study of dislocation interactions in thin films. In this study, the four distinct combinations of threads and intersecting misfit dipoles in both (001) and (111) film orientations were simulated and some of these interactions were studied at a range of film thicknesses. The strengths of these interactions ranged from $1.0\varepsilon_{ch}$ to $1.5\varepsilon_{ch}$. The orientation of the film affects interaction strength because of the different shapes that a thread can adopt as it interacts with the misfit. Pant *et al*. [29] showed that the thickness of the film affects the interaction in two different ways. First, a thinner film causes the curvature of a thread to increase in general compared with a thicker film, and requires a further increase for the thread to travel through a narrower misfit dipole. This prevents the thread from changing its shape easily because the required curvature changes are large. The upper bound on intersecting thread-misfit interaction strength of $1.5\varepsilon_{ch}$ occurred for films with thicknesses ~ 10 nm. For films that are hundreds of nanometers thick, a more reasonable upper bound is $1.3\varepsilon_{ch}$. This lower strength is because the thread can change its shape in such a way that requires less force to move it pass the misfit. Second, both the increase in the channeling stress and the increase in

interaction strength lead to higher local stresses during the interaction. These higher stresses constrain the misfit from moving into the film from the interface and limit the configurations that it can adopt. This is the reason for the different final configurations of the thread-misfit annihilation reactions shown in Fig. 2.9. In all cases, the strengths were less than predicted by Freund's analytical model [27].

Akasheh *et al.* [76, 109], using micro3D, conducted systematic studies of threads interacting with intersecting misfits in nanoscale strained coherent multilayers. They examined the effect of blocking by intersecting misfits for the four possible type of intersecting misfits in a (001) film in a multilayer structure. This is similar to the study by Pant *et al.* [29] except that Pant considered films with impenetrable boundaries having thicknesses of 80 nm or 800 nm and neglected image stresses. Akasheh *et al.* [76], on the other hand, studied coherent multilayers with elastic mismatch between the layers and layer thicknesses ranging from 6.4 nm to 51.1 nm and included the effects of image stresses by using a finite element overlay. Consistent with the results from Pant *et al.,* Akasheh *et al.* showed that the interaction strength between a thread an intersecting misfit is ~ 1.5 ε_{ch} for these very thin films and that the strongest interaction is between a thread and intersecting misfit having the same Burgers vector. The fact that including image stresses did not lead to appreciably different results than the results from the simulations of Pant *et al*., which did not include image stress effects, is consistent with the idea that for passivated films, image forces can be neglected [105].

The effect of threads interacting with misfits on parallel glide planes (Fig. 2.3c) was also examined by Pant *et al*. [29] for different film orientations and thicknesses. For these interactions, the upper limit on the interaction strength was about $1.7\varepsilon_{ch}$ when the parallel misfit was ~10 nm from the thread. In the case of an 800 nm Cu film, this interaction was shown to be stronger than the intersecting thread-misfit interaction when the spacing between the misfit and thread was less than 100 nm,

which corresponds to about 0.1% plastic strain. Because parallel interactions are dependent on the distance to the parallel misfit, the strength of these interactions will depend strongly on the distribution of misfits spacing in the film.

The 3D DDD simulations of interactions between threads and misfits have revealed several features that are important to film strength but would be difficult or impossible to study using analytical models or 2D simulations. First, the configuration of both the thread and the misfit change during the interaction. In many cases this change is significant and permanent. In all cases, it causes the interaction strength to be lower than predicted by the previous analytical interaction model [27]. Second, both the configuration and the strength of the interaction are dependent on film thickness with interaction stress increasing with decreasing film thickness.

The results of these simulations provide many insights into thread-misfit interactions, However, it is clear that strength of an interaction between any single thread and any single misfit dipole is not sufficient to account for film strength.

2.4.2.2 Thread-thread interactions

As with thread-misfit interactions, thread-thread interactions can be classified into interactions between threads lying either on intersecting (Fig. 2.3a) or parallel (Fig. 2.3b) slip planes. The strength of interactions between threading dislocations have not been studied analytically, perhaps because analytical solutions do not exist in closed form for dislocations that have varying curvature along their length, as do threads, or perhaps because they are not thought to be common enough to control strength.

Schwarz was the first to show that thread-thread interactions could be important. Using PARANOID, he examined the effect of threads interacting with other threads on parallel glide planes [71, 74]. He calculated both the loading and unloading interaction strengths of thread-thread dipoles. As expected, the interaction strength

depends strongly on the separation of the dipoles, with strength on loading exceeding $5\varepsilon_{ch}$ for separations of a few atomic planes in a 100 nm thick passivated film. He also noted that the trapping range, defined as the maximum distance between the glide planes of two threads such that the threads will interact to immobilize each other, increases with decreasing stress. He also observed that a third thread could come near a dipole and break the dipole or replace one of the threads in the dipole. This phenomenon was shown to give rise to a dislocation structure very similar to a dislocation structure observed in real semiconductor films, as shown in Figure 2.10. In simulations of dislocations in a buried layer, repeated activation of two Frank-Read sources, situated on closely-spaced parallel glide planes, produced threads which moved towards each other to form thread dipoles. As new threads were generated by the Frank-Read sources, each previously formed dipole would break, sending the dislocation ahead of it further along to form a new dipole in a cascade of dipole breaking and formation. The misfits associated with the thread dipoles were pushed into the substrate above and below the layer creating a beautiful structure that is very similar to that actually seen in a SiGe layer on Si. This work was the first to simulate thread-thread interactions and showed that these interactions are an important in films.

The simulations by Pant *et al.* [29] also included a systematic examination of thread-thread interactions. For threads on parallel slip planes 100 nm apart in an 800 nm film, the interaction strength was nearly $1.5\varepsilon_{\mathrm{ch}}$. But in an 80 nm film, the thread spacing had to be 10 nm to achieve the same strength. This thickness dependence arises from the increasing difficulty for shape change of the thread with decreasing film thickness. In a thick film, the threads can easily align to form a strong dipole, while in a thin film at the same thread spacing, the threads remain curved and the dipole is much weaker. So, like the thread-misfit interactions, the thread-thread interactions display strong thickness dependence, but in this case the interaction strength is greater for thicker films. Since threads have to be very close in order for the

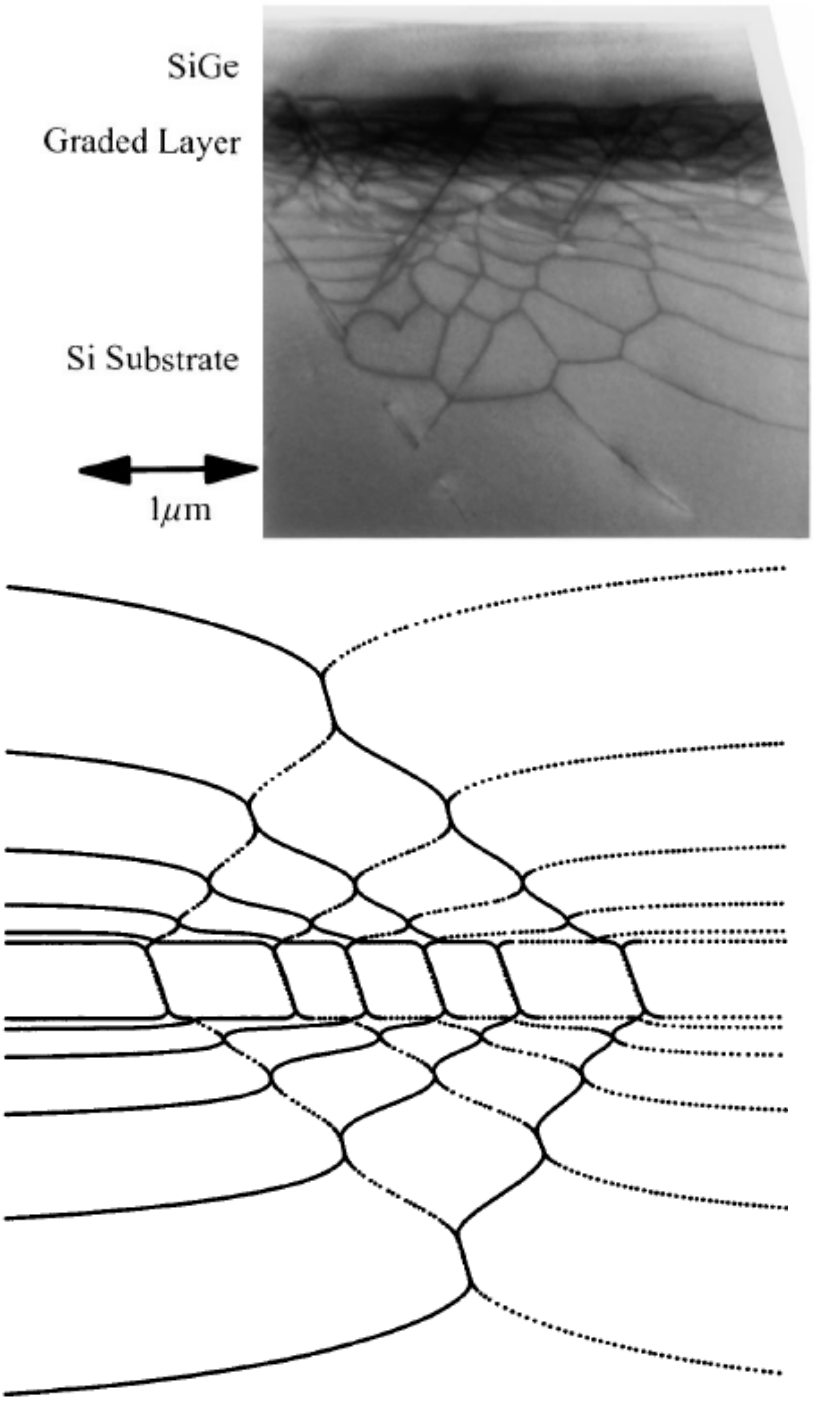

Figure 2.10. Top: Cross-sectional TEM of graded SiGe layer grown on Si. Dark lines correspond to dislocations. Bottom: Simulation results from repeated activation of two Frank-Read sources on parallel slip planes. (from Schwarz and LeGoues [74]) Reprinted figures with permission from Schwarz, KW, LeGoues, FK., Phys. Rev. Lett. 79:1877 (1997). Copyright (1997) by the American Physical Society.

interaction strength to be important in very thin films, this interaction may play an appreciable role in stopping threads only in thicker films.

Pant *et al*. [29] also systematically simulated interactions between threads on intersecting slip planes (Fig. 2.3b). For these interactions the interaction strengths span a very wide range from just above $1.0\varepsilon_{ch}$ up to ∞ for the case of annihilation. (By our definition, annihilation interactions have infinite strength because the threads involved are no longer in the film and thus, regardless of the applied stress, can never be moved out of that interaction.) In addition, some thread-thread junctions had strengths that were $\sim 10\varepsilon_{ch}$—much higher than any thread-misfit interaction. As with thread-thread dipoles, interaction strength between threads on intersecting slip planes increase with increasing film thickness.

As with the thread-misfit interactions, the configurations of the threads involved in thread-thread interactions play a significant role in determining the interaction strength and thus there is a significant thickness dependence, although unlike thread-misfit interactions, thread-thread interactions become stronger as the film becomes thicker. Encouragingly, the simulations have shown that some thread-thread interactions have strengths that are higher than the average stresses observed in films. However, it is important to know how common these strong interactions might be in a film since film strength is dependent on not only the strength of an interaction but also on how far a thread travels before stopping in the interaction.

2.4.2.3 Dislocation interactions summary

3D DDD simulations are able to capture the critical shape changes that determine both the strength and the final configuration of dislocation-dislocation interactions in thin films. Simulations of thread-thread and thread-misfit interactions have provided valuable insight into the behavior of dislocations in thin films and provide an initial

answer to the question: What stops threads? These simulations showed that interactions between threads and misfits are weak with strengths generally less than $1.3\varepsilon_{ch}$, and that interactions between threads and other threads can be very strong, relative to typical film stresses. In addition, changes in interaction strength with thickness in these simulations suggest that thread-misfit interactions should be more important in very thin films, while thread-thread interactions may become more important with increasing film thickness. Nevertheless, it is not possible to predict film strength or strain hardening directly from the strengths of isolated dislocation interactions. This is primarily because as a thread moves it changes the misfit density and structure, which in turn affects the local stress landscape. (In a displacement controlled experiment the global stress will decrease as the threads move.) The likelihood that any particular type of interaction will stop a thread depends on the local stress and the presence of dislocations with which the thread can interact at that stress level. Thus, the distance a thread travels before interacting is as important as the interaction strength in determining the strength of a film. In addition, it is also possible that more than two dislocations come together to interact (consider the multijunctions observed in bulk materials [110]). To link our knowledge of the strength of dislocation interactions to the strength of the entire film, large-scale simulations, discussed in the following section, are needed.

2.4.3 Large-scale dislocation dynamics simulations

To study how realistic dislocation structures evolve in thin films, large-scale simulations incorporating many dislocations are necessary. Such simulations provide the opportunity to find out what types of dislocation interactions and structures arise given a sufficient number of threads that move and interact naturally. These

simulations also allow study of how the local stress field develops and the relationships between the local stresses and the dislocation structure that forms.

All large-scale simulations to date use similar methodology. First, some reduced volume is defined, either a grain or a periodic unit cell. Then dislocations are inserted in the film. This is done either by introducing a starting set of dislocations or by introducing a starting configuration of Frank-Read sources. Either type of starting configuration requires the assumption of a preexisting dislocation structure that is somewhat artificial. After an initial dislocation configuration is assumed, a strain is applied and the dislocations are allowed to move and interact naturally in response to the stresses in the film.

The primary challenge to large-scale discrete dislocation dynamics simulations of films is that the computational cost is immense. In the absence of simplifying approximations, the computation time required to evaluate the contribution of N dislocation segments is proportional to N^2. To obtain good resolution, the size of the segments into which dislocations are discretized is made smaller in regions of higher curvature or where dislocations are in close proximity to each other. Thus N increases rapidly as the dislocation structure evolves. In addition, as dislocation density increases, the distance between dislocations decreases, the forces on the dislocation segments increase (on average), and the distance that the segments move in a fixed time according to the mobility law (Eq. 2.4) also increase. In order to maintain stability of the computation and to correctly model local dislocation interactions, it is necessary to limit the distance that any one segment moves during a time step. Thus, the time step is rapidly decreased as the dislocation structure evolves. Due to these adaptive time step and discretization schemes, the number of computations per unit plastic strain increases dramatically as dislocation density increases in large-scale simulations. As an example, fully resolved simulations by Pant *et al.* [53, 54], and Fertig *et al.* [53, 54] of ~100 threads relaxing ~$2\varepsilon_{ch}$ applied strain required of-order

100,000 cpu-hours. Because dealing with image forces is also computationally intensive and because of the observations that image forces at the top and bottom interfaces of the film tend to cancel [105], image forces have typically been neglected in large scale 3D DDD simulations of thin films.

Currently, two film configurations have been studied using large-scale 3D DDD simulations: passivated single crystal films and polycrystalline films, both freestanding and encapsulated. The single crystal studies have successfully addressed the questions remaining after the simulations of individual dislocations interactions: How do "weak" thread-misfit and "strong" thread-thread interactions combine to produce measured film strengths? How far do threads travel before stopping in an interaction? And, can we identify a link between individual interactions and global film behavior? Furthermore we argue that, just as with the 2D simulations, the real value in 3D DDD simulations is the ability to learn what features control strength and strain hardening so that simple, accurate, and predictive empirical models can be produced. The polycrystal studies have also produced sensible models and scaling laws, but, because dislocation-grain boundary interactions cannot be accurately modeled, are less satisfying. In the following sections, some key features and results from large-scale 3D DDD simulations of single- and poly-crystal films are presented and discussed.

2.4.3.1 Single-crystal films

The large-scale simulations of dislocations in single-crystal films have all been done using the PARANOID code [52-54, 81, 111]. The first results of such simulations were presented by Schwarz, who considered passivated (001) fcc films 100 nm thick [52]. Relaxation simulations were performed in layers with simulation cell sizes ranging from 2 to 8 μm on a side containing 16 to 2048 initial threads by

imposing an initial strain of 0.01 and allowing the threads to move and interact until all threads had stopped moving. Schwarz reported three primary results. First, as expected based on the interaction studies, thread-thread annihilations, thread-thread junctions, and thread-misfit annihilations, ultimately immobilized the majority of the threads. Second, the misfits created substantial spatial fluctuations in the stress felt by a thread as it moved through the film. Finally, these simulations showed that increasing initial thread density results in a decreased final residual stress. Schwarz suggested that a model based on stress "traps" that stop threads would most accurately describe relaxation in these films.

Schwarz *et al.* used similar DDD simulations conducted using periodic simulation cells to make direct comparisons with relaxation experiments in $Si_{1-x}Ge_x$ layers in which initial dislocation structures had been induced by implantation of He ions [111]. The initial threading density in the simulations was adjusted so that the final thread density in the fully relaxed simulation and experiment agreed. Without any other adjustable parameters, the simulations agreed with the experimental data both qualitatively, in terms of dislocation configuration, and quantitatively, in terms of residual strain; suggesting that these simulations reasonably approximate the actual behavior of dislocations in thin films. In other work [81], DDD simulation results were also shown to be in good agreement with experimental results from GaAs films.

Pant *et al.* [53] took this approach further and simulated not only loading but also unloading by conducting a series of sequential relaxations in a 200 nm thick passivated (001)-oriented fcc film (nominally Cu). An initial set of 32 loops (64 threads) with an equal number of loops on each possible slip system was seeded at random locations in a 4 μm square periodic simulation cell, a strain of $1.3\varepsilon_{ch}$ was applied and the threads allowed to run until they stopped. The applied strain was then incremented to 1.8 and $2.3\varepsilon_{ch}$ with full relaxations at each step. Unloading was carried out in a similar manner with smaller unloading increments for strains less than $1\varepsilon_{ch}$.

The dislocation structure and biaxial stress distribution after relaxation at $1.8\varepsilon_{ch}$ during loading are shown in Figure 2.11, and the average film stress and the dislocation density at each relaxed state in Figure 2.12. The results of the relaxations after the loading steps in these simulations were similar to those of Schwarz [52] in that the same types of thread-thread and thread-misfit interactions formed and the stress state became inhomogeneous. In addition, Lomer locks were observed.

The load steps were very illuminating. At each load step, most of the thread-misfit interactions broke allowing the threads to move forward into the film, while most of the thread-thread interactions held—consistent with the different strengths of the individual interactions (Sec. 2.4.2). Thus, threads accumulated in thread-thread interactions as plastic strain increased. Nonetheless thread-misfit interactions were observed to stop threads, even at an applied strain of $2.3\varepsilon_{ch}$. When threads did move, they were most often stopped in regions of low stress (consistent with Schwarz's prediction [52]) as can be seen in Fig. 2.11. These results show that the stress inhomogeneity in the film influences dislocation interactions. Despite the rather large strain steps, the strain hardening rates observed in the simulations (taken as the slope of the relaxed stresses with the applied strain) are in good agreement with experimental values for Cu films.

The unloading simulations of Pant *et al.* [53] produced a strong Bauschinger effect comparable to that seen in experimental data (compare Fig. 2.1 with Fig. 2.12.). During relaxation at 1.8 and $1.3\varepsilon_{ch}$ on unloading, the dislocation structure changed very little, as evidenced by the nearly constant dislocation density (Fig. 2.12). This is consistent with the unloading strengths of interactions discussed in Section 2.4.2. Below ε_{ch}, the threads run backwards, against the applied stress, to eliminate the misfits until, at $0.3\varepsilon_{ch}$, only misfits remain. Below $0.15\varepsilon_{ch}$, the misfit dipoles collapse, so that all of the plastic strain is recovered before the applied tensile strain decreases to

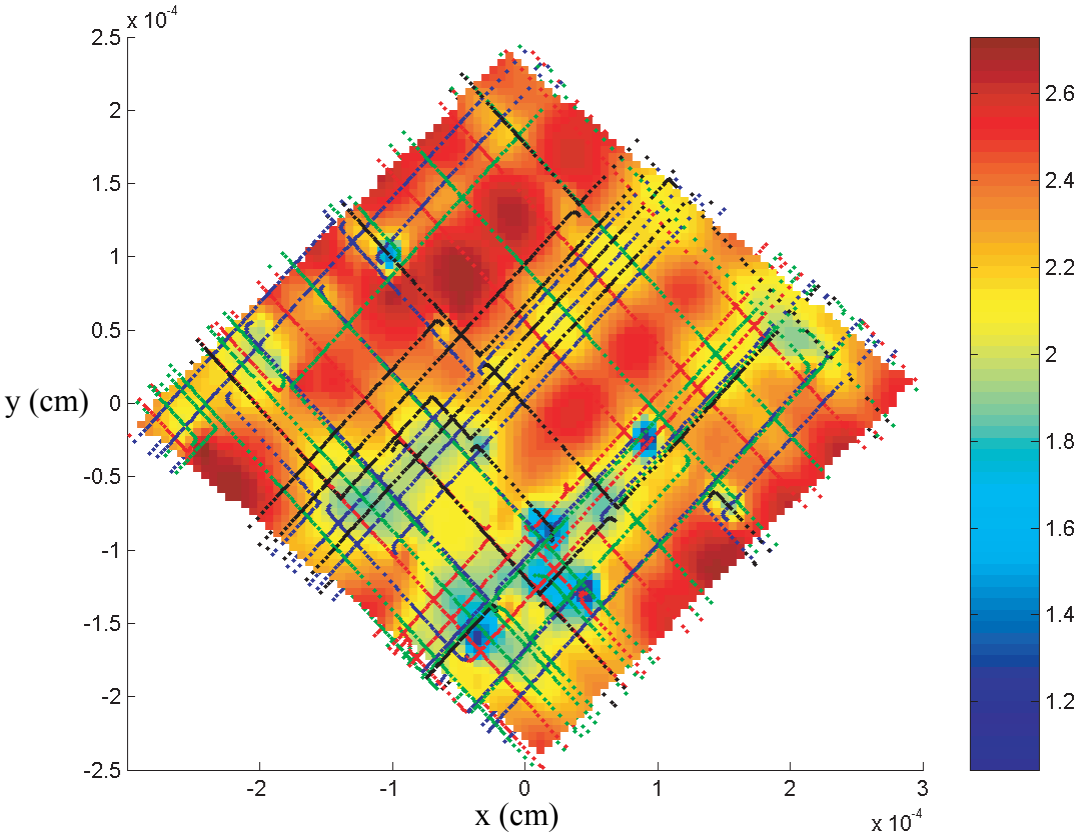

Figure 2.11. Dislocation configuration and the distribution of average biaxial stresses in an (001) film after relaxation from $1.8\varepsilon_{ch}$. Only the top misfit and the top half of each thread is shown for clarity. The stress field is very inhomogeneous and most dislocations are stopped in regions low local stress (from Pant et al. [53]).

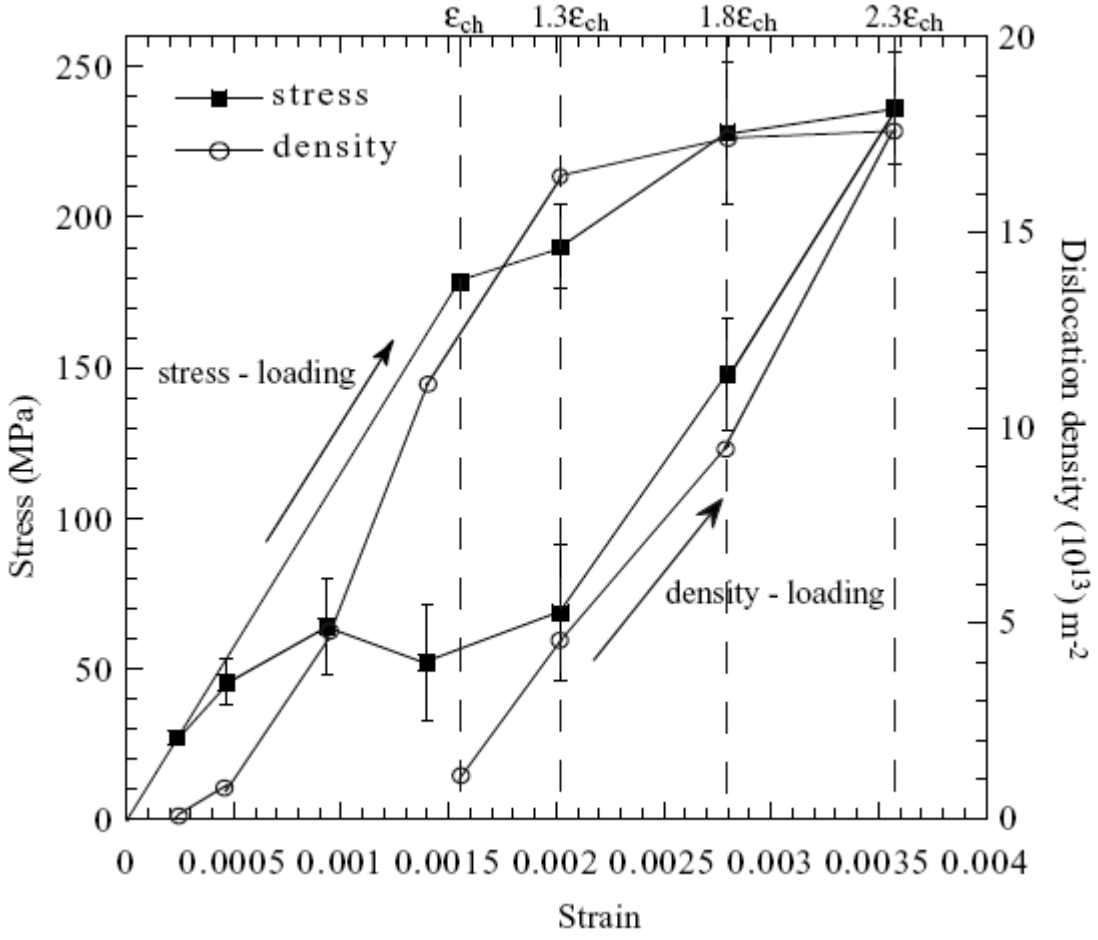

Figure 2.12. Average biaxial stress and dislocation density in (001) films after relaxation from different applied strain states during loading and unloading simulations. (from Pant et al. [53]).

zero. Thus the behavior is completely anelastic. These simulations provide a model for the origin of the large Bauschinger strains that are observed in thin films [40].

The simulations of Pant *et al.* [53] suggested that to develop a clear understanding of strength and strain hardening in single crystal films it would be necessary to understand how the inhomogeneity in the stress field evolves, what fraction of threads are stopped by each interaction type, and how far a thread travels before stopping, all as a function of the increasing misfit density during plastic deformation. With the intent to answer these questions, Fertig *et al*. [54] conducted more detailed simulations of stepwise loading, thoroughly analyzing the stress state and the interactions stopping threads in each relaxed configuration. These simulations were similar to those of Pant *et al*. [53] in that a series of sequential relaxations in a 200 nm thick passivated (001)-oriented fcc film (nominally Cu) were simulated using a 4 μm square periodic simulation cell. However in this case, the initial configuration consisted of 70 loops (140 threads) seeded randomly on the possible slip systems at random locations in the film. Strains of 1.3 to $3.3\varepsilon_{ch}$ were applied in $0.5\varepsilon_{ch}$ increments. As before, the threads were allowed to run until they stopped, creating a relaxed configuration after each load step. Like Pant *et al*.[53], Fertig *et al*. [54] also observed that film stresses were inhomogeneous in the relaxed configurations and that threads were nearly always stopped in regions of low stress, regardless of the type of interaction that stopped the thread.

Fertig *et al*. [54] went further and determined what types of interactions stopped every thread after each load step. The fates of the threads in the relaxed configurations are summarized in Figure 2.13, which shows the fraction of threads that have stopped due to thread-thread annihilation (TTA), thread-thread junction or dipole (NATT), thread-misfit annihilation (TMA), or other thread misfit interactions (NATM). At the end of each strain increment, the majority of the threads are stopped in thread-thread interactions not in thread-misfit interactions, as might be assumed. This result will, of

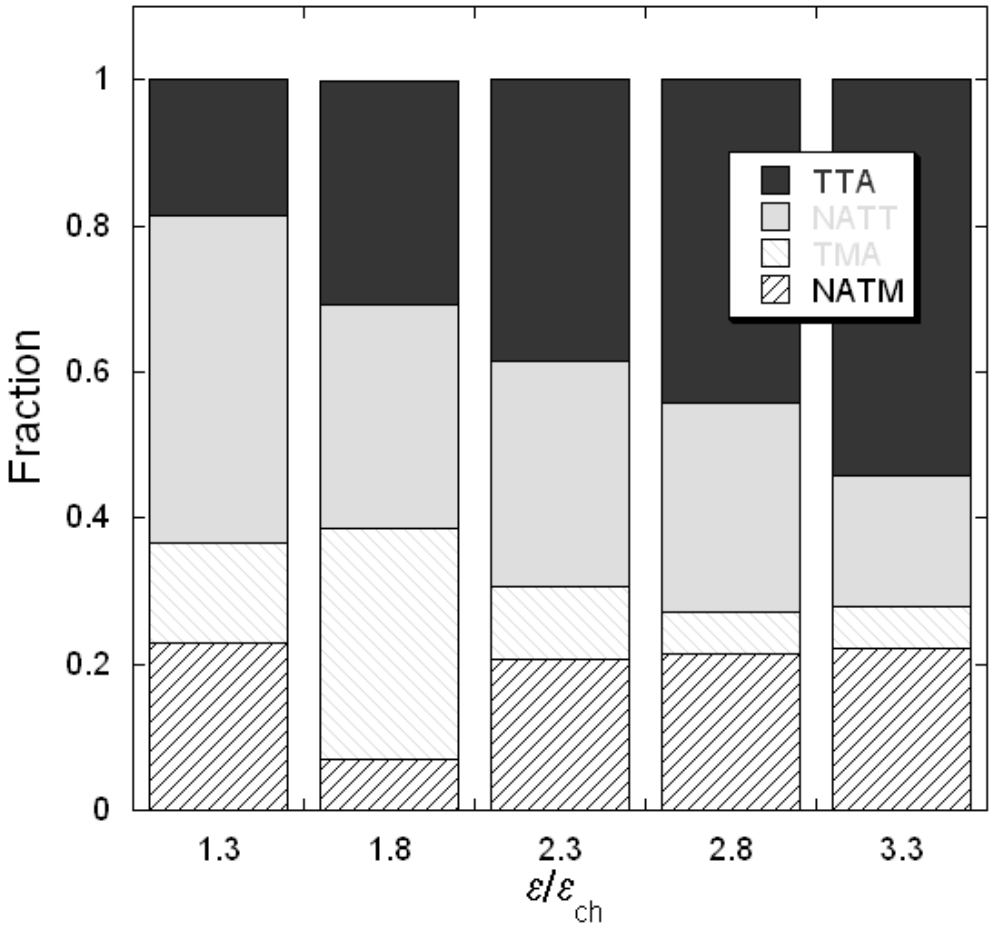

Figure 2.13. Interactions stopping threads after relaxation at each strain increment in the simulations by Fertig et al. [54]. Interactions are coded as TT = thread-thread, TM = thread-misfit, A = annihilation, NA = non-annihilating. TT interactions are seen to dominate at all strain levels and TM interactions to persist even at average stresses larger than nominal TM interaction strengths.

course, be dependent on the initial thread density, but it highlights the fact that the type of interaction that will stop a thread cannot be assumed *a priori*. In addition, thread-misfit interactions continue to stop threads at applied strains up to $3.3\varepsilon_{ch}$ despite the fact that at this strain level, the average biaxial film stress is much higher than the interaction strength of any thread-misfit interaction. Fertig *et al.* [54] showed that both the presence of a high fraction of thread-thread interactions at all stress levels, and the presence of thread-misfit interactions at high stress levels can be attributed to the inhomogeneous stress state.

In their single crystal simulations, Fertig *et al*. [54] found that the stress distribution rapidly became Gaussian and that the standard deviation increased significantly with increasing misfit density. This explains the presence of thread-misfit interactions at high average stresses since there were always regions where the local stress field was lower than the thread-misfit interaction strength and thread-misfit interactions occurred in these regions.

Fertig *et al.* [54] used this observation to develop a predictive model describing the distance a thread could travel before stopping in a thread-misfit interaction. Because the location that a thread will stop as a result of a thread-misfit interaction is governed by the local stress field relative to the interaction strength, the distance that a thread travels during relaxation is governed by the spatial fluctuation in the stress field. This is illustrated in Figure 2.14(a), which shows the resolved shear stress τ/τ_{ch} on a slip plane along a line through the middle of the film calculated from the relaxed configuration following an applied strain of $2.3\varepsilon_{ch}$. The shaded region represents the range of thread-misfit interaction strengths. If a thread moves through this stress field, the average distance that it will travel before stopping—the mean free path for dislocation motion—is just half of the average distance λ between regions of stress below some nominal thread-misfit interaction strength, τ_{TM}. Figure 2.14(b) shows λ as a function of τ_{TM} and the mean stress of the field $\bar{\tau}$. The different curves correspond

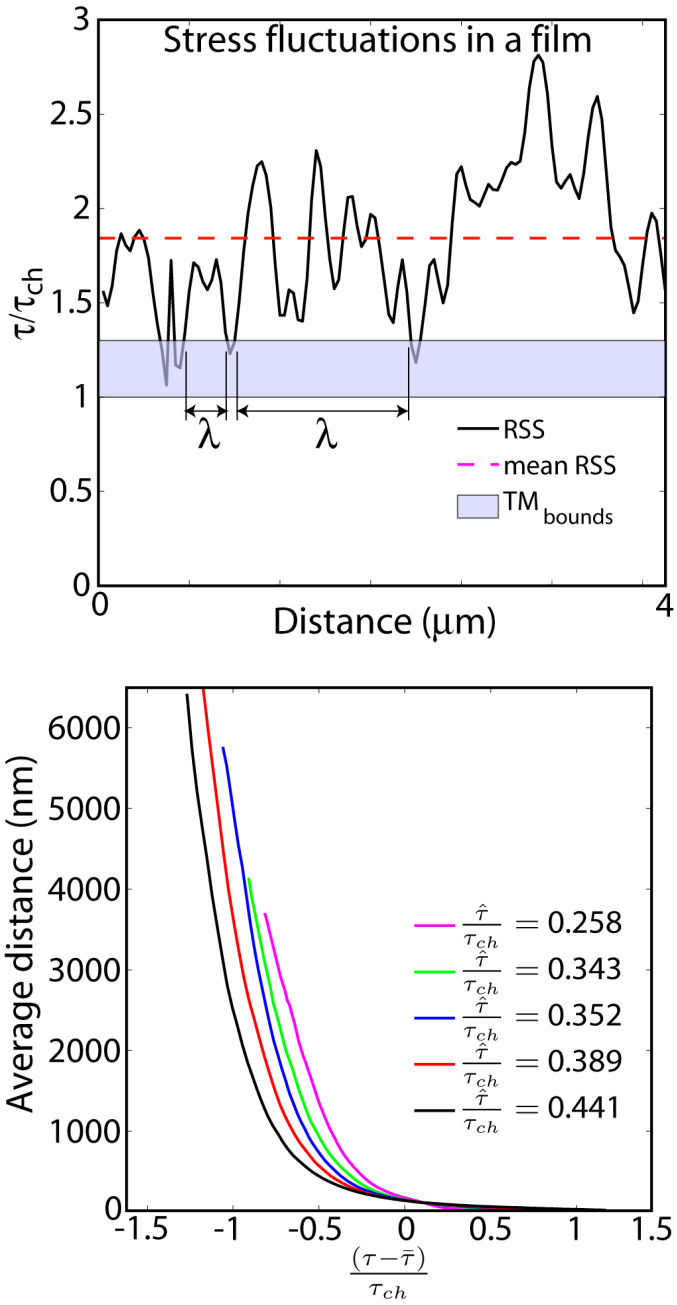

Figure 2.14. (a) Resolved shear stress along a line through the middle of a simulated 200 nm thick film that has relaxed an applied strain of $2.3\varepsilon_{ch}$. (b) Average distance between regions of stress lower than τ_{TM} in a field with mean stress $\bar{\tau}$ and standard deviation $\hat{\tau}$.

to stress fields with different standard deviations of stress $\hat{\tau}$ created by different misfit structures. Note that the average spacing between regions below the prescribed stress τ_{TM} decreases with increasing $\hat{\tau}$. Fertig *et al*. [54] showed that the $\lambda/2$ was in fact a good descriptor of the average distance traveled by a thread before it stopped in a thread-misfit interaction.

The inhomogeneity of the stress field also explains the prevalence of thread-thread interactions. As illustrated in Fig. 2.13, the number of threads stopped in TTA interactions steadily increases. That this increase is monotonic is not surprising, since threads can never leave this interaction. But, only about half of the threads that moved in the initial strain step move during the final strain step; so it is somewhat surprising that the number of threads that annihilate during each load step is nearly constant. For this to be the case, the threads must either move much farther during the relaxation step than was consistent with the amount of strain relaxation observed, or the inhomogeneous stress field affects the likelihood of thread-thread interaction. Fertig and Baker [112, 113] developed an analytical statistical model that showed that the latter is the case. Because threads move with a velocity proportional to the local resolved shear stress, threads move faster through regions of high stress and slower through regions of low stress. The result is that threads become more concentrated in regions of low stress, which increases the likelihood of a thread-thread interaction. Thus, thread-thread interactions should be more likely in an inhomogeneous stress field than in a homogeneous field. This is illustrated in Figure 2.15, which shows the likelihood of thread-thread interactions f in an inhomogeneous field normalized by the likelihood f_h in a homogeneous stress field plotted as a function of the coefficient of variation of the stress field. The smooth curve is analytically derived, while the open circles represent cellular automata simulations described in [113]. As the coefficient of variation of the stress field increases, the likelihood of thread-thread interaction increases, dramatically so when the coefficient of variation exceeds about 0.25. In the

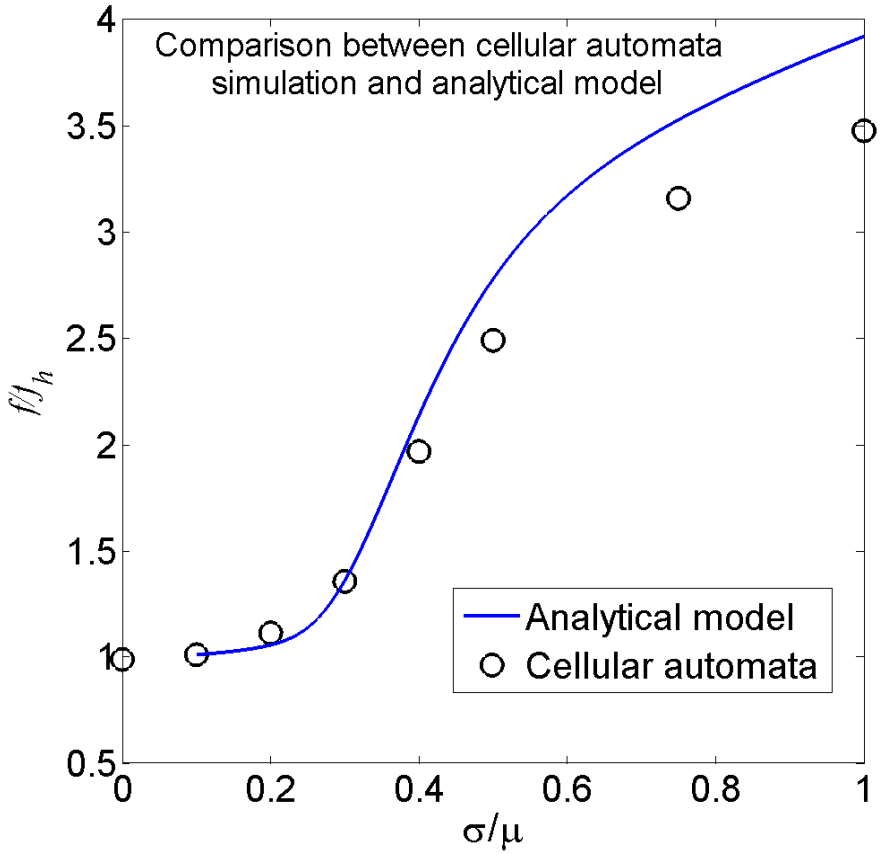

Figure 2.15. Fraction of threads f interacting in an inhomogeneous stress field normalized by the fraction of threads f_h that interact in a homogeneous field. The fields are characterized by mean μ and standard deviation σ of the resolved shear stresses on the dislocations. Increasing inhomogeneity of the stress field leads to increasing probability of thread-thread interactions since threads move more slowly, and become concentrated, in regions of low stress.

simulations, the coefficient of variation always exceeded this value. Thus, the threads were increasingly concentrated in low stress regions, which explains why they interacted with nearly constant frequency even when the global density of threads (as opposed to the effective density) decreased significantly.

Overall, the work of Fertig *et al.* [54] and Fertig and Baker [112, 113] provides a complete picture of strength and strain hardening in thin films based purely on dislocation interactions in an evolving stress field. On the one hand, "weak" thread-misfit interactions are effective because threads are trapped in these interactions in regions of low stress. The average distance of $\lambda/2$ that threads travel before being trapped determines the strain, and thus the strain hardening rate. On the other hand, "strong" thread-thread interactions occur frequently because threads are concentrated in regions of low stress. Fertig *et al.* [54] compared their simulation results with x-ray measurements of the thermomechanical behavior of the (001) grains in Cu thin films and found good agreement with both stresses and strain hardening rates.

Large-scale 3D DDD simulations of single-crystal films provide a much more refined answer to the question, "what stops threads?" than did simulations of individual dislocation interactions. In particular, the large-scale simulations demonstrate that knowledge of the strengths of dislocation interactions alone is insufficient to describe the strength of a film. Stress inhomogeneity was shown to play a critical role in determining which interactions would stop threads and where they would occur. These simulations have been able to reproduce configurations, stress levels, and strain hardening rates observed experimentally. Unfortunately, the thickness dependence has not yet been explored—probably due to the computational demands involved in running many fully-resolved simulations. While these single-crystal simulations appear to generate realistic descriptions of dislocation behavior in films, perhaps their most important function is that by observing them, one can develop concepts for how large numbers of dislocations behave and interact with each

other in films upon which analytical models that are simple, but more accurate, can be based. The stress fluctuation model suggested by Schwarz [52] and implemented by Fertig *et al.* [54] is one example.

2.4.3.2 Polycrystalline films

A number of simulations of polycrystalline films have been conducted [36-38, 97, 114] using 3D DDD simulations. These were motivated by the fact that many films are polycrystalline and at least in part by analytical and 3D results suggesting that dislocation interactions, certainly at least thread-misfit interactions, might not alone be able to account for film stresses. These simulations sought to determine how grain boundaries affect film strength, the functional form of the relationship between grain size and film stresses, and how important dislocation interactions are relative to grain boundaries in stopping threads.

Von Blanckenhagen *et al.* conducted a series of simulations of polycrystalline films using their own code [36]. In their initial models [36], they simulated a single grain where the grain boundaries and top (film/passivation) and bottom (film/substrate) interfaces were represented by impenetrable walls. Dislocations were generated by a Frank-Read source that was repeatedly activated as the applied strain was continuously increased, resulting in a dislocation pileup at the grain boundaries and interfaces. The effects of source size, grain size, and film thickness were investigated. They noted that for Frank-Read source activation, the dislocation loop must also squeeze between the pinning points and the grain boundary or interface, thus the minimum stress for source activation occurs for a source size of the smaller of *d/3* or *h/3*. In this study, yielding was assumed to occur if the stress on the lead dislocation reached an arbitrarily chosen value 0.057μ. For these conditions, the smaller of either the thickness or the grain diameter controlled the flow stress. They showed that the

analytical model presented by Friedman and Chrzan [115] accurately predicted film stresses for the case when the source size was much smaller than the grain size or film thickness. However, as the source size approached the size of the grain or the film thickness, the analytical model predicted flow stresses that were too low. As was seen in 2D simulations (*e.g.* [87]) and experiments (*e.g.* [23]) these simulations showed a change in the size dependence of the flow stress. For grains or thicknesses larger than some critical size, the flow stress follows a classical Hall-Petch relationship ($\sigma_f \propto 1/\sqrt{d}$ or $\sigma_f \propto 1/\sqrt{h}$). For grains or thicknesses smaller than this critical size, the flow stress varies as $1/d$ or $1/h$. Von Blanckenhagen *et al's* [37, 97] predictions of flow stress were much closer to experimentally observed values than those of Freund's analytical model [27] of blocking of a thread by a misfit.

In a subsequent study Von Blanckenhagen *et al.* [37] expanded this work to study the effect of a *distribution* of sources within a grain. In these simulations, the grain boundaries were still considered impenetrable, but dislocations were allowed to leave through the top and bottom interfaces, thus simulating a free-standing polycrystalline film. Sources with a range of lengths were seeded at random locations within the grain. Having many Frank-Read sources in a grain revealed several interesting results. First, similar to the effects of starting thread density in the single crystal simulations, von Blanckenhagen *et al.* found that the more sources they had, the lower the stress would be at a given applied strain. This was attributed to the fact that there would be more sources favorably oriented for deformation. In this region the flow stress is proportional to the inverse of the number of sources. However, a critical source density was found, above which additional sources do not contribute to further relaxation. This was attributed to the fact that complete relaxation does not require the activation of all the sources.

Von Blanckenhagen *et al.* [37] compared their simulations to experimental data from a microtensile test of a1 μm copper film on polyimide. The simulations appear to

capture the early yielding behavior, but the experiments show a wide plateau in stress at plastic strains, ε_{pl}, higher than ~0.5% that is not produced in the simulations. Hardening rates, defined as $\Delta\sigma/\Delta\varepsilon_{\mathrm{pl}}$, were calculated at $\varepsilon_{pl} < 0.5\%$ and shown to vary with $1/h^2$, which is consistent with dislocation sources in the volume of the grain. (If dislocation sources were from the grain boundaries, the scaling would simply be inversely proportional to the film thickness.) The scaling of hardening rates in experimental data was shown to lie in between a *1/h* and $1/h^2$ relationship. These authors note these simulations can predict the high stresses observed in real films, and also yield a *1/h* flow stress behavior, thus they conclude that in polycrystalline films, the key feature determining film strength is activation of a source, not dislocation interactions. If this is true, dislocation interactions may play only a minor role in the strength of polycrystalline films.

Espinosa *et al*. [38, 114] conducted very similar studies of 'free-standing' polycrystalline films using PARANOID. In this work, grains with impenetrable boundaries, varying thicknesses (200–1000 nm), and constant grain size (200 nm) were simulated. Frank-Read sources were randomly located in the boundaries with sizes distributed according to a Gaussian distribution. A constant density of sources per unit grain boundary area was maintained across these simulations. They observed that a grain size-dependent internal length scale set up by the dislocation structure became the dominant length scale for thicker films, such that a threshold thickness existed above which dislocation behavior and film stress was invariant with thickness. This thickness saturation occurred when the thickness was somewhat larger than the grain size.

The simulations of polycrystalline films have successfully provided models for the functional form of the flow stress and hardening rates. However, these simulations are less satisfying—although potentially no less correct—than the single crystal simulations because they depend heavily on two unverified assumptions. First, in all

simulations of polycrystalline films to date, grain boundaries have been assumed to be impenetrable obstacles. In real materials, however, a dislocation may be stopped by boundary, or the boundary can absorb, reflect, transmit, and/or nucleate dislocations [30, 31]. Second, the results of these polycrystalline film simulations are heavily contingent on the assumption of nucleation of dislocations at Frank-Read sources in the interior of a grain. Very little is known quantitatively about dislocation sources in films. Furthermore, these "polycrystalline" models simulate relaxation in a single grain embedded in a bulk or film where the stresses outside the grain are not relaxed. Thus, the effects of dislocations in neighboring grains on the behavior of dislocations in the grain of interest are not included. Until nucleation, dislocation-grain boundary interactions, and the effects of elastic and plastic behavior of neighboring grains are better understood, confidence in the accuracy of polycrystalline film simulations will remain elusive.

2.5. Other simulation methods

Two other simulation techniques have been employed for three-dimensional simulation of dislocations in thin films: the phase field and level set methods. These techniques address the same class of problems that 3D DDD simulations consider, namely, dislocation motion in thin films, but they may be better suited for modeling particular dislocation behaviors such as climb, cross-slip, or interaction with impurities. In the follow subsections, we briefly outline how each method works and its particular strengths relative to DDD simulations.

2.5.1. Phase field method

Dislocation dynamics in thin films have been simulated using the phase field method; an excellent overview of this method and a comparison with discrete dislocation dynamics simulations is given in [99]. In this method, the slip due to dislocation motion is represented by an eigenstrain. Because slip occurs only on a finite number of crystallographic planes there are a finite number of eigenstrain tensors, *e.g.* for slip on primary slip planes in an fcc material, superposition of eight different eigenstrain tensors (2 for each slip system) can describe the total eigenstrain in the material. Thus, eight tensor fields $\boldsymbol{\phi}_\alpha(\boldsymbol{x})$ would be used to describe the dislocations in an fcc material, where $\boldsymbol{\phi}_a$ is a tensor and $\boldsymbol{x}$ is a position vector. The field is evolved according to the Ginzberg-Landau equation

$$\frac{\partial \phi_\alpha}{\partial t} = -k \frac{\delta F[\phi_\alpha]}{\delta \phi_\alpha}, \tag{6}$$

where $F[\phi_\alpha]$ is an energy functional of the eigenstrain field; and no sum over repeated indices is implied.

The phase field method offers several advantages over other dislocation simulation techniques. The numerical implementation is more straightforward than discrete dislocation dynamics simulations because the phase field method requires no specialized topological treatment for the dislocation. The method also handles anisotropic elasticity much more easily than DDD codes. In addition, the phase field method can utilize well-developed numerical tools for solving partial differential equations. Finally, the phase field method is ideally suited to simultaneously incorporate other microstructural features such as impurities or phase transformations. Despite these strengths, phase field methods suffer from spatial resolution limitations. Because the equations are solved on a grid over the whole volume, microstructural features smaller than the grid spacing cannot be resolved. This means that the details

of dislocation-dislocations interactions cannot be accurately modeled without a very fine grid spacing ~1nm. This would make large-scale simulations computationally unfeasible. Consequently, this method would be unsuitable for any study for which details of dislocation interactions are important, such as those described in Sections 2.4.2 and 2.4.3.

Wang *et al*. [116] have used phase field methods to simulate dislocations in misfitting epitaxial films. In order to account for the image forces from free surfaces, they used an additional evolution equation for what they termed virtual strain. This equation was coupled to and simultaneously solved with the evolution of the eigenstrain fields described above. After demonstrating quantitative agreement with an analytical solution of the stress due to a screw dislocation near a free surface, they qualitatively modeled four different thin film dislocation phenomena: propagation of a single thread protruding from the substrate into the film; and operation of a Frank-Read source for a film on an infinite substrate, a thin substrate, and a in a misfitting multilayer. In these simulations, a thread was observed to propagate in through the film, although comparison to the channeling stress was not made. The simulation also captured misfit pileups as the Frank-Read source operated multiple times. In the film on an infinite substrate the misfits were driven into the substrate, whereas the misfits remained at the interface in films on thin substrates or misfitting multilayers. These results showed qualitative agreement for all the modeled phenomena, but quantitative comparisons were not made.

2.5.2. Level set method

Recently, an approach based on level set methods has been adapted for dislocation dynamics simulations of thin films [75, 117, 118]. This method is used because it easier to combine the effects of dislocation climb, cross-slip, and glide and because it

doesn't require explicit discretization of the dislocation [118]. In this method, a dislocation is represented as the intersection of the level sets of two three-dimensional functions $\phi(\mathbf{x},t)=0$ and $\psi(\mathbf{x},t)=0$, where **x** is a three-dimensional vector and t is time. The time evolution of these equations must satisfy

$$\begin{aligned}\phi_t + \mathbf{v}\cdot\nabla\varphi &= 0\\ \psi_t + \mathbf{v}\cdot\nabla\psi &= 0\end{aligned}. \tag{7}$$

Once the dislocation line is calculated, the stresses are computed by FFT of the elastic Green's function. The instantaneous jump in strain at the core of a Volterra dislocation is treated by smearing the delta function describing the displacement gradient. The velocity **v** is calculated using a mobility tensor **M** such that **v** = **Mf**, where **f** is the force on the dislocation. In thin films, the half-space elastic Green's function is used to ensure that surface tractions are zero [75, 118]. A simulated film is assumed to be periodic in the plane of the film. If a thread intersects a free surface, its sense vector is assumed to be normal to the surface at the surface; the creation of surface steps is ignored. These simulations showed that level set methods could reasonably model a variety of dislocation behaviors in thin films such as cross slip, thread junction formation, and thread annihilation. Of these effects, thread junctions were shown to present a kinetic barrier to motion of other threads near the junction, possibly providing a further mechanism to dislocation pileup.

Despite the promise of level set methods, particularly in the study of climb and cross slip, several limitations on its widespread use remain. First, unlike DD methods that discretize dislocations based on dislocation curvature, level set methods utilize a numerical grid, which limits the topological configurations that can be described. Second, it is not clear that this method can be easily parallelized, a feature that would be required for large-scale simulations. The level set method does not model sharp corners well, so a corrective velocity term is applied to improve the approximation; it is not clear what effect this might have on the simulation results. Finally, visualization

of the dislocation line is more difficult than in traditional discrete dislocation dynamics methods because not only must the intersection between the two level sets be calculated, but interpolation must also be performed on each numerical cell to determine the dislocation line

2.6. Summary and discussion

Experimentally, thin films show stresses and strain hardening rates that are higher than would be predicted based on bulk scaling laws (Fig. 2.1). Setting aside relaxation due to diffusional flow, models and simulations of thin film mechanical behavior have focused on constraints on dislocation motion. These include the dimensional constraint created by the necessity of creating misfit dislocation line length as a thread moves through the channel of the film, interactions of dislocations with other dislocations, and interactions of dislocations with grain boundaries (Section 2.1). Analytical models (Section 2.2) correctly describe the channeling strain and its dependence on the reciprocal film thickness $1/h$, but overpredict the strength of dislocation interactions because *ad hoc* dislocation configurations are assumed in such models and are inflexible. 2D simulations (Section 2.3) allow computationally efficient study of interactions among many dislocations, and can include sources, image stresses, and simple impenetrable grain boundaries. 2D simulations have been used to produce a model for the experimentally observed $1/h$ dependence of the flow stress, but 2D simulations cannot model the interactions or changes in shape that occur in realistic 3D dislocation structures. Thus, these results are difficult to interpret.

For the cost of computational time, 3D DDD simulations (Section 2.4) can be used to create models in which dislocations move and interact in a physically reasonable way. In thin films, this type of simulation can be quite realistic because the thickness constraint limits both the configurations that dislocations can adopt and the number of

dislocations that must be modeled in order to obtain an accurate description of dislocation structures. Interactions between individual dislocations have been studied in detail and two distinct approaches have been developed for large-scale simulations of dislocation behavior in thin films following different sets of assumptions about the boundary conditions. In one approach, single crystal simulations are performed based on the assumption that threads move laterally through a film large distances compared with the film thickness (Fig. 2.2). Single crystal simulations follow logically from the analytical work to quantify the channeling stress and the strength of blocking interactions. These simulations provide detailed and accurate knowledge of how both the dislocation structure and the stress field evolve during deformation. In the other approach, polycrystal simulations are performed consistent with the observation that, in polycrystalline films, the mean grain size is comparable to the film thickness [119] so that interactions with boundaries and interfaces dominate. In these simulations, channeling never really occurs.

The results of both approaches have been compared with experimental results and have shown good agreement. However, the main value of large scale 3D DDD simulations lies not in their ability to generate quantitative agreement with experiments. Except in rare cases (*e.g.* [111]) it is difficult to know experimental initial and boundary conditions well enough to generate an accurate simulation. Rather the main value of these simulations is the ability to use them to *discover* the phenomena that control deformation in thin films and to use them, in turn, to generate simple conceptual or analytical models that can be used to predict film behavior.

For example, the 3D DDD simulations demonstrated that knowledge of both the strength of dislocation interactions and the inhomogeneity in the stress field that develops during deformation are necessary to describe the strength of a single crystal film. Thread-misfit interactions continue to play a role in stopping threads even when the average film stress exceeds the interaction strength because interactions can still

occur in low stress regions. The likelihood of thread-thread interactions is greatly increased because threads are concentrated in low-stress regions and because the regions of low stress dramatically increase the capture cross-section of the thread. This understanding leads to the prospect that a complete model for film strength and strain hardening may be developed based on stress fluctuations and a range of dislocation interaction strengths. Indeed a first step in this direction has been taken [112].

Of course, it is always desirable to benchmark the accuracy of modeling and simulation results against experiments. At the moment, the connection between 3D DDD simulations and film behavior is tenuous at best. In our view, improvements in both simulations and experiments in five categories are needed:

1. *Understanding of dislocation sources*: Both the single crystal and polycrystal simulations depend on *ad hoc* assumptions to get dislocations into the film. In the single crystal simulations a starting configuration of threads or loops is assumed. This has relatively little qualitative effect on the outcome for the simulations performed to date. However, the polycrystal simulation results depend critically on the fact that a particular configuration of Frank-Read sources is selected. To obtain even qualitative confidence in these simulations, some knowledge that the assumed source configuration is reasonable is needed. The difficulty of modeling dislocation nucleation correctly is that very little experimental work exists from which to construct an accurate picture. Transmission electron microscopy experiments have shown that dislocations can nucleate at grain boundaries [73, 120] and from interfaces [73], but knowledge of how to incorporate dislocation sources in thin film simulations is not yet available.

2. *Behavior of dislocations at grain boundaries and interfaces*: As has been noted several times in this review, the DDD simulations conducted thus far have simply treated grain boundaries as impenetrable obstacles, *ad hoc*, whereas experiments [30, 31] show a wide range of behavior: absorption, absorption and reemission,

transmission, and reflection. It is difficult to imagine that the effect of grain boundaries can be accurately incorporated before a solution to this problem is found. The polycrystal simulations cannot predict film strength because the resistance of a grain boundary to penetration by dislocations must be assumed. In addition, it is possible for the core of a dislocation to spread out into the interface between the film and an amorphous substrate or passivation layer. This behavior has been observed experimentally [21, 69, 121, 122], calculated analytically [68], and modeled using molecular dynamics simulations [55]. Dislocation dynamics simulations do not yet include these effects, although they have been shown to significantly affect the stress required for thread motion [67]. Accurate treatment of realistic dislocation behavior at grain boundaries and interfaces could be accomplished by systematic atomistic simulations that can be used concurrently, or to create a set of rules for use in DDD simulations.

3. *More complete dislocation behavior*: Most DDD simulations of thin films to date handle full Volterra type dislocations that glide on their slip planes. However, real dislocations can be dissociated into partials, may cross-slip or climb, or may be jogged as a result of dislocation interactions. To incorporate these effects, realistic dislocation core treatments must be found. Currently dislocation cores are either treated as smeared out (e.g. [100, 104]) or a cutoff radius is assumed, as in the case of PARANOID. The form of the core may have an impact on the types of interactions seen, particularly if the core is dissociated into compact partial dislocations (*e.g.* [94, 123]). The effect of the treatment of the dislocation core on dislocation behaviors such as climb, cross-slip, and junction formation remain to be examined, and could substantially change the configuration of a dislocation during an interaction or the evolution of a dislocation structure in time.

4. *Image forces*: To date, calculations of image forces in large-scale 3D DDD simulations have been avoided due to the computational demands. This is typically

done by selecting a symmetric passivated or unpassivated planar thin film geometry where such effects can be ignored [105]. However, in order to simulate films and structures with more realistic and interesting geometries, image force calculations will have to be included.

5. *Inhomogeneous/anisotropic materials*: In real materials, inhomogeneous structures are common, for example polycrystalline films oftern have mixed texture and therefore are composed of grains with different biaxial moduli due to elastic anisotropy. This leads to inhomogeneous stress states due to strain transfer from grain to grain [124]. Transmission electron microscopy work has shown that stresses near the grain boundary may indeed be different [125] than the grain interior. Incorporating these effects will almost certainly require coupling DDD simulations to a finite element model.

Incorporating all of these features will likely require a combination of a great deal of experimental work, particularly direct observations of dislocation behaviors, but also production and characterization of samples with well-known configurations and boundary conditions that can be directly compared with simulations. It will also benefit from the application of true multi-scale modeling in which appropriate parts of the problem are simultaneously handled using finite element or atomistic methods.

Regardless of the extent to which these tools are made available, there is a wide range of topics that would benefit from study using dislocation dynamics simulations. To date there are still not conclusive mechanistic explanations for either the thickness dependence or the grain size dependence of strength and strain hardening in films. Simulations that cover the range of strains, microstructures, and interfacial conditions seen in real thin film samples have not yet been reported.

Despite the challenges that remain for DDD simulations, the future looks bright. As a “virtual laboratory” in which to examine specific dislocation behaviors, these simulations are excellent tools. Continuing increase in computational resources means

that large-scale simulations will become more feasible. And increasing advances in experimental techniques should enable collection of more data for comparison to simulations for further simulation refinement.

Acknowledgements

This review was created with support from the National Science Foundation under grant DMR-0311848 as part of a symposium to honor F.R.N. Nabarro and his seminal contributions to dislocation theory at the 2008 Materials Research Society Spring Meeting, March 24-28, 2008.

REFERENCES

[1] Vinci RP, Zielinski EM, Bravman JC. Thermal strain and stress in copper thin films. Thin Solid Films 1995;262:142.

[2] Keller R, Baker SP, Arzt E. Quantitative analysis of strengthening mechanisms in thin Cu films: effects of film thickness, grain size, and passivation. J. Mater. Res. 1998;13:1307.

[3] Baker SP, Kretschmann A, Arzt E. Thermomechanical behavior of different texture components in Cu thin films. Acta Mater. 2001;49:2145.

[4] Baker SP. Plastic deformation and strength of materials in small dimensions. Mater. Sci. Eng. A 2001;319-321:16.

[5] Nix WD. Mechanical properties of thin films. Metall. Trans. A 1989;20:2217.

[6] Freund LB, Suresh S. Thin Film Materials: Stress, Defect Formation and Surface Evolution. Cambridge, United Kingdom: Cambridge University Press, 2003.

[7] Arzt E. Overview no. 130 - Size effects in materials due to microstructural and dimensional constraints: A comparative review. Acta Mater. 1998;46:5611.

[8] Kraft O, Freund LB, Phillips R, Arzt E. Dislocation plasticity in thin metal films. MRS Bull. 2002;27:30.

[9] Vinci RP, Vlassak JJ. Mechanical behavior of thin films. Annual Review of Materials Science 1996;26:431.

[10] Freund LB. Dislocation Mechanisms of Relaxation in Strained Epitaxial-Films. MRS Bull. 1992;17:52.

[11] Dehm G, Balk TJ, von Blanckenhagen B, Gumbsch P, Arzt E. Dislocation dynamics in sub-micron confinement: recent progress in Cu thin film plasticity. Zeitschrift Fur Metallkunde 2002;93:383.

[12] Frost HJ, Ashby MF. Deformation-mechanism maps: The plasticity and creep of metals and ceramics. Oxford: Pergamon Press, 1982.

[13] Keller R-M, Baker SP, Arzt E. Stress-temperature behavior of unpassivated thin copper films. Acta Mater. 1999;47:415.

[14] Koleshko VM, Belitsky VF, Kiryushin IV. Stress relaxation in thin aluminum films. Thin Solid Films 1986;142:199.

[15] Venkatraman R, Chen S, Bravman JC. The Effect of Laser Reflow on the Variation of Stress with Thermal Cycling in Aluminum Thin-Films. Journal of Vacuum Science & Technology a-Vacuum Surfaces and Films 1991;9:2536.

[16] Volkert CA, Alofs CF, Liefting JR. Deformation mechanisms of Al films on oxidized Si wafers. J. Mater. Res. 1994;9:1147.

[17] Shen YL, Suresh S, He MY, Bagchi A, Kienzle O, Ruhle M, Evans AG. Stress evolution in passivated thin films of Cu on silica substrates. J. Mater. Res. 1998;13:1928.

[18] Weiss D, Gao H, Arzt E. Constrained diffusional creep in UHV-produced copper thin films. Acta Mater. 2001;49:2395.

[19] Vinci RP, Forrest SA, Bravman JC. Effect of interface conditions on yield behavior of passivated copper thin films. J. Mater. Res. 2002;17:1863.

[20] Shu JB, Clyburn SB, Mates TE, Baker SP. Effect of oxygen on the thermomechanical behavior of passivated Cu thin films. J. Mater. Res. 2003;18:2122.

[21] Keller-Flaig RM, Legros M, Sigle W, Gouldstone A, Hemker KJ, Suresh S, Arzt E. In situ transmission electron microscopy investigation of threading dislocation motion in passivated thin aluminum films. J. Mater. Res. 1999;14:4673.

[22] Thompson CV. The Yield Stress of Polycrystalline Thin-Films. J. Mater. Res. 1993;8:237.

[23] Venkatraman R, Bravman JC. Separation of Film Thickness and Grain-Boundary Strengthening Effects in Al Thin-Films on Si. J. Mater. Res. 1992;7:2040.

[24] Matthews JW. Defects associated with the accommodation of misfit between crystals. Journal of Vacuum Science and Technology 1975;12:126.

[25] Freund LB. The Stability of a Dislocation Threading a Strained Layer on a Substrate. J. Appl. Mech. 1987;54:553.

[26] Nix WD. Yielding and strain hardening of thin metal films on substrates. Scr. Mater. 1998;39:545.

[27] Freund LB. A criterion for arrest of a threading dislocation in a strained epitaxial layer due to an interface misfit dislocation in its path. J. Appl. Phys. 1990;68:2073.

[28] Schwarz KW, Tersoff J. Interaction of threading and misfit dislocations in a strained epitaxial layer. Appl. Phys. Lett. 1996;69:1220.

[29] Pant P, Schwarz KW, Baker SP. Dislocation interactions in thin FCC metal films. Acta Mater. 2003;51:3243.

[30] de Koning M, Miller R, Bulatov VV, Abraham FF. Modelling grain-boundary resistance in intergranular dislocation slip transmission. Philos. Mag. A 2002;82:2511.

[31] de Koning M, Kurtz RJ, Bulatov VV, Henager CH, Hoagland RG, Cai W, Nomura M. Modeling of dislocation-grain boundary interactions in FCC metals. Journal of Nuclear Materials 2003;323:281.

[32] Lee TC, Robertson IM, Birnbaum HK. Prediction of Slip Transfer Mechanisms across Grain-Boundaries. Scripta Metallurgica 1989;23:799.

[33] Robertson IM, Lee TC, Rozenak P, Bond GM, Birnbaum HK. Dynamic Observations of the Transfer of Slip across a Grain-Boundary. Ultramicroscopy 1989;30:70.

[34] Lee TC, Robertson IM, Birnbaum HK. TEM in situ Deformation Study of the Interaction of Lattice Dislocations with Grain-Boundaries in Metals. Philos. Mag. A 1990;62:131.

[35] Clark WAT, Wagoner RH, Shen ZY, Lee TC, Robertson IM, Birnbaum HK. On the Criteria for Slip Transmission across Interfaces in Polycrystals. Scr. Metall. Materialia 1992;26:203.

[36] von Blanckenhagen B, Gumbsch P, Arzt E. Dislocation sources in discrete dislocation simulations of thin-film plasticity and the Hall-Petch relation. Model. Simul. Mater. Sci. Eng. 2001;9:157.

[37] von Blanckenhagen B, Arzt E, Gumbsch P. Discrete dislocation simulation of plastic deformation in metal thin films. Acta Mater. 2004;52:773.

[38] Espinosa HD, Panico M, Berbenni S, Schwarz KW. Discrete dislocation dynamics simulations to interpret plasticity size and surface effects in freestanding FCC thin films. International Journal of Plasticity 2006;22:2091.

[39] Gao H, Zhang L, Nix WD, Thompson CV, Arzt E. Crack-like grain-boundary diffusion wedges in thin metal films. Acta Mater. 1999;47:2865.

[40] Baker SP, Keller-Flaig RM, Shu JB. Bauschinger effect and anomalous thermomechanical deformation induced by oxygen in passivated thin Cu films on substrates. Acta Mater. 2003;51:3019.

[41] Shu JB. Plastic Deformation and Thermomechancial Behavior of Passivated Copper Thin Films on Silicon Substrates. Materials Science and Engineering. Ithaca, NY: Cornell University, 2003. p.196.

[42] Shen YL, Ramamurty U. Constitutive response of passivated copper films to thermal cycling. J. Appl. Phys. 2003;93:1806.

[43] Xiang Y, Vlassak JJ. Bauschinger effect in thin metal films. Scr. Mater. 2005;53:177.

[44] Gruber PA, Böhm J, Onuseit F, Wanner A, Spolenak R, Arzt E. Size effects on yield strength and strain hardening for ultra-thin Cu films with and without passivation: A study by synchrotron and bulge test techniques. Acta Mater. 2008;56:2318.

[45] Eiper E, Keckes J, Martinschitz KJ, Zizak I, Cabie M, Dehm G. Size-independent stresses in Al thin films thermally strained down to-100 degrees C. Acta Mater. 2007;55:1941.

[46] Fitzgerald EA. Gesi/Si Nanostructures. Annual Review of Materials Science 1995;25:417.

[47] Schwarz KW, Liu XH, Chidambarrao D. Dislocation modeling for the silicon world. Mater. Sci. Eng. A 2001;309-310:229.

[48] Schwarz KW, Chidambarrao D. Dislocation modeling for the microelectronics industry. Mater. Sci. Eng. A-Struct. Mater. Prop. Microstruct. Process. 2005;400:435.

[49] Freund LB. The Driving Force for Glide of a Threading Dislocation in a Strained Epitaxial Layer on a Substrate. J. Mech. Phys. Solids 1990;38:657.

[50] Douin J, Pettinari-Sturmel F, Coujou A. Dissociated dislocations in confined plasticity. Acta Mater. 2007;55:6453.

[51] Schwarz KW. Simulation of dislocations on the mesoscopic scale. I. Methods and examples. J. Appl. Phys. 1999;85:108.

[52] Schwarz KW. Discrete dislocation dynamics study of strained-layer relaxation. Phys. Rev. Lett. 2003;91:145503.

[53] Pant P, Schwarz KW, Baker SP. Dislocation dynamics simulations of plastic deformation in thin films. Unpublished 2008.

[54] Fertig RS, Pant P, Schwarz KW, Baker SP. Dislocation dynamics simulations of dislocation interactions and stresses in thin films. In preparation 2008.

[55] Rodney D, Deby JB, Verdier M. Atomic-scale modelling of plasticity at a metal film/amorphous substrate interface. Model. Simul. Mater. Sci. Eng. 2005;13:427.

[56] Sedlacek R, Kratochvil J, Werner E. The importance of being curved: bowing dislocations in a continuum description. Philosophical Magazine 2003;83:3735.

[57] Sedlacek R, Werner E. Constrained shearing of a thin crystalline strip: Application of a continuum dislocation-based model. Phys. Rev. B 2004;69:134114.

[58] Schwarz C, Sedlacek R, Werner E. Application of a continuum dislocation-based model to a tensile test on a thin film. Mater. Sci. Eng. A 2005;400-401:443.

[59] Hirth JP, Lothe J. Theory of Dislocations. New York: John Wiley and Sons, Inc., 1982.

[60] Freund LB. The mechanics of dislocations in strained-layer semiconductor materials. Advances in Applied Mechanics 1994;30:1.

[61] Friedman LH, Chrzan DC. Scaling theory of the Hall-Petch relation for multilayers. Phys. Rev. Lett. 1998;81:2715.

[62] Friedman LH. Towards a full analytic treatment of the Hall-Petch behavior in multilayers: putting the pieces together. Scr. Mater. 2004;50:763.

[63] Frank FC, van der Merwe JH. One-Dimensional Dislocations. I. Static Theory. Proceedings of the Royal Society of London. Series A, Mathematical and Physical Sciences 1949;198:205.

[64] Frank FC, van der Merwe JH. One-Dimensional Dislocations. II. Misfitting Monolayers and Oriented Overgrowth. Proceedings of the Royal Society of London. Series A, Mathematical and Physical Sciences 1949;198:216.

[65] Matthews JW, Mader S, Light TB. Accommodation of Misfit Across the Interface Between Crystals of Semiconducting Elements or Compounds. J. Appl. Phys. 1970;41:3800.

[66] Matthews JW, Blakeslee AE. Defects in epitaxial multilayers. I. Misfit dislocations. Journal of Crystal Growth 1974;27:118.

[67] Baker SP, Zhang L, Gao HJ. Effect of dislocation core spreading at interfaces on strength of thin-films. J. Mater. Res. 2002;17:1808.

[68] Gao HJ, Zhang L, Baker SP. Dislocation core spreading at interfaces between metal films and amorphous substrates. J. Mech. Phys. Solids 2002;50:2169.

[69] Kuan TS, Murakami M. Low-Temperature Strain Behavior of Pb Thin-Films on a Substrate. Metall. Trans. A 1982;13:383.

[70] Schwarz KW. Interaction of dislocations on crossed glide planes in a strained epitaxial layer. Phys. Rev. Lett. 1997;78:4785.

[71] Schwarz KW. Simulation of dislocations on the mesoscopic scale. II. Application to strained-layer relaxation. J. Appl. Phys. 1999;85:120.

[72] Stach EA, Schwarz KW, Hull R, Ross FM, Tromp RM. New Mechanism for Dislocation Blocking in Strained Layer Epitaxial Growth. Phys. Rev. Lett. 2000;84:947.

[73] Dehm G, Balk TJ, Edongue H, Arzt E. Small-scale plasticity in thin Cu and Al films. Microelec. Engr. 2003;70:412.

[74] Schwarz KW, LeGoues FK. Dislocation patterns in strained layers from sources on parallel glide planes. Phys. Rev. Lett. 1997;79:1877.

[75] Quek SS, Wu Z, Zhang Y-W, Xiang Y, Srolovitz DJ. Dislocation junctions as barriers to threading dislocation migration. Appl. Phys. Lett. 2007;90:011905.

[76] Akasheh F, Zbib HM, Hirth JP, Hoagland RG, Misra A. Dislocation dynamics analysis of dislocation intersections in nanoscale metallic multilayered composites. J. Appl. Phys. 2007;101:084314.

[77] Kukta RV, Freund LB. Three-dimensional numerical simulation of interacting dislocations in a strained epitaxial surface layer. In: Bulatov V, editor. Multiscale Modeling of Materials, vol. 538. Pittsburgh, PA: Materials Research Society Proceedings, 1999. p.99.

[78] Freund LB. Dislocation Interactions in Relaxation of a Strained Epitaxial Layer. Scr. Metall. Materialia 1992;27:669.

[79] Weihnacht V, Bruckner W. Dislocation accumulation and strengthening in Cu thin films. Acta Mater. 2001;49:2365.

[80] Wolf D, Yamakov V, Phillpot SR, Mukherjee A, Gleiter H. Deformation of nanocrystalline materials by molecular-dynamics simulation: relationship to experiments? Acta Mater. 2005;53:1.

[81] Lynch C, Chason E, Beresford R, Freund LB, Tetz K, Schwarz KW. Limits of strain relaxation in InGaAs/GaAs probed in real time by in situ wafer curvature measurement. J. Appl. Phys. 2005;98:073532.

[82] Van der Giessen E, Needleman A. Discrete Dislocation Plasticity - a Simple Planar Model. Model. Simul. Mater. Sci. Eng. 1995;3:689.

[83] Nicola L, Van der Giessen E, Needleman A. 2D dislocation dynamics in thin metal layers. Mater. Sci. Eng. A-Struct. Mater. Prop. Microstruct. Process. 2001;309:274.

[84] Nicola L, Van der Giessen E, Needleman A. Discrete dislocation analysis of size effects in thin films. J. Appl. Phys. 2003;93:5920.

[85] Nicola L, Van der Giessen E, Needleman A. Two hardening mechanisms in single crystal thin films studied by discrete dislocation plasticity. Philosophical Magazine 2005;85:1507.

[86] Nicola L, Xiang Y, Vlassak JJ, Van der Giessen E, Needleman A. Plastic deformation of freestanding thin films: Experiments and modeling. J. Mech. Phys. Solids 2006;54:2089.

[87] Nicola L, Van der Giessen E, Needleman A. Size effects in polycrystalline thin films analyzed by discrete dislocation plasticity. Thin Solid Films 2005;479:329.

[88] Hartmaier A, Buehler MJ, Gao HJ. Multiscale modeling of deformation in polycrystalline thin metal films on substrates. Adv. Eng. Mater. 2005;7:165.

[89] Hartmaier A, Buehler MJ, Gao H. A discrete dislocation plasticity model of creep in polycrystalline thin films. Defects and Diffusion in Metals: An Annual Retrospective Vi 2003;224-2:107.

[90] Shen Y-L, Leger RW. Parametric atomistic analysis of dislocation-interface interactions in thin metallic films. Materials Science and Engineering: A Mechanical Behaviour of Micro- and Nano-scale Systems 2006;423:102.

[91] Kubin LP, Canova G, Condat M, Devincre B, Pontikis V, Brechet Y. Dislocation microstructures and plastic flow: A 3D simulation. Solid State Phenomena 1992;23-24:455.

[92] Devincre B, Kubin LP. Simulations of Forest Interactions and Strain-Hardening in Fcc Crystals. Model. Simul. Mater. Sci. Eng. 1994;2:559.

[93] Hirth JP, Rhee M, Zbib H. Modeling of deformation by a 3D simulation of multiple, curved dislocations. J. Comput-Aided Mater. Des. 1996;3:164.

[94] Shenoy VB, Kukta RV, Phillips R. Mesoscopic Analysis of Structure and Strength of Dislocation Junctions in fcc Metals. Phys. Rev. Lett. 2000;84:1491 LP

[95] Weygand D, Friedman LH, van der Giessen E, Needleman A. Discrete dislocation modeling in three-dimensional confined volumes. Mater. Sci. Eng. A-Struct. Mater. Prop. Microstruct. Process. 2001;309:420.

[96] Rhee M, Stolken JS, Bulatov VV, de la Rubia TD, Zbib HM, Hirth JP. Dislocation stress fields for dynamic codes using anisotropic elasticity: methodology and analysis. Mater. Sci. Eng. A-Struct. Mater. Prop. Microstruct. Process. 2001;309:288.

[97] von Blanckenhagen B, Gumbsch P, Arzt E. Dislocation sources and the flow stress of polycrystalline thin metal films. Philos. Mag. Lett. 2003;83:1.

[98] Zbib HM, de la Rubia TD, Bulatov V. A multiscale model of plasticity based on discrete dislocation dynamics. J. Eng. Mater. Technol.-Trans. ASME 2002;124:78.

[99] Bulatov VV, Cai W. Computer Simulations of Dislocations. New York: Oxford University Press, 2006.

[100] Arsenlis A, Cai W, Tang M, Rhee M, Oppelstrup T, Hommes G, Pierce TG, Bulatov VV. Enabling strain hardening simulations with dislocation dynamics. Model. Simul. Mater. Sci. Eng. 2007;15:553.

[101] Tsao JY, Dodson BW. Excess Stress and the Stability of Strained Heterostructures. Appl. Phys. Lett. 1988;53:848.

[102] Brown LM. The self-stress of dislocations and the shape of extended nodes Philosophical Magazine 1964;10:441.

[103] Zbib HM, Rhee M, Hirth JP. On plastic deformation and the dynamics of 3D dislocations. International Journal of Mechanical Sciences 1998;40:113.

[104] Cai W, Arsenlis A, Weinberger CR, Bulatov VV. A non-singular continuum theory of dislocations. J. Mech. Phys. Solids 2006;54:561.

[105] Liu XH, Schwarz KW. Modelling of dislocations intersecting a free surface. Model. Simul. Mater. Sci. Eng. 2005:1233.

[106] Hartmaier A, Fivel MC, Canova GR, Gumbsch P. Image stresses in a free-standing thin film. Model. Simul. Mater. Sci. Eng. 1999;7:781.

[107] Gomez-Garcia D, Devincre B, Kubin L. Dislocation dynamics in confined geometry. J. Comput-Aided Mater. Des. 1999;6:157.

[108] Groh S, Devincre B, Kubin LP, Roos A, Feyel F, Chaboche JL. Dislocations and elastic anisotropy in heteroepitaxial metallic thin films. Philos. Mag. Lett. 2003;83:303.

[109] Akasheh F, Zbib HM, Hirth JP, Hoagland RG, Misra A. Interactions between glide dislocations and parallel interfacial dislocations in nanoscale strained layers. J. Appl. Phys. 2007;102.

[110] Bulatov VV, Hsiung LL, Tang M, Arsenlis A, Bartelt MC, Cai W, Florando JN, Hiratani M, Rhee M, Hommes G, Pierce TG, De La Rubia TD. Dislocation multi-junctions and strain hardening. Nature 2006;440:1174.

[111] Schwarz KW, Cai J, Mooney PM. Comparison of large-scale layer-relaxation simulations with experiment. Appl. Phys. Lett. 2004;85:2238.

[112] Fertig RS, Baker SP. Threading dislocation interactions in an inhomogeneous stress field: a statistical model. In preparation 2008.

[113] Fertig RS, Baker SP. Relationship between film stress and dislocation microstructure evolution in thin films. In: LaVan D, Spearing M, Vengallatore S, Silva

Md, editors. Microelectromechanical Systems -- Materials and Devices, vol. 1052. Boston, MA: Mater. Res. Soc., 2007. p.DD07.

[114] Espinosa HD, Berbenni S, Panico M, Schwarz KW. An interpretation of size-scale plasticity in geometrically confined systems. Proceedings of the National Academy of Sciences of the United States of America 2005;102:16933.

[115] Friedman LH, Chrzan DC. Continuum analysis of dislocation pile-ups: influence of sources. Philos. Mag. A 1998;77:1185.

[116] Wang YU, Jin YM, Khachaturyan AG. Phase field microelasticity modeling of dislocation dynamics near free surface and in heteroepitaxial thin films. Acta Mater. 2003;51:4209.

[117] Xiang Y, Cheng L-T, Srolovitz DJ, Weinan E. A level set method for dislocation dynamics. Acta Mater. 2003;51:5499.

[118] Quek SS, Xiang Y, Zhang YW, Srolovitz DJ, Lu C. Level set simulation of dislocation dynamics in thin films. Acta Mater. 2006;54:2371.

[119] Thompson CV, Floro J, Smith HI. Epitaxial Grain-Growth in Thin Metal-Films. J. Appl. Phys. 1990;67:4099.

[120] Owusu-Boahen K, King AH. The early stages of plastic yielding in polycrystalline gold thin films. Acta Mater. 2001;49:237.

[121] Dehm G, Weiss D, Arzt E. In situ transmission electron microscopy study of thermal-stress-induced dislocations in a thin Cu film constrained by a Si substrate. Mater. Sci. Eng. A 2001;309-310:468.

[122] Dehm G, Arzt E. In situ transmission electron microscopy study of dislocations in a polycrystalline Cu thin film constrained by a substrate. Appl. Phys. Lett. 2000;77:1126.

[123] Martínez E, Marian J, Arsenlis A, Victoria M, Perlado JM. Atomistically informed dislocation dynamics in fcc crystals. Acta Mater. 2008;56:869.

[124] Vodnick AM, Nowak DE, Labat S, Thomas O, Baker SP. Out-of-plane stresses arising from grain interactions in textured thin films. In preparation 2009.

[125] Balk TJ, Dehm G, Arzt E. Parallel glide: Unexpected dislocation motion parallel to the substrate in ultrathin copper films. Acta Mater. 2003;51:4471.

[126] Schwarz KW. Local rules for approximating strong dislocation interactions in discrete dislocation dynamics. Model. Simul. Mater. Sci. Eng. 2003:609.

[127] Kukta RV. Observations on the Kinetics of Relaxations in Epitaxial Films Grown on Conventional and Compliant Substrates: A Continuum Simulation of Dislocation Glide Near an Interface. Division of Engineering. Providence, RI: Brown University, 1998. p.188.

[128] Weygand D, Friedman LH, Giessen EVd, Needleman A. Aspects of boundary-value problem solutions with three-dimensional dislocation dynamics. Model. Simul. Mater. Sci. Eng. 2002;10:437.

[129] Zbib HM, de la Rubia TD. A multiscale model of plasticity. International Journal of Plasticity 2002;18:1133.

[130] Bulatov V, Cai W, Fier J, Hiratani M, Hommes G, Pierce T, Tang M, Rhee M, Yates K, Arsenlis T. Scalable line dynamics in ParaDiS. IEEE/ACM SC2004 Conference - Bridging Communities, Nov 6-12 2004. Pittsburgh, PA, United States: Institute of Electrical and Electronics Engineers Inc., New York, NY 10016-5997, United States, 2004. p.367.

[131] Tang M, Cai W, Xu G, Bulatov VV. A hybrid method for computing forces on curved dislocations intersecting free surfaces in three-dimensional dislocation dynamics. Model. Simul. Mater. Sci. Eng. 2006;14:1139.

CHAPTER 3
DISLOCATION DYNAMICS SIMULATIONS OF DISLOCATION INTERACTIONS AND STRESSES IN THIN FILMS

R. S. Fertig[1], P. Pant[1], K. W. Schwarz[2], S. P. Baker[1]

[1]*Department of Materials Science and Engineering, Cornell University, Ithaca, NY 14853*

[2]*IBM Watson Research Center, P.O. Box 218, Yorktown Heights, NY 10598*

ABSTRACT – The dislocation interactions that stop threading dislocations (threads) during relaxation at increasing applied strains in single-crystal thin films are investigated using large-scale three-dimensional dislocation dynamics simulations. Threads were observed to stop via interactions with both threads and misfits. Both types of interactions were shown to be contingent on stress inhomogeneity in the film. Low stress regions in the film enabled threads to stop in weak thread-misfit interactions even at high average film stresses. Threads were concentrated in low stress regions, which facilitated their interaction with other threads. Threads were shown to accumulate in thread-thread interactions, and stop only temporarily in thread-misfit interactions. The mean free path for dislocation motion, a key factor in determining film strength and strain hardening, is shown to be well-predicted from details of the inhomogeneous stress state arising from the applied strain and the misfit structure. The behaviors of these threads are analyzed to present a more complete picture of film relaxation.

3.1 Introduction

Crystalline thin films on substrates are used in a wide variety of applications [1] including semiconductor devices, biomedical components, fuel cells, solar cells, and wear-resistant coatings. While the primary function of such films is often electrical or chemical, thin films often support stresses that can be an order of magnitude greater than could be supported by the corresponding bulk material [1-9]. These high stresses can lead to film failures [10, 11] in the form of fracture, delamination, creep, or void or hillock formation. Consequently, the mechanical behavior of thin films on substrates has been the subject of much study.

High stresses can only occur when plastic deformation is limited. If the grain size is large enough compared with the film thickness, as in epitaxial semiconductor or annealed metal films, plastic deformation occurs by the motion of threading dislocations, or "threads," that extend through the thickness as shown in Figure 3.1. In this case, high strength requires preventing thread motion, and understanding the strength of such films can be reduced to understanding what stops threads.

This problem has received much attention. In a homogeneous film, threads can be stopped by a thickness constraint, other dislocations, or grain boundaries. The thickness constraint is well-known [2, 12-16]. For a thread to move (Fig. 3.1), it must lay down misfit dislocations, or "misfits," at film/substrate and film/passivation interfaces; which is energetically favorable only if the strain energy relaxed by the moving thread is sufficient to create the misfits. This leads to a critical stress (or strain) for dislocation motion, referred to here as the channeling stress (σ_{ch}) (or strain (ε_{ch})) [17], which is proportional to the inverse of the film thickness [2, 12-16]. While the thickness constraint provides a lower limit on strength, it accounts for only a fraction of the scale dependent stresses in thin films [5, 18]. Grain boundaries are

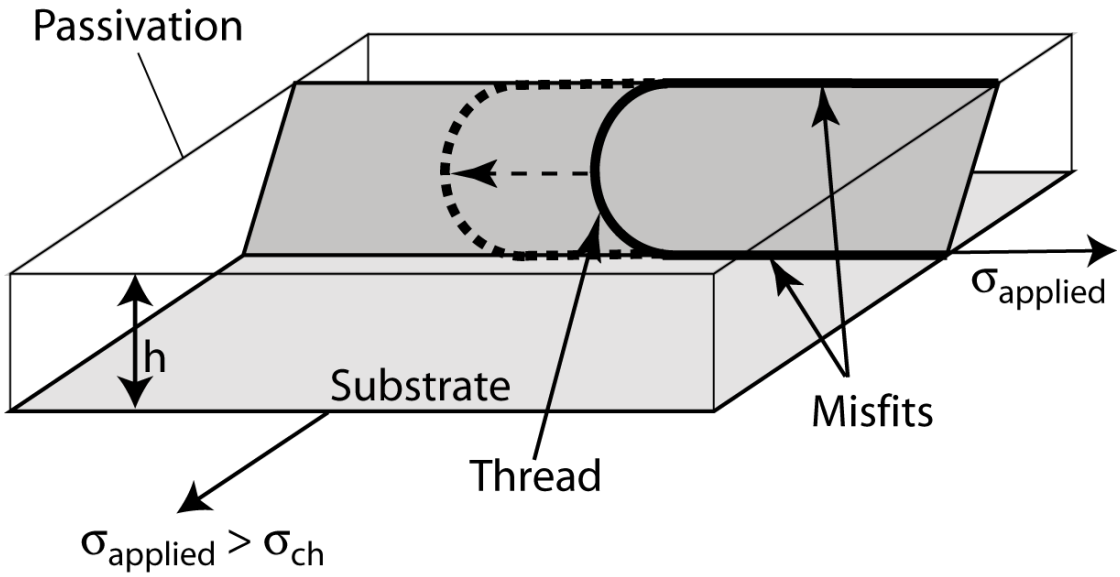

Figure 3.1. Stress relaxation in thin films occurs by motion of threading dislocations (threads), which extend through the film thickness. At applied strains greater than the channeling strain ε_{ch}, the thread advances, leaving misfit dislocations (misfits) at the interfaces.

expected to play a role in stopping dislocations in a polycrystalline film. This has been described elsewhere [19, 20] and will not be considered here. The present results apply strictly to single crystal films.

In the present work, we focus on the contributions of dislocation interactions to film strength. A moving thread may be stopped by interactions with other threads and misfits. The strength of each interaction is defined as the minimum remotely-applied biaxial stress required to cause the thread to break free of the interaction and continue moving through the film. Thus, a thread subject to a stress higher than σ_{ch} will move until it encounters an interaction strong enough to stop it, and, once stopped, will not move again until the local stress is raised above the interaction strength.

Initial efforts to understand how dislocation interactions contribute to film strength focused on the strength of dislocation interactions. We have reviewed these efforts elsewhere [9]. Several efforts have been made to determine the strength of "pairwise" interactions between the thread from one dislocation half-loop and the thread or the misfits from another. Both analytical calculations [16, 21] and more accurate discrete dislocation dynamics (DDD) simulations [22-25] showed that thread-misfit (TM) interactions are weak, with maximum strengths less than about $1.3\sigma_{ch}$ [22-25], much less than the observed strengths of films. However DDD simulations also showed that certain thread-thread (TT) interactions can be quite strong—more than an order of magnitude stronger than the strongest TM interactions [25] and much stronger than typical film stresses. But it is not clear from these studies how the overall film strength is determined from a distribution of interaction strengths.

Recently, much more detail has been obtained using DDD simulations to examine the behavior of ensembles of many dislocations in single-crystal films [26-29]. Schwarz conducted simulations [26] in which initial configurations of loops were allowed to run in response to a fixed applied strain. All of the predicted interactions

[22] were observed, with a significant fraction of threads annihilated or “immobilized” in strong interactions. The remaining threads became trapped in local stress fluctuations, providing a qualitative account of how threads are stopped. Schwarz [26] also noted that the amount of stress relaxation increased with increasing initial thread density. Other similar simulations [27, 28] showed that dislocation interactions can account for the relaxed stresses observed in heteroepitaxial strained semiconductors. Pant *et al.* simulated loading and unloading in thin Cu films as a series of stepwise relaxations [25]. They found stress levels and strain hardening rates that agreed closely with experimental data from Cu films; searched for, but did not find, more complex interactions (Lomer-locks were observed but did not appear to play a significant role in film strength); and characterized the stress fields as a function of dislocation density, showing that threads were indeed stopped in regions of low stress. Overall, the DDD results [22-28] show quantitatively that dislocation interactions alone can account for the stress levels in films and illustrate qualitatively many of the key features that determine dislocation behavior and strength in thin films. However, they have not shown how these factors interact to determine film strength.

Here, we present results of a study in which we used three-dimensional DDD simulations similar to those reported previously [19-25] to determine how strength of interactions and dislocation motion conspire to determine strength of thin films. A key insight in this work is that, since the strain in a film on a substrate arises from the constraint of the substrate, deformation takes place under strain control. The stress is determined by the amount of plastic relaxation, which is in turn determined by the number of mobile dislocations and the distance that each one moves. This can be thought of in terms of the canonical description of plastic strain,

$$\varepsilon_p \propto \rho_M b\bar{x}, \tag{3.1}$$

where ρ_M is the density of mobile dislocations, *b* the Burgers vector, and $\bar{x}$ the average distance that a dislocation travels. In this case, the interaction strengths determine ρ_M and the dislocation structure and applied stress determine $\bar{x}$.

Similar to Pant *et al.* [25], we model loading of a film as a series of stepwise relaxations. We quantify the dislocation interactions responsible for stopping threads as well as the stress field at each strain level. We show how the types of interactions stopping threads and the inhomogeneity of the stress field evolve in a coupled way with increasing plastic strain. The inhomogeneity of the stress field plays a critical role in film strength by permitting weak TM interactions to stop threads even when the average film stress exceeds their interaction strengths, and by facilitating strong TT interactions by concentrating threads in regions of low stress. These mechanisms determine the "mean free path" that a dislocation can travel before becoming trapped in a dislocation interaction. These concepts provide the first steps towards a predictive model of film strength based on dislocation interactions.

3.2. Discrete dislocation dynamics simulations

The three-dimensional discrete dislocation dynamics program PARANOID [30, 31] was used for our simulations. In this code, dislocations are discretized into tracking points connected by straight line segments. The glide force on each tracking point is calculated by summing the applied stress, the stresses due to other dislocations, and the self-stress of the dislocation due to curvature [30]. The self-stress is calculated using a modified Brown splitting procedure, which ensures convergent results for arbitrarily small dislocation segments. This allows regions of a dislocation with high curvature or close proximity to other dislocations to be finely discretized at each time step to accurately model the behavior. At every time step, each dislocation

tracking point is moved a distance corresponding to a velocity that is proportional to the glide force, and the dislocation is then rediscretized.

An infinite, 200 nm thick, fcc, single-crystal film with (001) planes parallel to the film plane was simulated using a periodic unit cell with in-plane dimensions of 4 μm × 4 μm. Figure 3.2 shows a section of the simulated film in plan view with a shaded periodic unit cell in the center. The dashed lines represent the intersection of selected slip planes with the film surface. In the simulation, a dislocation that exits the periodic unit cell at point A re-enters at point B on the other side, corresponding to a dislocation entering from the neighboring cell. To minimize the effects of the periodic boundary conditions, slip plane traces were rotated 5.7º with respect to the cell boundaries, forcing the minimum spacing between the misfits generated by a thread that traverses a unit cell more than once to be about 400 nm.

The film was modeled as a thin layer in an infinite solid with boundaries that are impenetrable to dislocations at the top and bottom of the film. This configuration approximates a passivated film on a substrate, where both passivation and substrate have the same elastic properties as the film. Isotropic material properties of copper were used with shear modulus μ = 42.3 GPa, Poisson ratio ν = 0.3, and Burgers vector b = 0.255 nm. Using these values, the channeling strain and stress in the simulation were found to be $\varepsilon_{ch} = 1.55 \times 10^{-3}$ and σ_{ch} = 178.4 MPa, respectively. These are in excellent agreement with values obtained from equations presented by Freund [15] for a passivated 200 nm thick (001) Cu film using $b/2$ as the dislocation core cutoff radius.

Initially, the periodic unit cell was seeded with 70 randomly-located dislocation glide loops, which supplied 140 threads. Each loop was randomly assigned to one of the eight primary slip systems that can relax a biaxial strain in a (001) film. An equal biaxial strain was applied to this configuration, beginning with $1.3\varepsilon_{ch}$, and was

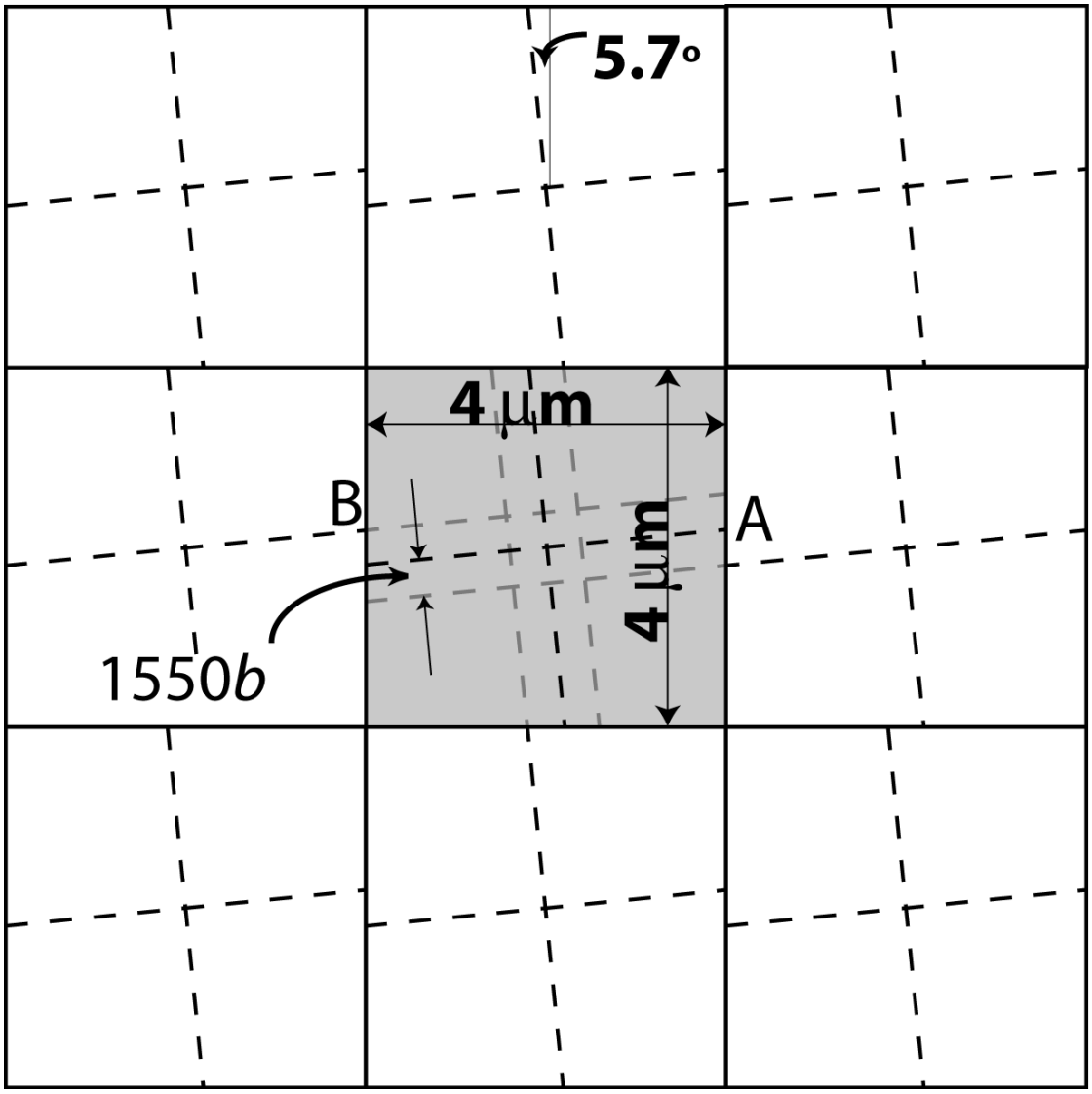

Figure 3.2. Plan view of the simulated film showing the periodic unit cell repeated 9 times. A dislocation leaving the shaded cell at point A re-enters the shaded cell at point B.

increased incrementally in steps of $0.5\varepsilon_{ch}$ to $3.3\varepsilon_{ch}$. After each strain increment, some threads in the film moved. The strain was held constant at each strain level until every thread stopped moving. The resulting configuration was thus a relaxed configuration. The relaxed configurations were analyzed to determine the types of dislocation interactions that stopped each thread. Film stresses were calculated for each relaxed configuration. The stresses were calculated at the film midplane on points of a 125 × 125 element grid, which corresponds to a point spacing of 32 nm.

To quantitatively study the types of interactions that stop threads, we defined several categories of dislocation interactions. Figure 3.3 shows segments of a simulation cell showing examples of these different types of interactions. Following Pant *et al.* [25], interactions were divided into thread-thread (TT) and thread-misfit (TM) interactions. Each category was further subdivided into annihilating and non-annihilating interactions. A thread-thread annihilation (TTA) interaction occurs when two threads on intersecting glide planes with opposite Burgers vectors come together and annihilate, removing both threads from the system. The dashed line in Fig. 3.3a shows the intersection of two slip planes where two threads annihilated in a TTA interaction. TTA interactions have unlimited interaction strength because the involved threads obviously cannot continue moving.

We define a non-annihilating thread-thread (NATT) interaction as the case where two threads stop within one-half of the film thickness of each other, as measured at the midplane of the film. This interaction is either a junction between threads on intersecting slip planes, an interaction between threads on nonparallel slip planes but with parallel misfits, or a dipole formed by threads on parallel slip planes. Fig. 3.3a shows a NATT junction that occurred along the intersection of slip planes. The strength of a NATT interaction depends on the Burgers vectors of the threads

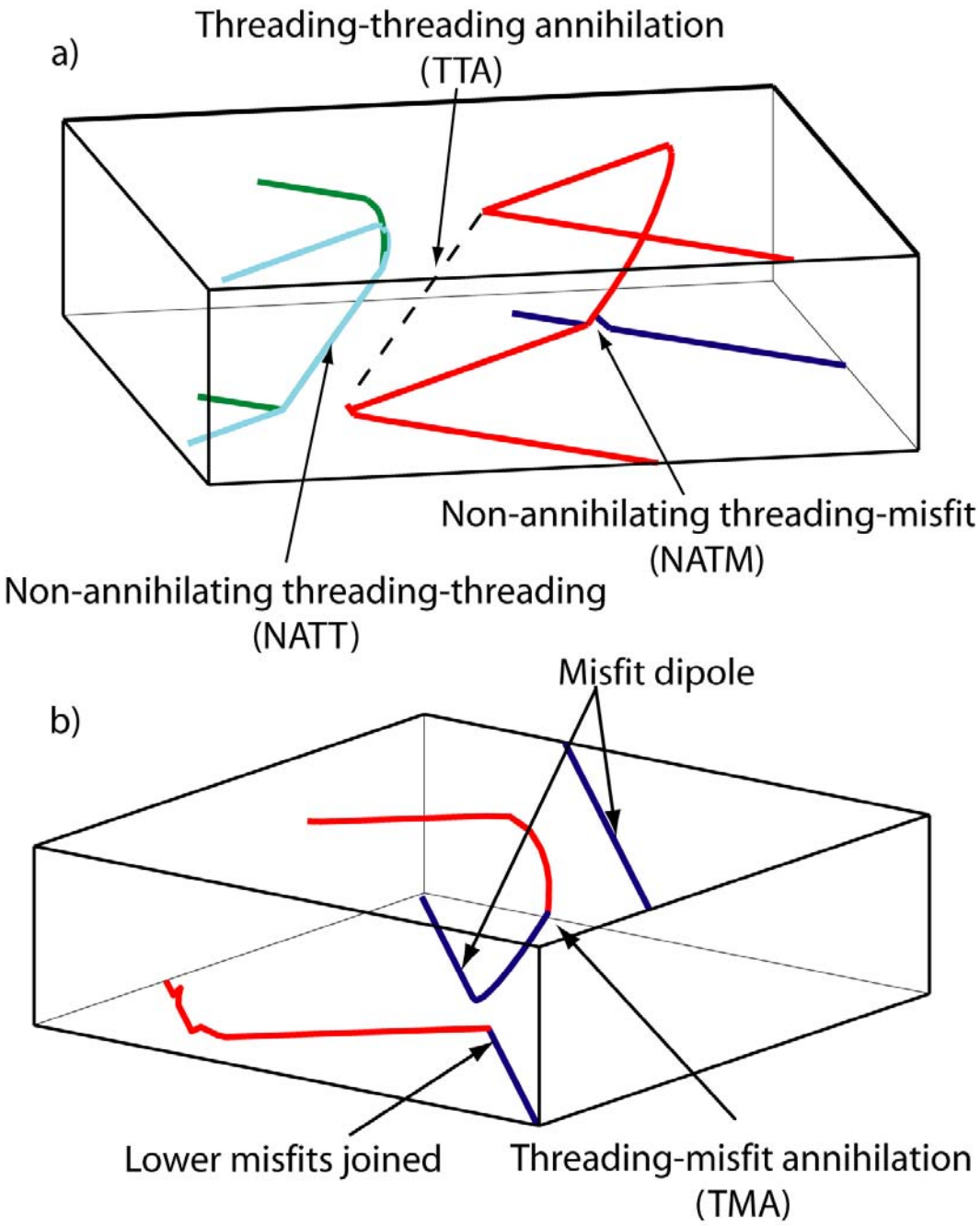

Figure 3.3. Examples of dislocation interactions from the simulation. a) The thick solid line shows a NATT interaction, and the dashed line a TTA interaction along the intersections of slip planes. The junction between a thread and misfit is an example of a NATM interaction. b) A TMA interaction creates a thread that exists on two different slip planes.

involved. For (111) films, some have been shown to be an order of magnitude stronger than any TM interaction [25], significantly higher than observed film stresses.

Thread-misfit interactions are similarly divided. The thread-misfit annihilation (TMA) interaction, illustrated in Fig. 3.3b, is one of the strongest TM interactions, with an interaction strength of about $1.2\sigma_{ch}$ for 800 nm thick films [25]. This interaction is described in greater detail elsewhere [25, 32]. Briefly, it occurs when a portion of a misfit moves away from the interface to align and annihilate with part of an approaching thread. In (001) films, one of the misfits left behind by the thread joins with the crossing misfit to form a right angle due to their perpendicular slip traces. The other misfit left behind by the thread then connects to the remaining part of the crossing misfit, creating a thread that exists on two different slip planes and can move on either, given an appropriate stress.

The non-annihilating thread-misfit (NATM) interactions consist of the remainder of interactions not classified into any previous categories, with strengths ranging from $1.0\sigma_{ch}$ to $1.2\sigma_{ch}$ for 800 nm films [25]. One type of NATM interaction is shown in Fig. 3.3a.

3.3. Results and Analysis

In this section, we first present the dislocation configurations, average film stress, and dislocation densities from the simulations. We then detail the types of interactions that stopped threads at each of the applied strain levels. Next, we examine the inhomogeneous nature of the film stress and the manner in which it evolved with increasing plastic strain. Finally, we correlate the inhomogeneous stresses with the dislocation interactions.

3.3.1. General results

Following each strain increment, threading dislocations moved through the film, laying down misfit dislocations that relaxed the applied strain. Threads moved until they either encountered an interaction that was strong enough to stop them or the stress was relaxed below σ_{ch}. Plan views of the relaxed structures at applied strains of 1.3, 1.8 and 3.3 ε_{ch}, are shown in Figures 3.4a, b, and c, respectively. Figure 3.4d shows a side view of the same structures, with the thickness direction stretched for better viewing. The different colors correspond to different Burgers vectors. Examples of TM and TT interactions are highlighted by squares and circles, respectively. In Fig. 3.4a, the leftmost square encloses a TMA interaction and the right square a NATM interaction. Both circles enclose NATT interactions, with the top circle showing a junction and the bottom circle a dipole. Consistent with the idea of a range of interaction strengths, some threads never moved out of their initial interactions even after subsequent increments in strain. Other threads broke free from their interaction at every strain increment. For example, the threads involved in the TT interaction circled at the top of Figures 3.4a, b, and c remained in this interaction throughout all loading increments, whereas the thread dipole highlighted by the lower circle did not remain past the first increment. None of the boxed TM interactions remained for even one subsequent loading increment.

As an initial approach to understanding how the dislocation structures shown in Fig. 3.4 are related to film strength, it is instructive to compare these with the average stresses in the film as might be measured in an x-ray [33] or substrate curvature [7] experiment. Figure 3.5 shows the average biaxial stress (circles) and dislocation density (diamonds) calculated for each of the relaxed dislocation structures. The stresses and strains are normalized by the channeling stress and strain, respectively.

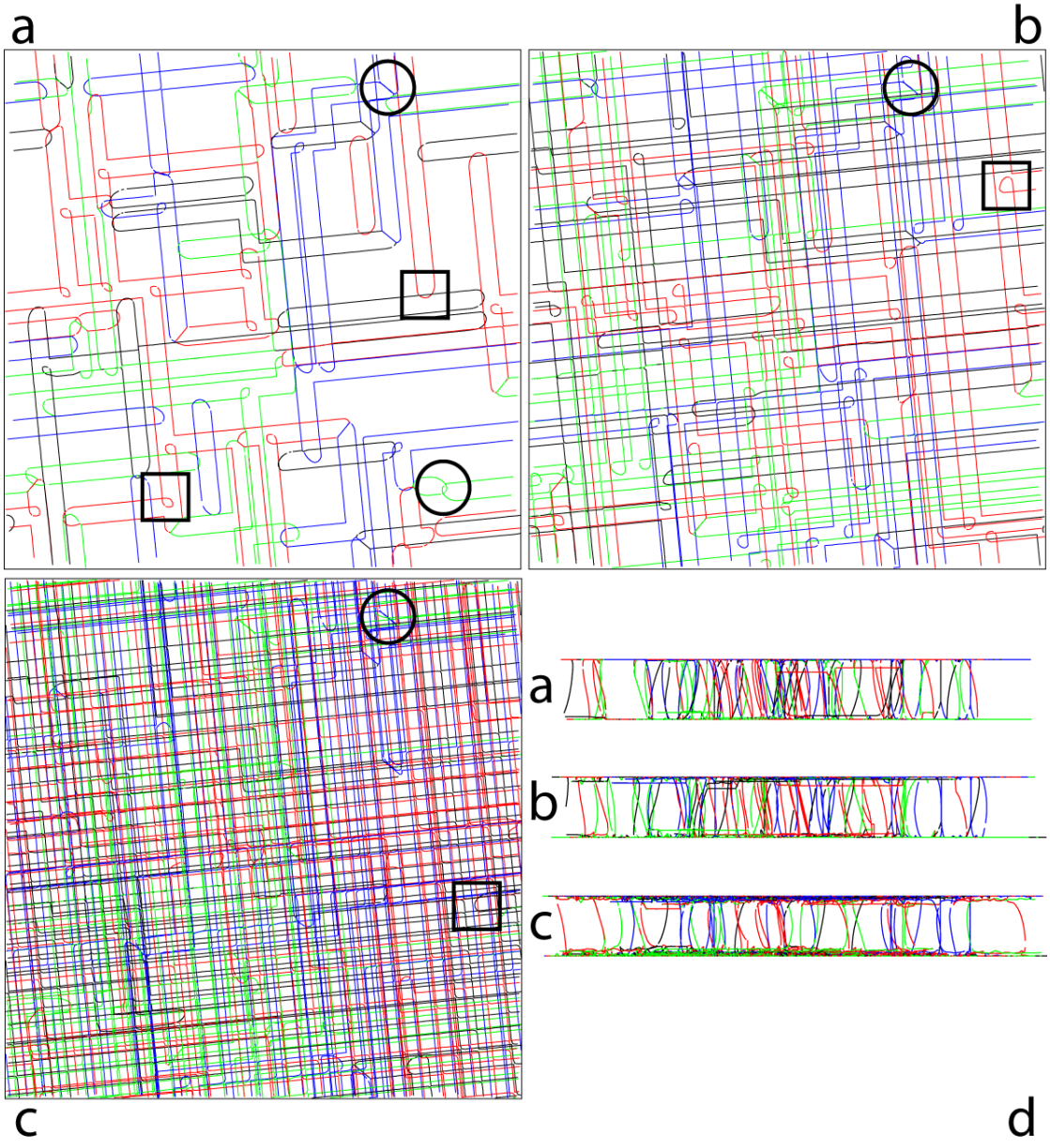

Figure 3.4. Equilibrium dislocation structures with circles highlighting TT interactions and squares highlighting TM interactions after loading to a) 1.3ε_{ch}, b) 1.8ε_{ch}, and c) 3.3ε_{ch}. d) Side views of these configurations.

.

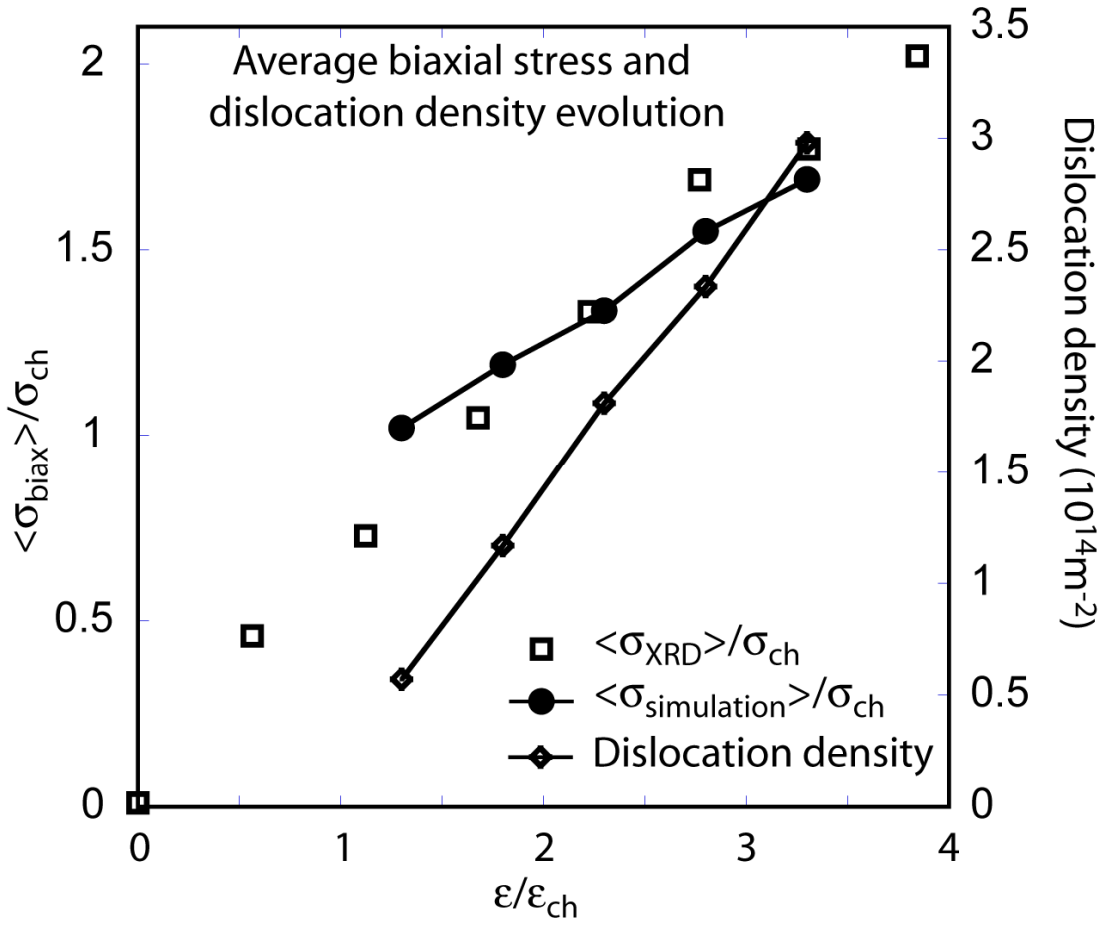

Figure 3.5. Average biaxial film stress, $<\sigma_{biax}>$, as a function of applied strain, ε, normalized to the channeling stress and strain, respectively. Filled circles depict simulation results. Open squares show stresses obtained from synchrotron X-ray diffraction data for the (001) texture component in a 500 nm passivated polycrystalline Cu film [34]. Note the agreement between both absolute stresses and strain hardening rates. Dislocation density in each relaxed configuration from the simulations is also shown (open diamonds).

For comparison, normalized stresses obtained from synchrotron x-ray diffraction measurements of (001) grains in a 500 nm thick passivated polycrystalline Cu film are also shown (squares) [34]. The average film stresses for both the simulation and the real film are observed to exceed the maximum strength of a TM interaction of $1.3\sigma_{ch}$by a considerable margin. The relaxed stress from the simulations varies linearly with the applied strain with a slope of $0.34Y$, where Y is the biaxial modulus [2]. The stress strain relationship for the experimental data is also linear, with a slope of $0.47Y$. The dislocation density from the simulations also varies linearly with the applied strain. The maximum dislocation density of about 3×10^{14} m^{-2} at $3.3\varepsilon_{ch}$ is more than an order of magnitude greater than the starting density of 2.7×10^{13} m^{-2} and is due entirely to an increase in misfit density, since no new threads were nucleated. The smooth increase in dislocation density is somewhat surprising given the highly irregular misfit structure shown in Fig. 3.4(a-c).

It is easy to see from Figures 4 and 5 that the strength of a film cannot be simply related to the strength of dislocation interactions. In particular, despite the fact that the average biaxial stress (Fig. 3.5) during the final three loading increments exceeded the strength of *any* TM interaction, TM interactions were observed to stop threads at even the highest level of applied strain. In fact, all types of interactions were observed stopping threads in the relaxed structures at all applied strain levels. This raises the question: why are threads stopped by TM interactions when the average film stress exceeds their interaction strengths? To answer this question, we need a better understanding of both the types of interactions that stop threads and the stress state at each strain step.

3.3.2. Dislocation interactions

We first look at the types of interactions that stopped threads at each strain step. Because not all threads moved during every strain increment, we differentiate between the threads that moved during a particular load increment, which we call *mobile* threads, from those that did not, which we call *static* threads. For example, at $1.3\varepsilon_{ch}$, all 140 threads moved some distance because none were involved in interactions before the application of strain. Thus all threads were mobile during the $1.3\varepsilon_{ch}$. They stopped moving due to the interactions shown in Fig. 3.4a. The increment in strain to $1.8\varepsilon_{ch}$ caused 85 of these threads to break free from the interaction that had stopped them at $1.3\varepsilon_{ch}$. The 85 threads that moved were termed *mobile* threads for the $1.8\varepsilon_{ch}$ strain increment. The 55 threads that did not move during that strain increment were termed *static* threads for the $1.8\varepsilon_{\mathrm{ch}}$ strain increment. Each thread was evaluated to determine if it was mobile or static during each strain interval.

Figure 3.6 shows the fraction of the initial 140 threads that were *static* during each load increment and the types of interactions that made the threads static. (Because there were no static threads at $1.3\varepsilon_{ch}$, this increment is not plotted.) The data show that threads tend to accumulate in the stronger TT interactions and, once in these interactions, do not easily break free. Thus, the number of static threads increases with increasing strain and these threads are static almost entirely because of TT interactions. (The apparent decrease at $>3.3\varepsilon_{ch}$ appears because no further increment was simulated to determine which of the interactions besides TTA interactions were static.) TM interactions play only a small role in making threads static. TT interactions thus act to permanently reduce the density of mobile threads. Figure 3.7 shows the number of mobile threads during each strain increment. At a strain of $3.3\varepsilon_{ch}$, the number of mobile threads was reduced by nearly 65%. Of course, the number of

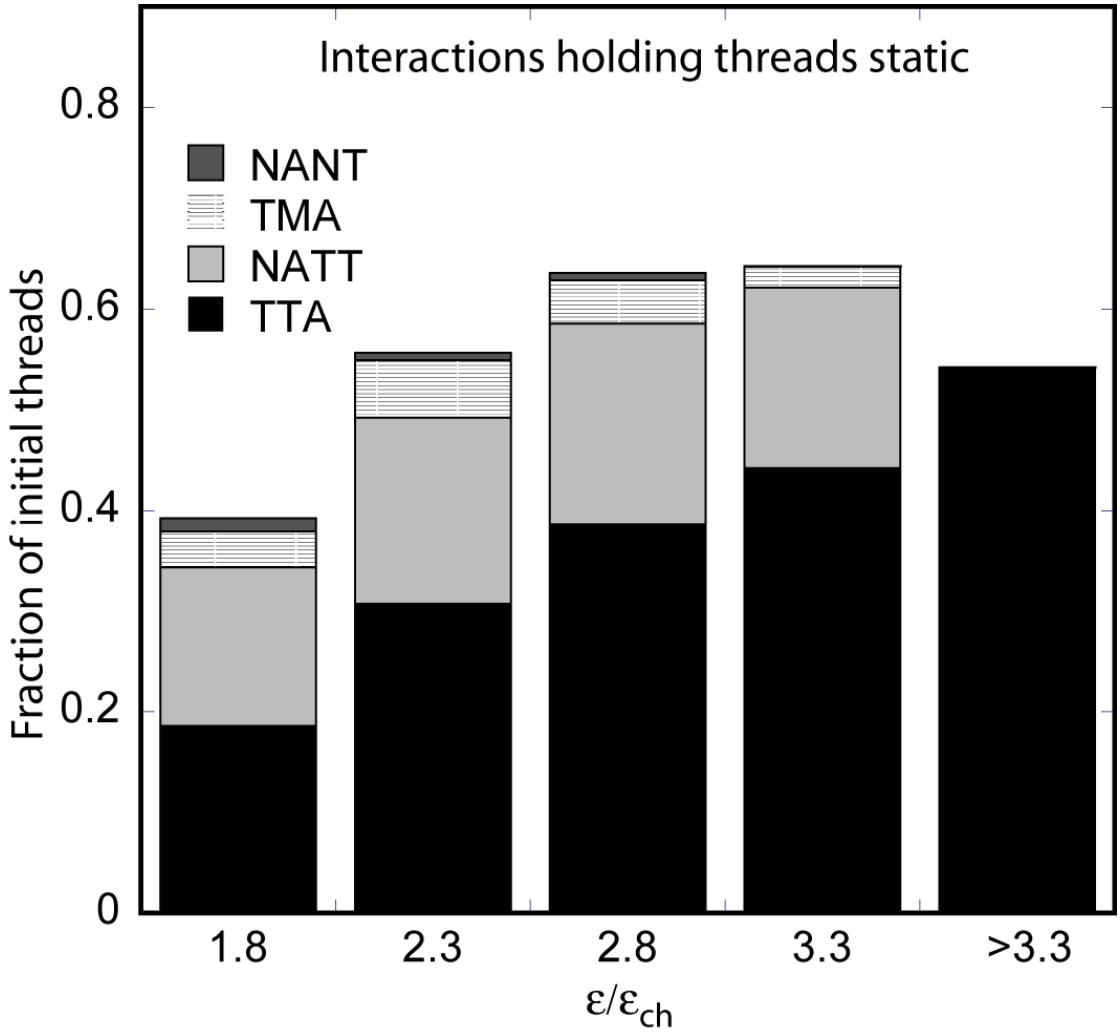

Figure 3.6. Fraction of total threads (140) made static by each interaction type at each equilibrium configuration. Strong TT interactions hold threads, preventing them from participating in further relaxation at higher strains.

.

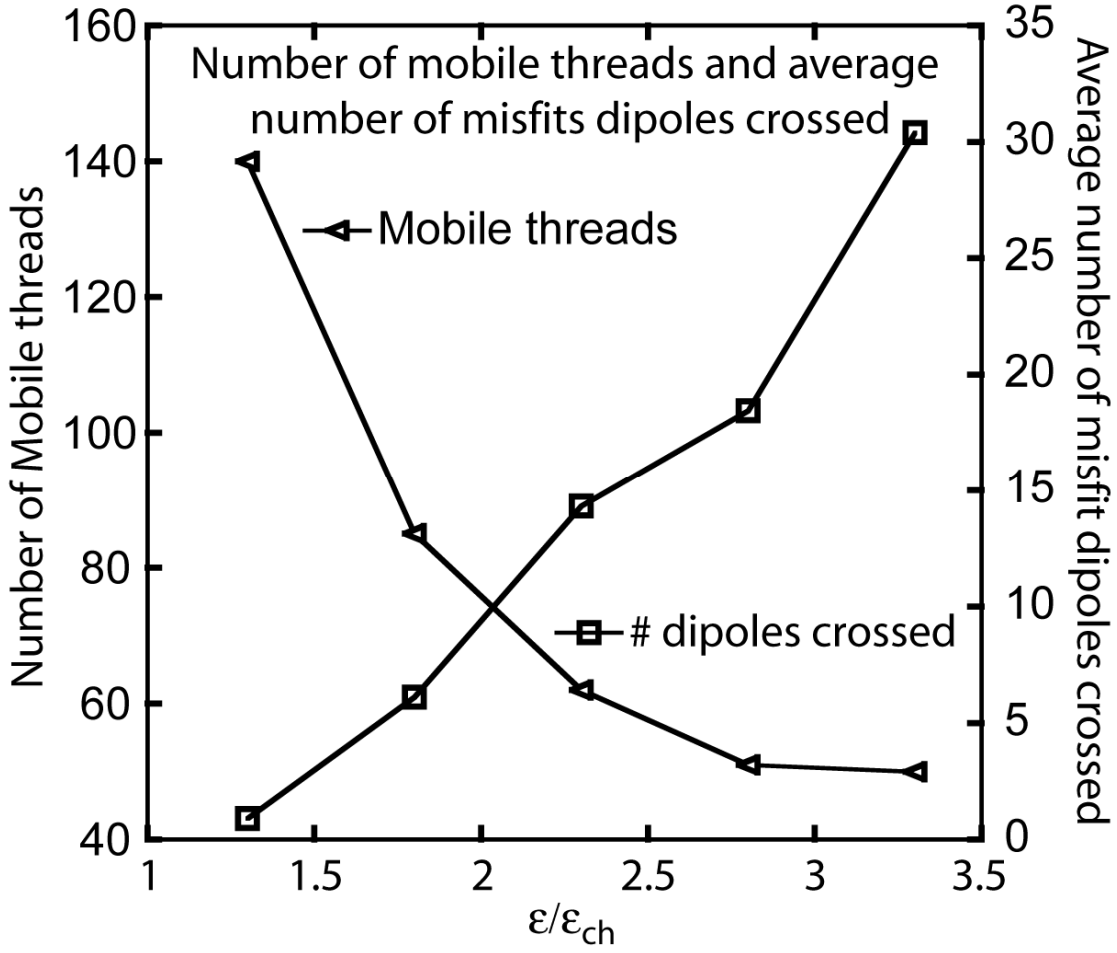

Figure 3.7. Number of mobile threads at each applied strain level and the average number of misfits crossed by a thread during each load increment. The number of mobile threads constantly decreases due to thread annihilation and other strong interactions, which prevent threads from moving under subsequent strain increments.

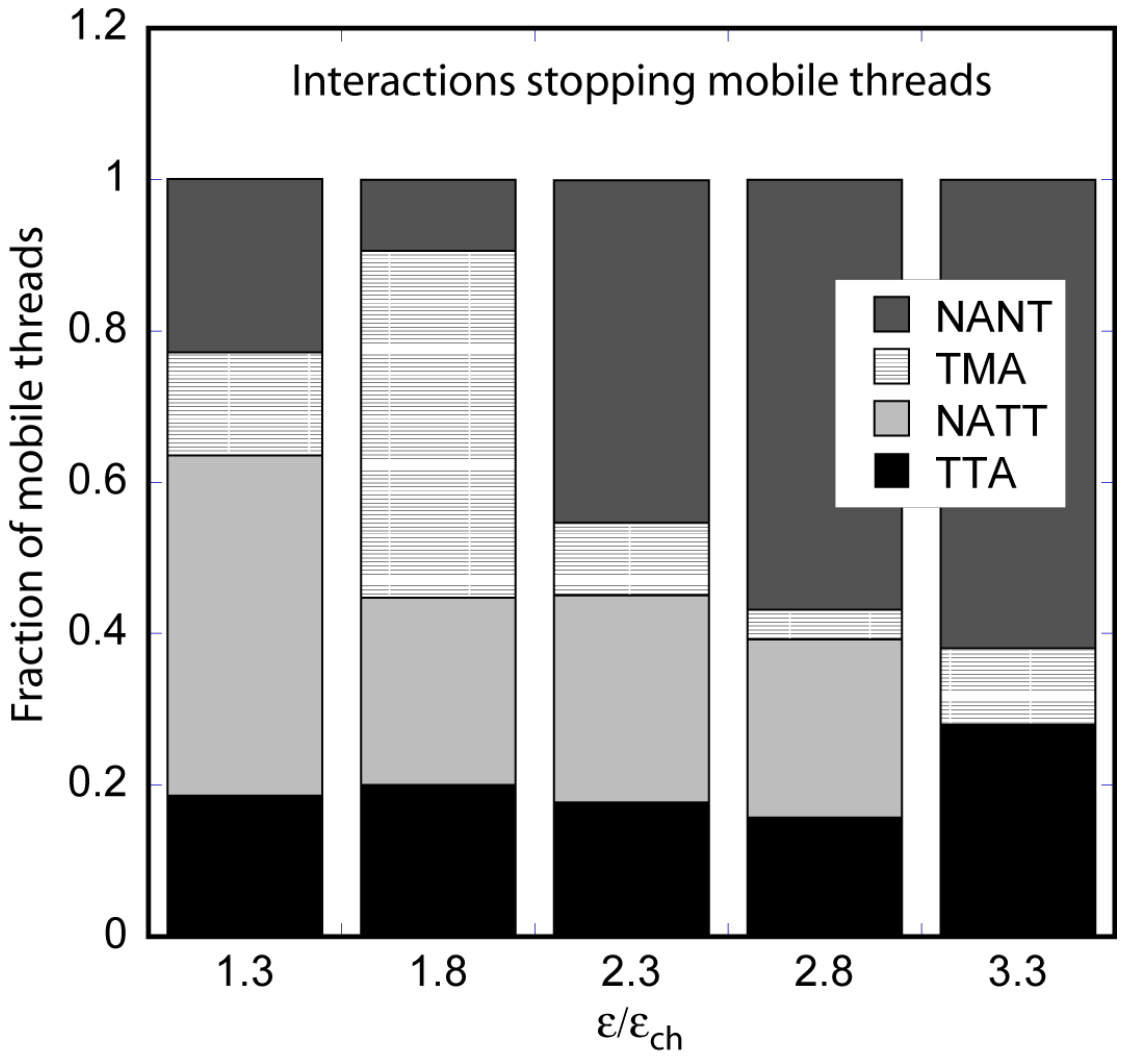

Figure 3.8. Fraction of each interaction type stopping mobile threads at each load increment.

threads held “static” by TTA interactions always increases because an annihilated thread no longer exists and clearly can never move again. This can be qualitatively observed in Figure 3.4d where fewer threads are observed at $3.3\varepsilon_{ch}$ than at $1.3\varepsilon_{ch}$. Fig. 3.7 also shows that as the misfit density increases and the number of mobile threads decreases with increasing applied strain, each mobile thread crosses more and more misfit dipoles before stopping.

Corresponding to Figure 3.7, Figure 3.8 shows the fraction of *mobile* threads stopped by each interaction type after each strain increment. The dominant interactions that stopped mobile threads were more varied than the interactions holding threads static. In contrast to the interactions holding threads static, which were primarily TT interactions, these data indicate that *both* TM and TT interactions play an important role in stopping mobile threads at *all* strain levels.

Two counterintuitive results emerge from the data shown in Fig. 3.8. First, at low film stress (relaxed stresses less than $1.3\sigma_{\text{ch}}$—applies to films loaded to 1.3 and $1.8\varepsilon_{\text{ch}}$, see Fig. 3.5), one might expect TM interactions to stop the majority of mobile threads since their interaction strengths are sufficient to do so and each thread crosses several misfits; see Fig’s 4a, 4b, and 7. Instead TT interactions are dominant. This was primarily because weak thread-thread dipoles and weak junctions were able to form at low strain. These dipoles and weak junctions did not play significant roles in stopping threads after the first strain increment. The second counterintuitive result is the presence of TM interactions at high strain. Not only do TM interactions exist when the average film stress exceeds their interaction strengths, as mentioned above, but they are the *dominant* interaction stopping mobile threads at these strain levels. On average, threads were observed to cross many misfit dipoles (~30) before being stopped (Fig. 3.7). This suggests that the controlling factor in stopping threads was the local stress landscape, not the mere existence of a misfit dipole.

3.3.3. Stress inhomogeneity

We now look more carefully at local film stresses to highlight the link between stress inhomogeneities and dislocation interactions. Figure 3.9a shows the local resolved shear stress on the $(1\,\bar{1}\,1)[0\,1\,1]$ slip system at the film midplane in the relaxed structure at $3.3\varepsilon_{ch}$. The irregular misfit structure gives rise to strongly inhomogeneous stresses, ranging from about 0.4 to $3.0\,\tau_{ch}$, where τ_{ch} is the channeling stress resolved onto an active slip system. Figure 3.9b shows distributions of the resolved shear stress averaged over the active slip systems in the relaxed configurations. These data show that even at the highest applied strain ($3.3\varepsilon_{ch}$) there are still local regions in the film with stresses below the strength of a TM interaction. The data also show that the stress distribution becomes normally distributed and that the standard deviation increases with increasing applied strain. These results demonstrate that the stress felt by any single thread is not described well by the average film stress. Consequently, to understand film relaxation, we must understand the relationship between local stress fluctuations and dislocation interactions.

The correlation between local stresses and interaction locations is illustrated in Figure 3.10a, which shows the radial-averaged resolved shear stress landscape around a thread, averaged over all threads, as a function of radial distance from the thread. The values plotted in Fig. 3.10a represent the deviation from the mean resolved shear stress, normalized by the standard deviation. Threads stopped in regions where the stress was about one standard deviation lower than the average film stress at all applied strains. To determine differences between TM and TT interactions, we examined each separately. Figures 10b and 10c show resolved shear stresses normalized by the standard deviation for threads stopped in TT interactions and those stopped in TM interactions, respectively. The threads stopped by TM interactions are

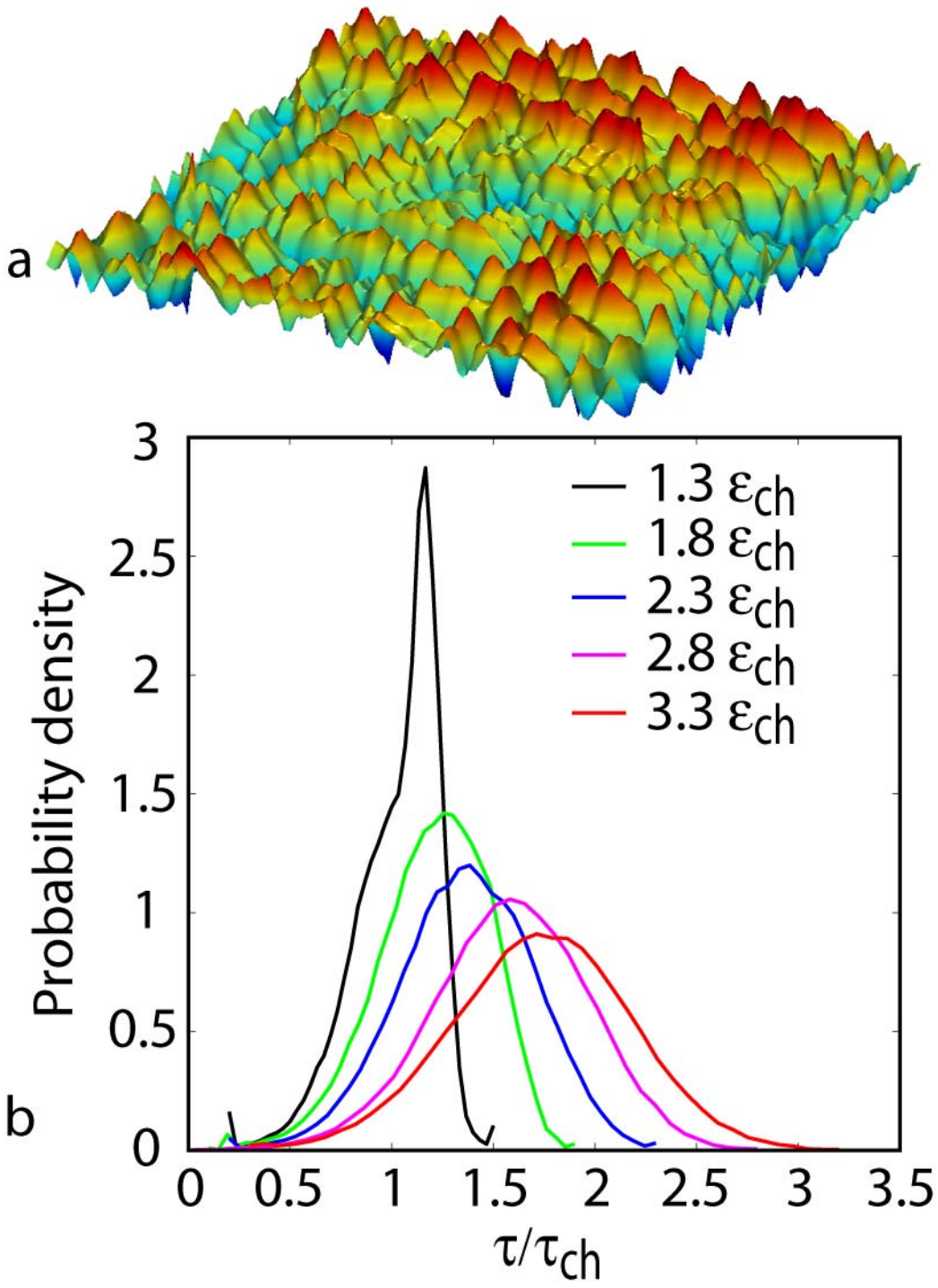

Figure 3.9. a) Average biaxial stress calculated at the midplane of the film at an applied strain of 3.3ε_{ch}. b) Probability distribution of resolved shear stresses averaged over the active slip systems in the relaxed configurations.

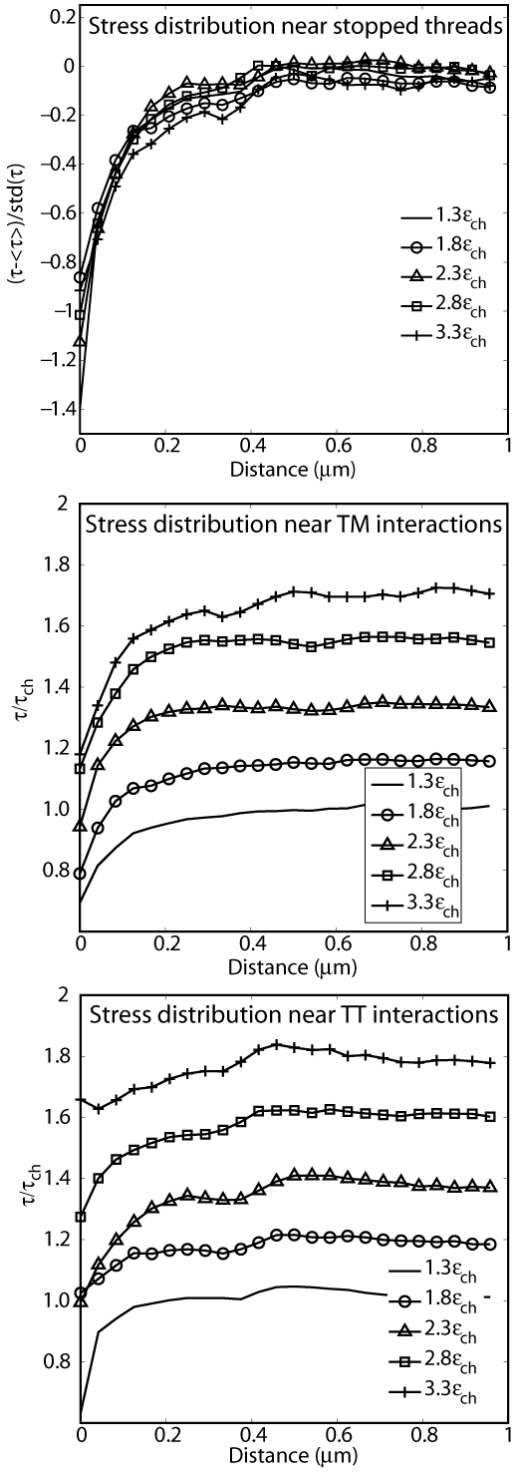

Figure 3.10. Average resolved shear stresses around a thread as a function of radial distance from the thread for a) all threads (deviation from mean, normalized by standard deviation), b) TT interactions, and c) TM interactions.

stopped at local stresses less than the greatest TM interaction strength of $1.3\sigma_{ch}$. Thus, even if the average film stress is higher than the TM interaction strength, a thread may still be stopped by a TM interaction in a region of low stress. The threads in TT interactions are also stopped in regions of lower stress, although, consistent with the higher interaction strengths of these interactions, the average stresses around a thread in a TT interaction are higher than those around one in a TM interaction. However, TT interactions are strong enough to stop threads regardless of where they occur. So why do they occur in regions of low stress? The prevalence of TT interactions in low stress regions suggests that threads are being concentrated by stress fluctuations. The likelihood of TT interactions is higher in these regions because the local thread density is greater there, a result which was recently verified using cellular automata simulations [35]. Thus, stress inhomogeneity in the film facilitates not only TM interactions, but also TT interactions.

3.4. Discussion

The simulations presented above suggest that the strength of a ductile single crystal film is determined not only by the strengths of dislocation interactions, but also by the spatially inhomogeneous stress field that develops as the misfit dislocation structure evolves. Given the range of dislocation interaction strengths, the inhomogeneous stress field plays a significant role in determining both the number of mobile dislocations and the distance that each one travels. Weak TM interactions ($\sigma_{\mathrm{ch}} < \sigma_{\mathrm{TM}} < 1.3\sigma_{\mathrm{ch}}$) and strong TT interactions ($\sigma_{\mathrm{film}} < \sigma_{\mathrm{TT}}$) are found to play distinct roles. Stress fluctuations allow TM interactions to stop threads even when average film stresses exceed TM interaction strengths, and provide an upper bound to the distance that a dislocation can travel between regions of low stress. In addition, stress

fluctuations increase the likelihood of strong TT interactions by concentrating threads in regions of low stress. These interactions can permanently prevent the involved threads from being mobile at higher stresses and thus control the mobile dislocation density. In other words, the inhomogeneities in the stress field influence both the mobile dislocation density, ρ_M, and the average distance that dislocations can travel, $\bar{x}$, in Equation 3.1.

These observations suggest that it is possible to develop new models of film strength by considering both the strength of thread-stopping interactions and the inhomogeneity in the stress field. In the following sections we take the first steps towards such a model by using the simulation data to describe the distance that dislocations travel before being stopped at various load steps. We also consider the sensitivity of the results to the simulation parameters and the application of this type of model to real films.

3.4.1. Emerging picture of thin film relaxation and strain hardening

During relaxation, a thread will move to relax the film stress if the resolved shear stress on the thread exceeds both the channeling stress and the strength of any interaction that is currently stopping it. As the thread moves, the misfit dislocation structure evolves, relaxing the average film stress and giving rise to an aperiodic, spatially inhomogeneous stress field. When a mobile thread is involved in either a TT or TM interaction, it will stop if the interaction occurs in a local region of stress lower than the strength of the interaction.

To understand the strength of films, it is necessary to understand how far mobile threads travel before becoming immobilized in TM or TT interactions. Our simulations showed that during a particular relaxation step, mobile threads stopped

preferentially in regions of low stress (Fig. 3.10). However, a fundamental distinction exists between "strong" TT interactions and TM interactions. We define strong TT interactions as those with interaction strengths that are greater than the stress in the film. Although, TT interactions range in strength from σ_{ch} to ∞, weak NATT interactions (weak junctions and thread dipoles) were significant only during the first relaxation step (1.3 ε_{ch}). During this step, the dislocation structure was artificial, with 140 initial threads and no deposited misfits, permitting an unrealistically large number of weak NATT interactions to occur. During the rest of the simulations these weak NATT interactions do not play a significant role and we neglect them.

By definition, strong TT interactions do not *require* a low stress region. In contrast, TM interactions can occur *only* in regions where the stress is below about $1.3\sigma_{ch}$. Thus, the factors controlling the distance that a thread travels before being stopped in a TM interaction are expected to be different from those controlling the distance that a thread travels before stopping in a TT interaction. The distance that a thread travels before stopping in a TM interaction will be directly dependent on the average film stress and magnitude of the stress fluctuations. In contrast, the distance traveled by a thread before stopping in a TT interaction will depend on these quantities only implicitly, through their effect on the probability that a TT interaction will form.

3.4.1.1. Thread-Misfit interactions and dislocation mean free path

The distance that a thread can travel before being stopped in a TM interaction must be related to the spacing of the low stress regions in the film. This is illustrated in Fig. 3.11, which shows the local resolved shear stress on an active $\{111\}\langle\bar{1}10\rangle$ slip system along a straight line through the center of the film at the midplane at an applied strain of $3.3\varepsilon_{ch}$. The dashed line is the average biaxial film stress, and the shaded area

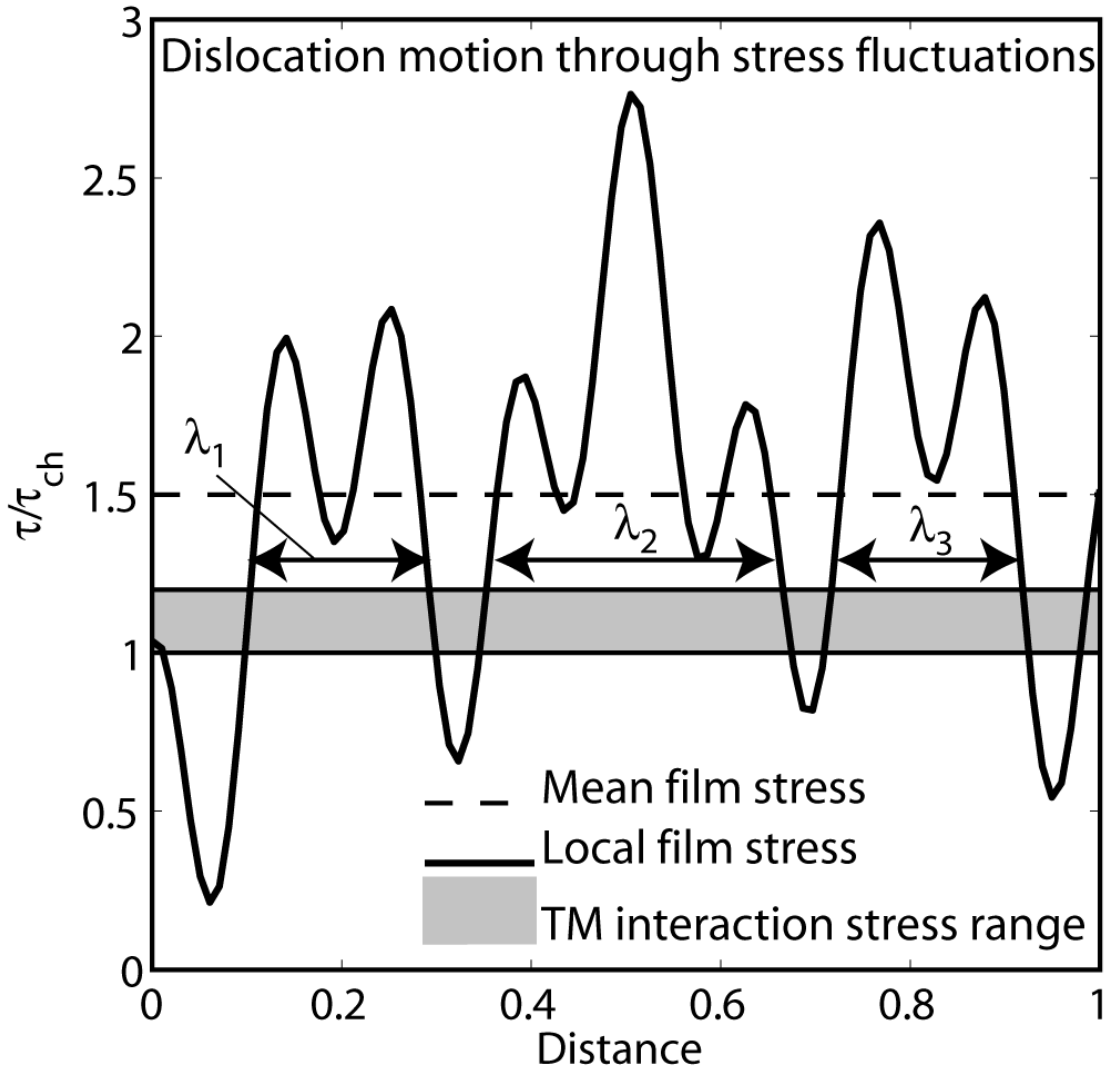

Figure 3.11. Stress fluctuation schematic. A dislocation may move when it is in a region of where the stress is above the shaded line.

represents the range of TM interaction strengths. A thread moving through the field cannot be stopped by a TM interaction unless the interaction occurs where the local stress is within this shaded region. Thus, the average distance that a thread travels before stopping in a TM interaction is related to the length of a mean free path λ in which the stress is always greater than the TM interaction strength. Because the film stress is relaxed by a misfit dipole, the likelihood of a misfit lying in the region of low stress is quite high. If we assume that an appropriate misfit exists wherever the stress dips below the interaction strength, then a thread would not be able to pass though any such region. The average distance d that a thread is expected to travel during the relaxation step before stopping at a TM interaction is then $d = \langle \lambda \rangle / 2$. Because the thread may also be stopped by TT interactions before traveling this distance, d represents the *upper* limit of the average distance that a thread will travel before stopping. (Note that the mean free path defined in this manner is only pertinent to stopping by TM interactions.)

The average mean free path, $d = \lambda/2$, was calculated from the stress distributions determined from the simulations, such as the one shown in Fig. 3.11, and was compared to the actual mean distance d_m traveled by threads in the DDD simulations during each relaxation step (Table 3.1). Because the stress field is continuously changing during relaxation at each strain step, the mean free path continuously changes as well. However, upper and lower bounds can be determined. The upper bound on the mean free path was calculated immediately after the strain increment but before any dislocations started moving, using the lowest TM interaction strength of τ_{ch}. The lower bound was calculated after dislocation motion had stopped, at the end of the strain increment, assuming the highest TM interaction strength of $1.3\tau_{ch}$. A rough estimate of the predicted average distance that a thread would travel during each relaxation step was obtained by averaging the upper and lower bounds. In Figure 3.12,

we compare this predicted average distance (dashed curve) with the actual distances from our simulations (squares). The solid curves represent the upper and lower bounds. We observe that our stress fluctuation model correctly bounds the distance traveled, and that the average of the bounds is in good agreement with the actual distance traveled. This is consistent with the idea that the stress inhomogeneity and TM interactions determine an upper bound on the average distance that a thread travels. Note that this is an upper bound because TT interactions also occur. Thus, the actual distance dislocations travel could be shorter. Since *d* describes the mean freepath well, this indicates that the threads stopped by TT interactions must travel roughly the same distance as those stopped by TM interactions. However, this is not a general result because the distance that a thread travels before stopping in a TT interaction depends on thread density [26], *e.g.* our choice of starting thread density.

We wish to develop an analytical model for *d* in terms of the stress distribution in the film We note that, as illustrated in Fig. 3.11, the level of the interaction strength τ_{TM} relative to the stress distribution is an important quantity for determining the distance that a thread travels before stopping in a TM interaction. We characterize this as using the difference between τ_{TM} and a measure of the bottom of the stress distribution. A measure of the stress level in the low stress regions may be estimated simply as $(\bar{\tau} - \hat{\tau})$, where $\hat{\tau}$ is the standard deviation of the resolved shear stress on a particular slip plane and $\bar{\tau}$ is the mean resolved shear stress. The choice of this measure is motivated by Fig. 3.10, which shows stresses at interacting threads of about $(\bar{\tau} - \hat{\tau})$. Thus, we propose, as a term to quantify the effect of stress inhomogeneity on TM interactions:

$$\tau_{diff} = \frac{\tau_{TM} - (\bar{\tau} - \hat{\tau})}{\tau_{ch}}, \tag{3.2}$$

Table 3.1. Average distance d_m traveled by each thread during a particular applied strain increment and the misfit spacing s at the end of the increment.

Applied strain	$\langle d_m \rangle$ (nm)	$\langle s \rangle$ (nm)
1.3	389	426
1.8	1129	185
2.3	1652	115
2.8	1631	88
3.3	2080	68

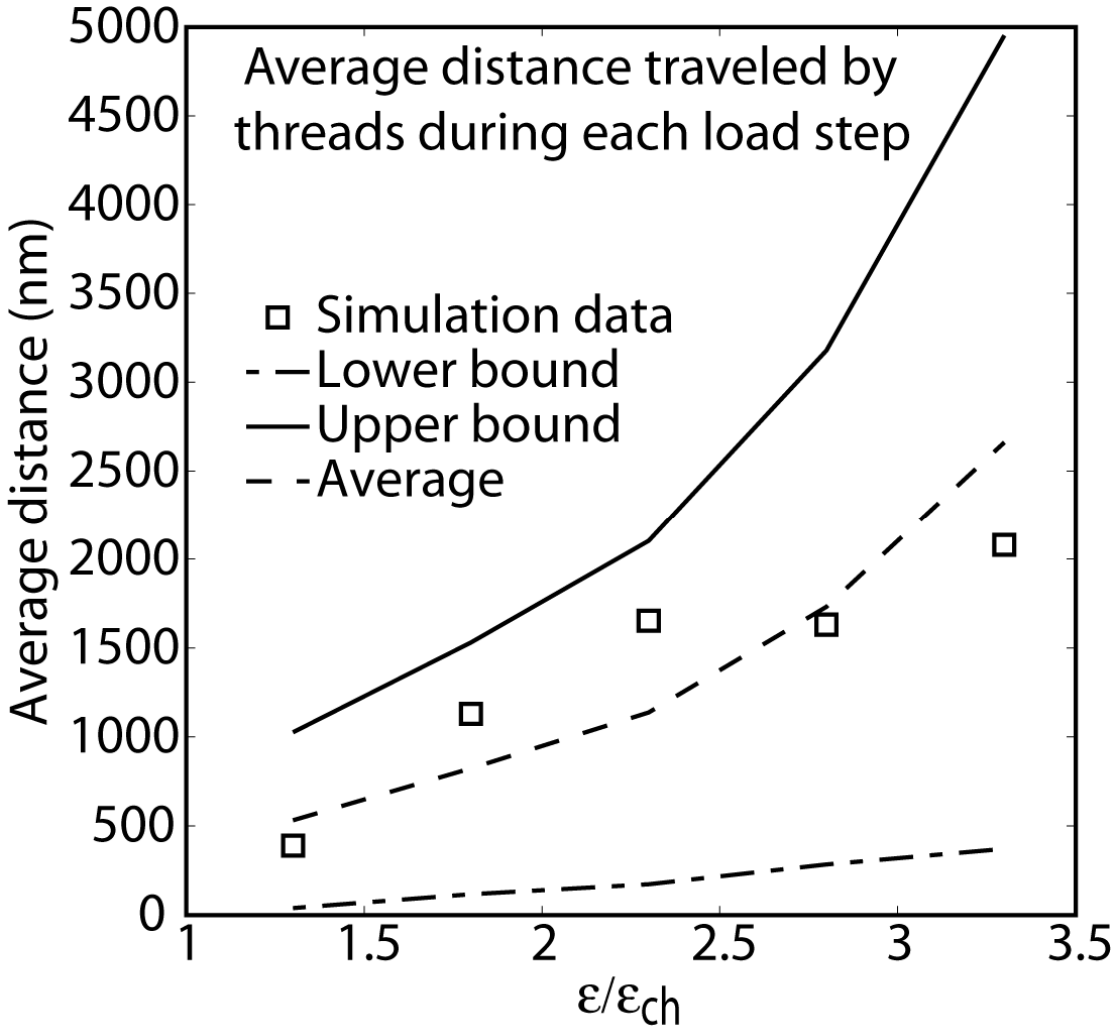

Figure 3.12. Comparison of fluctuation model with simulation data. Average distance traveled by a thread shown by stars. Bounds based on TM interaction strengths shown by squares and circles.

where, for convenience in comparing stress inhomogeneity across different film thicknesses or orientations, we normalized by the channeling stress. As τ_{diff} decreases, the distance that threads travel before being stopped in a TM interaction increases.

Thus, we have identified four terms that are important to determining dislocation behavior in films: mean stress, standard deviation of stress, channeling stress, and the strengths of TM interactions. To determine the relationship between these terms and the mean free path that a thread will travel before interacting with a misfit, we used the stress states in the equilibrium configurations of the DD simulation. The average travel distance, *d*, predicted by the mean free path in each of the equilibrium stress fields was calculated as described above and plotted as a function of τ_{diff}. The results are shown in Figure 3.13. We observe that the curves in Fig. 3.13 all follow the form

$$d = C\exp\left[-\eta\left(\frac{\tau_{TM} - (\bar{\tau} - \hat{\tau})}{\tau_{ch}}\right)\right], \tag{3.3}$$

where *C* and η are constants. For this film, *C* ~ 200 nm and η ~ 4. These data confirm that for a given dislocation structure, the average distance traveled by a thread is related to mean stress, standard deviation of stress, channeling stress, and the strength of a thread-misfit interaction.

3.4.1.2. Thread-Thread interactions

Stress inhomogeneity, as measured by the standard deviation of stress, affects TM interactions and TT interactions differently. In our simulations, the primary role that TT interactions play is in controlling the number of mobile threads in subsequent steps. As such, they play a pivotal role in the incremental loading of a film. Two parameters are important for understanding TT interactions: mobile thread density and

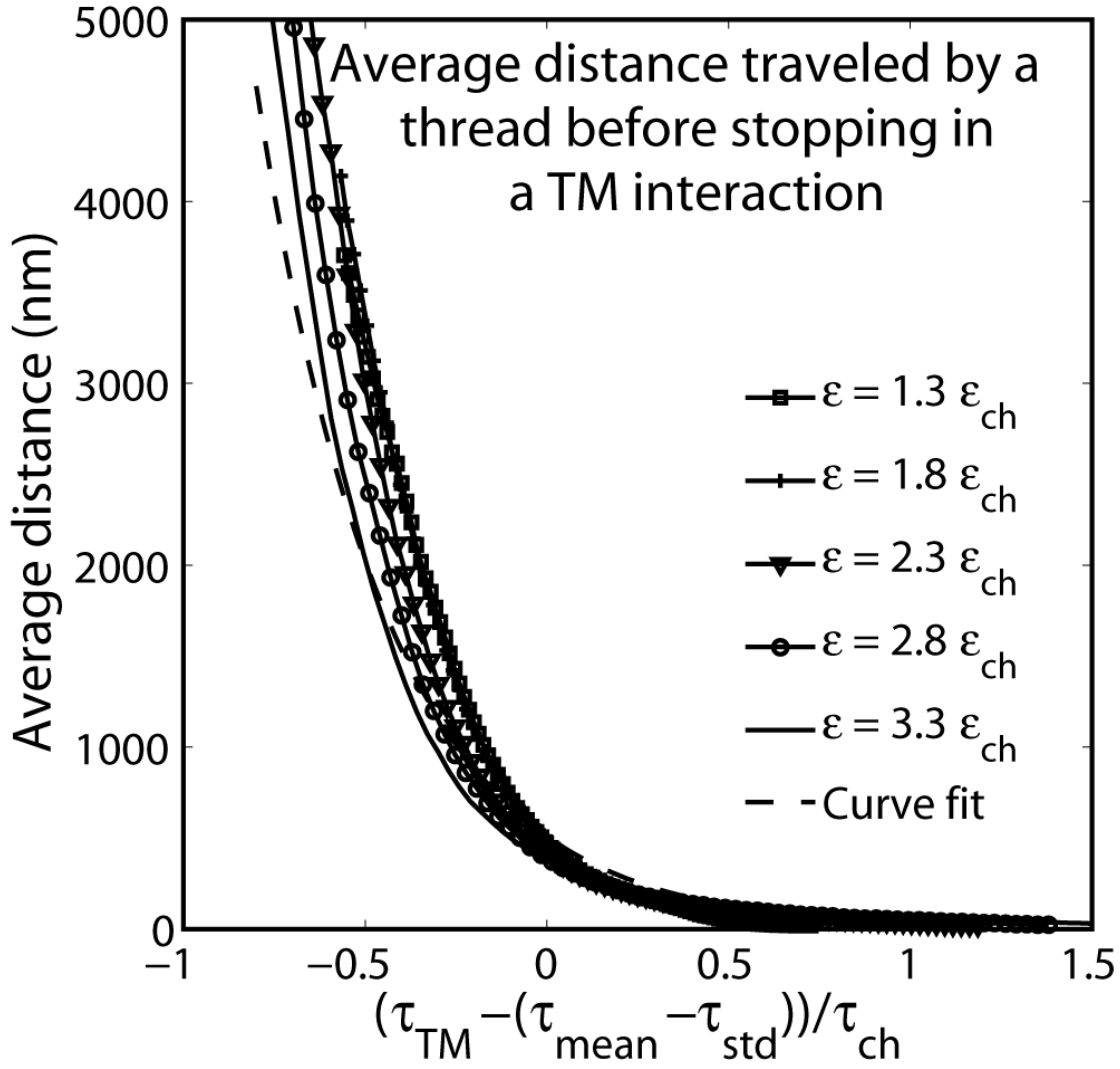

Figure 3.13. Average distance traveled by a thread as predicted by the mean free path as a function of a measure of the resolved shear stress in a low stress region of the film $\frac{\tau - (\bar{\tau} - \hat{\tau})}{\tau_{ch}}$*. The curves correspond to equilibrium dislocation structures at the simulated applied strains.*

interaction radius. In this section we outline the effects of these parameters on TT interactions and how they are influenced by stress inhomogeneity.

The role of mobile thread density in TT interactions is straightforward—larger mobile thread densities mean more TT interactions. We have shown elsewhere that the fraction of threads in TT interactions is proportional to the number of mobile threads N, and the number of TT interactions is proportional to N^2 [36]. Our results also showed that TT interactions, like TM interactions, occurred preferentially in regions of low stress. However, while low stress for TM interactions is sharply defined by TM interaction strength, low stress for TT interactions requires only that stresses are low relative to other stresses in the film. TT interactions occur in regions of low stress because threads move with a velocity proportional to the stress applied to them. They move quickly through regions of high stress and slowly through regions of low stress, thus spending more time in low stress regions, making the thread density higher in low stress regions than in high stress regions, and making TT interactions in regions of low stress more likely [35, 36]. Looking only at the effects of thread concentration, the likelihood of TT interaction increases with increasing $\frac{\hat{\tau}}{\bar{\tau} - \tau_{ch}}$ [36]. Thus, an increase in the magnitude of stress fluctuations makes this thread concentration effect more pronounced.

The other parameter important to TT interactions is the interaction radius r, which is the average maximum distance that two threads can be apart and still exert an attractive force on each other that is strong enough to pull them together to form a junction or annihilate. We define r such that when two mobile threads are within r of each other, their attraction will be strong enough to overcome the channeling stress and any applied stress. The radius r depends on the local stress on the slip system τ and will vary as $r \propto 1/(\tau - \tau_{ch})$, owing to the singular nature of the elastic field caused

by a dislocation. Consider two threads moving on intersecting slip planes. If the applied film stress is large, the threads will have to be very close for their attractive force to overcome the force on them due to the applied stress. As the applied stress is reduced, their attractive force will overcome the force from the applied stress at larger distances. Thus, when the mean film stress exceeds the channeling stress, the interaction radius will be larger in low stress regions, further biasing TT interactions to occur in these regions.

3.4.1.3. Multiple relaxation steps and strain hardening

In our simulations, we have used the dislocation structures and stresses in the relaxed states following a series of discrete jumps in the applied strain. It is important to consider how closely these results describe what would happen in a continuously loaded film. To test this, we examined the effect of strain increment size on our simulation results by starting with the equilibrium dislocation structure at $1.3\varepsilon_{ch}$ and evaluating the evolution of the dislocation structure and stress distribution as the applied strain was increased to $1.8\varepsilon_{ch}$ in strain increments of 0.25, 0.125, and $0.0625\varepsilon_{ch}$. We observed that the final stress level reached and the types of interactions that occurred at $1.8\varepsilon_{ch}$ did not substantially deviate from those obtained with the initial step size of $0.5\varepsilon_{c}$. Therefore, we conclude that our results are not strongly influenced by step size.

Since continuous loading can be thought of as a series of strain increments and subsequent relaxation steps, where the step size and the relaxation time both go to zero, we expect that the most important conclusions of our stepwise simulations will still hold for continuous loading, provided that the dislocation response is quasi-static. The distance that a thread will travel before stopping will still be well described by the

spacing of low-stress regions, and, in the absence of dislocation sources, the number of mobile threads available to relax the strain will decrease as threads become immobilized in static interactions. Both the increasing stress inhomogeneity with increasing strain and the reduction in the mobile thread density will contribute to strain hardening. Of course, during continuous loading, the number of mobile threads can always be tracked, but the definition of a static thread will depend on the increment in stress over which one expects the dislocation to remain static..

3.4.2. Additional consideration of simulation parameters

The highly-resolved simulations reported here were computationally intensive (approx. 100,000 hours of CPU time) and lack of computation time prevented us from exploring more variables. Nevertheless, the effects due to variations in the initial number of threads and the film thickness can be described based on these, and other, simulations.

First, as mentioned above, the number of initial threads will affect the relative amounts of the different types of dislocation interactions that occur. For example, if 10 initial threads were used instead of our 140, we would expect fewer TT interactions. Also, since fewer regions of high stress could be relaxed, we would expect the stress inhomogeneity to increase and the film to relax less. Consistent with this view, higher thread densities have been shown in previous simulations to correspond with greater relaxation [26]. Our conclusions regarding the effect of stress inhomogeneity on TT and TM interactions do not depend on the initial thread density. Thus, even the existence of dislocation sources in a film will not change our basic conclusions about how TM and TT interaction strengths and stress inhomogeneities conspire to establish the strength and strain hardening in a film.

A change in the simulated film thickness will affect the results by changing the interaction strengths, modifying the development of the inhomogeneous field, and possibly by qualitatively changing the interactions. The interaction strengths have been shown to be thickness dependent [25]: TM interactions get weaker with increasing film thickness and TT interactions get stronger. Thus, interactions in a thicker film will tend to bias the interaction fractions in favor of TT interactions. The interaction radius of the thread will be larger because of the reduced channeling stress, also facilitating a greater fraction of TT interactions. Stress inhomogeneity will be diminished in thicker films because the misfits will be farther apart, so that their stresses, which are inversely proportional to the distance from the misfit, will account for a smaller percentage of stress in the film.. This will reduce strain hardening in thicker films.

3.4.3. Application to real films

We have used our simulation results to motivate a framework for thinking about dislocation motion and stress relaxation in thin films. We now extend these ideas to real films that contain both grain boundaries and dislocation sources. The application to dislocation sources is simple: the presence of sources will reduce strain hardening and increase the number of TT interactions through the production of additional threads. If the thread density doubles, threads need only to move half as far to relax the same amount of strain. This has been shown in previous simulations [26]. The additional threads increase the likelihood of TT interactions simply because there are more threads with which to interact [36].

Grain boundaries affect a film mechanically in two ways: they affect the motion of dislocations and they can create stress inhomogeneities in the film. Dislocations can be

absorbed, reflected, or transmitted at grain boundaries—increasing the stress required for dislocation motion [37-39]. Stress inhomogeneities in a film can be created by the mismatch in elastic properties that occur at some grain boundaries and have even been observed to cause dislocations to move on planes that do not relax applied biaxial strains in a film [40]. The presence of such dislocations is sure to increase the intrinsic stress required to drive a dislocation into the film but was not studied here .

Because the grain size is fixed and the mean free path for dislocation motion changes with misfit density and mean stress the model proposed in Section 4.1 allows us to postulate the existence of a critical film stress, below which TM and TT interactions will dominate and above which thread-grain boundary interactions will dominate. We predict that a thread will, on average, travel a distance $\lambda/2$. The grain boundaries would be expected to dominate the stopping of threads when $\lambda/2$ approaches the average size of the grain. We have shown that an increase in stress inhomogeneity increases the strain hardening rate. If $\lambda/2$ is greater than the grain size, we expect an additional strain hardening mechanism to be present. Thus, because an additional mechanism is present to stop dislocations, we expect a polycrystalline film to have a higher strain hardening rate than its single crystal counterpart. This is consistent with the results we observed in Fig. 3.4, which was from the (001) grains of a polycrystalline film: the strain hardening rate in the polycrystalline film is greater than that of the simulated film.

3.5. Conclusions

We studied stress levels and strain hardening in a passivated single-crystal thin film on a hard substrate using three-dimensional dislocation dynamics simulations, approximating continuous loading as a series of discrete load steps followed by stress

relaxations. Our results revealed several critical features of dislocation behavior and motivate a new picture of dislocation-based relaxation of thin films.

Deformation in films can be viewed as arising from the motion of threading dislocations (threads) that leave misfit dislocations (misfits) behind at interfaces. Thus, strength and strain hardening can be understood in terms of what stops threads at different stress and strain levels. We found that the misfit structure that arises in the film during deformation gives rise to local stress fluctuations, the magnitude of which increase with increasing misfit density. As a result of this spatially-inhomogeneous stress field, both thread-thread and thread-misfit interactions play a important roles in stopping threads, and thus in determining film strength and strain hardening, at all stress levels.

Threads stop via interactions with other dislocations in local regions of low stress. Because low-stress regions exist even at high average stress levels, thread-misfit interactions, which are relatively weak compared with typical film strengths, play a significant role in stopping threads, even when the average stress in the film is high. Thread-thread interactions, which have strengths that can be much higher than typical film strengths are also facilitated by stress inhomogeneities because (1) they are concentrated in areas of low stress by velocity fluctuations, and (2) the area of a thread capture cross-section is largest in regions of low stress.

Thread-thread interactions also play an important role in strain hardening since they typically render threads immobile up to very high applied strain levels. Thus threads tend to accumulate in these interactions, and the density of threads available to relax stresses declines as plastic strain increases. In comparison, thread-misfit interactions typically break following much more modest increases in film stress, allowing the involved thread to participate in strain relaxation at higher film stresses.

We have identified the average distance that a thread travels before stopping in a thread-misfit interaction as a key measure of the film's ability to relax stress and thus the stress and strain hardening rate for a given dislocation structure. This mean free path for dislocation motion is governed by the distance between regions of stress lower than the strength of a thread-misfit interaction. The average distance that a thread travels before stopping in a thread-thread interaction also plays a role and is governed by thread density and capture cross-section, both of which are implicitly dependent on average film stress and the magnitude of the stress fluctuations.

Based on these observations, an analytical formulation for the dislocation mean free path was generated based on attributes of the stress state. The mean free path and the unique functions of TT and TM interactions provide a clear link between individual dislocation behavior, dislocation structure, and strength and strain hardening in thin films.

Acknowledgements

This research was supported by the National Science Foundation under grant DMR-0311848, and was conducted using the resources of the Cornell University Center for Advanced Computing, which receives funding from Cornell University, New York State, the National Science Foundation, and other leading public agencies, foundations, and corporations.

REFERENCES

[1] Freund LB, Suresh S. Thin Film Materials: Stress, Defect Formation and Surface Evolution. Cambridge, United Kingdom: Cambridge University Press, 2003.

[2] Nix WD. Mechanical properties of thin films. Metall. Trans. A 1989;20:2217.

[3] Arzt E. Overview no. 130 - Size effects in materials due to microstructural and dimensional constraints: A comparative review. Acta Mater. 1998;46:5611.

[4] Vinci RP, Vlassak JJ. Mechanical behavior of thin films. Annual Review of Materials Science 1996;26:431.

[5] Baker SP. Plastic deformation and strength of materials in small dimensions. Mater. Sci. Eng. A 2001;319-321:16.

[6] Venkatraman R, Bravman JC. Separation of Film Thickness and Grain-Boundary Strengthening Effects in Al Thin-Films on Si. J. Mater. Res. 1992;7:2040.

[7] Baker SP, Keller-Flaig RM, Shu JB. Bauschinger effect and anomalous thermomechanical deformation induced by oxygen in passivated thin Cu films on substrates. Acta Mater. 2003;51:3019.

[8] Keller R, Baker SP, Arzt E. Quantitative analysis of strengthening mechanisms in thin Cu films: effects of film thickness, grain size, and passivation. J. Mater. Res. 1998;13:1307.

[9] Fertig RS, Baker SP. Simulation of dislocations and strength in thin films: A review. Prog. Mater. Sci. 2009;54:874.

[10] Espinosa HD, Berbenni S, Panico M, Schwarz KW. An interpretation of size-scale plasticity in geometrically confined systems. Proceedings of the National Academy of Sciences of the United States of America 2005;102:16933.

[11] Schwaiger R, Dehm G, Kraft O. Cyclic deformation of polycrystalline Cu film. Philosophical Magazine 2003;83:693.

[12] Frank FC, van der Merwe JH. One-Dimensional Dislocations. I. Static Theory. Proceedings of the Royal Society of London. Series A, Mathematical and Physical Sciences 1949;198:205.

[13] Matthews JW, Blakeslee AE. Defects in epitaxial multilayers. II. Dislocation pile-ups, threading dislocations, slip lines, and cracks. Journal of Crystal Growth 1975;29:273.

[14] Matthews JW, Blakeslee AE. Defects in epitaxial multilayers. I. Misfit dislocations. Journal of Crystal Growth 1974;27:118.

[15] Freund LB. The Stability of a Dislocation Threading a Strained Layer on a Substrate. J. Appl. Mech. 1987;54:553.

[16] Freund LB. The Driving Force for Glide of a Threading Dislocation in a Strained Epitaxial Layer on a Substrate. J. Mech. Phys. Solids 1990;38:657.

[17] Nix WD. Yielding and strain hardening of thin metal films on substrates. Scr. Mater. 1998;39:545.

[18] Keller R-M, Baker SP, Arzt E. Stress-temperature behavior of unpassivated thin copper films. Acta Mater. 1999;47:415.

[19] Thompson CV. The Yield Stress of Polycrystalline Thin-Films. J. Mater. Res. 1993;8:237.

[20] von Blanckenhagen B, Arzt E, Gumbsch P. Discrete dislocation simulation of plastic deformation in metal thin films. Acta Mater. 2004;52:773.

[21] Freund LB. A criterion for arrest of a threading dislocation in a strained epitaxial layer due to an interface misfit dislocation in its path. J. Appl. Phys. 1990;68:2073.

[22] Schwarz KW, Tersoff J. Interaction of threading and misfit dislocations in a strained epitaxial layer. Appl. Phys. Lett. 1996;69:1220.

[23] Schwarz KW. Interaction of dislocations on crossed glide planes in a strained epitaxial layer. Phys. Rev. Lett. 1997;78:4785.

[24] Gomez-Garcia D, Devincre B, Kubin L. Dislocation dynamics in confined geometry. J. Comput-Aided Mater. Des. 1999;6:157.

[25] Pant P, Schwarz KW, Baker SP. Dislocation interactions in thin FCC metal films. Acta Mater. 2003;51:3243.

[26] Schwarz KW. Discrete dislocation dynamics study of strained-layer relaxation. Phys. Rev. Lett. 2003;91:145503.

[27] Schwarz KW, Cai J, Mooney PM. Comparison of large-scale layer-relaxation simulations with experiment. Appl. Phys. Lett. 2004;85:2238.

[28] Lynch C, Chason E, Beresford R, Freund LB, Tetz K, Schwarz KW. Limits of strain relaxation in InGaAs/GaAs probed in real time by in situ wafer curvature measurement. J. Appl. Phys. 2005;98:073532.

[29] Pant P, Schwarz KW, Baker SP. Dislocation dynamics simulations of plastic deformation in thin films. Unpublished 2006.

[30] Schwarz KW. Simulation of dislocations on the mesoscopic scale. I. Methods and examples. J. Appl. Phys. 1999;85:108.

[31] Schwarz KW. Local rules for approximating strong dislocation interactions in discrete dislocation dynamics. Model. Simul. Mater. Sci. Eng. 2003:609.

[32] Stach EA, Schwarz KW, Hull R, Ross FM, Tromp RM. New Mechanism for Dislocation Blocking in Strained Layer Epitaxial Growth. Phys. Rev. Lett. 2000;84:947.

[33] Baker SP, Kretschmann A, Arzt E. Thermomechanical behavior of different texture components in Cu thin films. Acta Mater. 2001;49:2145.

[34] Nowak DE, Baker SP. Early yielding and stress recovery in (111) and (100) texture components in Cu thin films determined using synchrotron X-ray diffraction.

Thin Films - Stresses and Mechanical Properties X, vol. 795. Boston, MA, USA: Mater. Res. Soc, 2004. p.449.

[35] Fertig RS, Baker SP. Relationship between film stress and dislocation microstructure evolution in thin films. In: LaVan D, Spearing M, Vengallatore S, Silva Md, editors. Microelectromechanical Systems -- Materials and Devices, vol. 1052. Boston, MA: Mater. Res. Soc., 2007. p.DD07.

[36] Fertig RS, Baker SP. Threading dislocation interactions in an inhomogeneous stress field: a statistical model. In preparation 2008.

[37] de Koning M, Miller R, Bulatov VV, Abraham FF. Modelling grain-boundary resistance in intergranular dislocation slip transmission. Philos. Mag. A 2002;82:2511.

[38] de Koning M, Kurtz RJ, Bulatov VV, Henager CH, Hoagland RG, Cai W, Nomura M. Modeling of dislocation-grain boundary interactions in FCC metals. Journal of Nuclear Materials 2003;323:281.

[39] Lee TC, Robertson IM, Birnbaum HK. TEM in situ Deformation Study of the Interaction of Lattice Dislocations with Grain-Boundaries in Metals. Philos. Mag. A 1990;62:131.

[40] Balk TJ, Dehm G, Arzt E. Parallel glide: Unexpected dislocation motion parallel to the substrate in ultrathin copper films. Acta Mater. 2003;51:4471.

CHAPTER 4
CAPTURE CROSS-SECTION OF THREADING DISLOCATIONS IN THIN FILMS

Ray S. Fertig and Shefford P. Baker

Department of Materials Science and Engineering, Cornell University, Ithaca, NY 14853

ABSTRACT – In this paper the annihilation of two threads with opposite Burgers vectors moving on orthogonal slip planes in a thin film is examined. Film thicknesses and applied loads are systematically varied and the initial configurations of threads that lead to annihilation are mapped out for each film thickness and applied stress. The area of the region of initial configurations that lead to annihilation is the capture cross-section of the thread. The size of the capture cross-section is shown to be highly sensitive to the applied stress relative to the constraint on dislocation motion imposed by film thickness.

4.1 Introduction

Thin films are used in a wide variety of applications ranging from microelectronics to biomedical devices to solar cells. In many applications films support stresses in excess of the ultimate stresses of their bulk counterparts by an order of magnitude [1]. The reasons for this are not fully understood. These high stresses contribute to failure mechanisms such as fracture, delamination, and stress voiding. Thus, understanding the mechanical behavior of thin films is crucial to improving thin film performance and reliability.

High stresses are only possible when dislocation motion is difficult. In thin films, threading dislocations (threads), which run through the thickness of the film, move through the film to relax the film stress by depositing misfit dislocations (misfits) at film interfaces or creating steps at the film surfaces. Thus, to understand high film stresses we must know what stops threads. One impediment to thread motion is a dimensional constraint—the so-called channeling stress [2, 3]. The channeling stress is simply the minimum stress required to move a dislocation in a film. It arises from balancing the energy increase due to adding a misfit dislocation with the strain energy decrease from the stress relaxed by the dislocation. Above the channeling stress, in single-crystal films, threads are stopped by interacting with other dislocations, both threads and misfits. Using discrete dislocation dynamics simulations [4], we have shown that interactions between two threads stop a large fraction of the mobile threads in a film. Because many thread-thread interactions are very strong, they often permanently immobilize threads, which leads to a reduction in the number of threads available to relax the film stress and, consequently, to strain hardening.

The frequency of interaction between threads is controlled by three factors: thread mobility, the density of the threads, and the capture cross-section of the thread. The capture cross-section represents the locus of points around a thread such that another thread inside this region will form a junction or annihilate with the first thread. The size of this capture cross-section has been studied previously, but only as it relates to cross-slip, climb, or layer growth [5-13]. Our simulations showed that threading dislocation interactions are more likely between threads on intersecting slip planes depositing orthogonal (in the case of (001) films) misfits than for any other possible threading dislocation combinations [14].

The goal of the work reported here is to determine size and shape of the capture cross-section for a thread annihilating with another thread on an intersecting slip plane

moving in an orthogonal direction. In contrast to previous investigations [12, 15] that have considered cross-slip/climb as the mechanism for annihilation with the limiting stress being the Peierls stress, we focus on dislocation glide in response to an applied stress as the mechanism for annihilation with the limiting stress being the channeling stress [2, 3]. We seek to determine whether there are particular stress regimes where the capture cross-section is either very large or very small.

4.2 Model

In a real film, threads are curved, of mixed character, and are confined to their glide planes [3]. To treat this problem in an efficient and tractable way, we model this situation using straight screw segments that are confined to their slip planes. While possibly different in detail or magnitude, we expect this model to be qualitatively correct.

We consider threads *A* and *B* having pure screw character moving on intersecting $\{100\}$ slip planes in a cubic (001) film, as shown in Figure 4.1. The stress field of these dislocations was approximated as the stress field of two infinite screw dislocations with sense vectors $\xi_A = \xi_B = [0\,0\,1]$. The Burgers vectors for the dislocations were $b_A = [0\,0\,b]$ and $b_B = -b_A$, such that they would annihilate if they formed a junction. These assumptions allowed the stress field of each dislocation to be written as

$$\sigma_{dis} = \frac{\mu b}{2\pi R^2}\begin{bmatrix} 0 & 0 & y \\ 0 & 0 & -x \\ y & -x & 0 \end{bmatrix}, \tag{4.1}$$

where *x* and *y* are coordinates in the $[100]$ and $[010]$ directions in the film plane, $R = \sqrt{x^2 + y^2}$, μ is the shear modulus, and the origin is at the point of intersection of the two glide planes. Uniform shear stresses, $\tau_{xz} = \tau_{yz} = \tau$, were applied to the film,

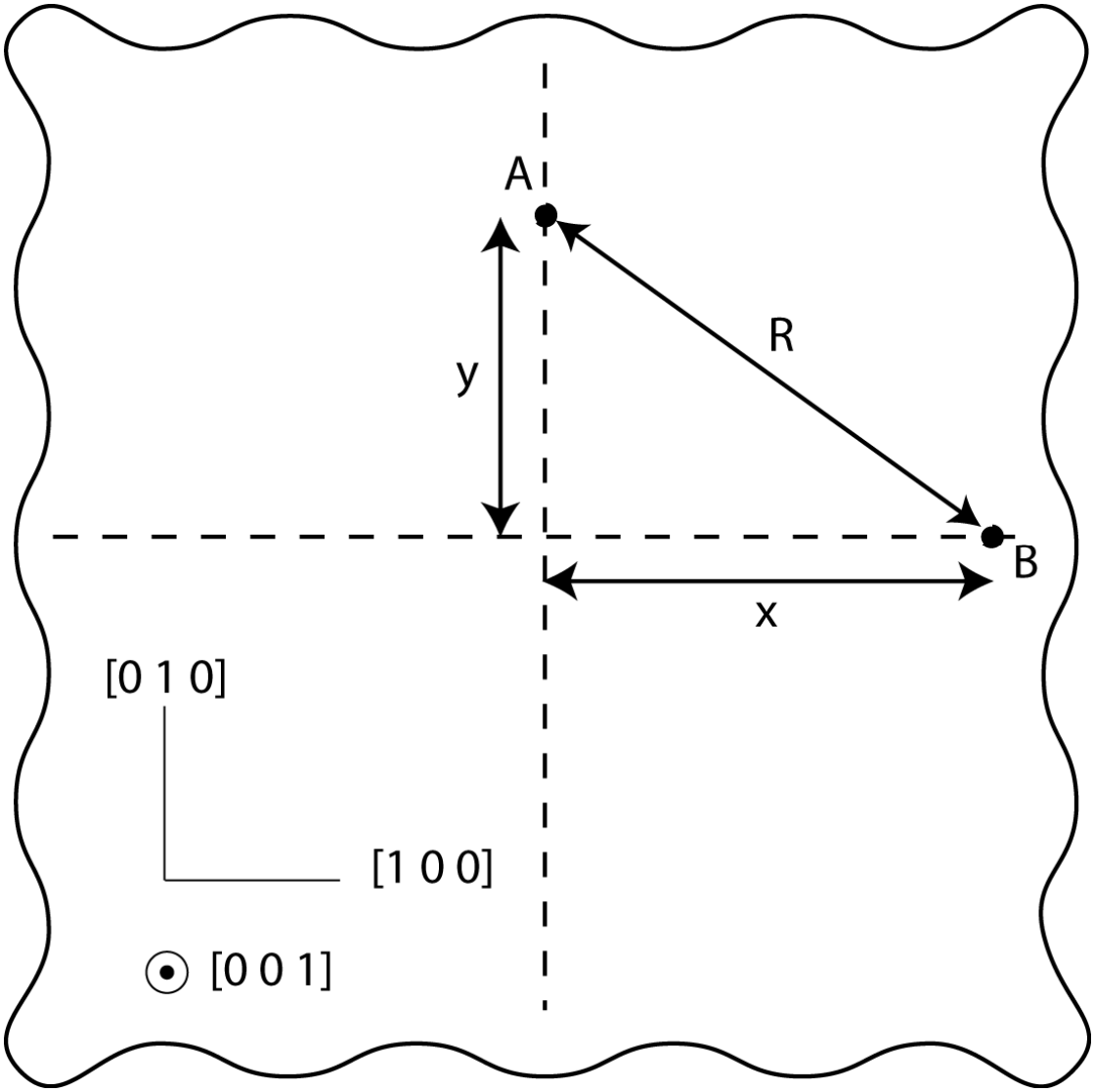

Figure 4.1. Schematic of the model setup. The goal of the model is to determine the capture cross-section of dislocation B as determined by its interaction with A.

resulting in an equal applied force on both dislocations. The total stress felt by either dislocation due to the applied stress and the stress field of the other dislocation was

$$\sigma_A = \sigma_B = \frac{\mu b}{2\pi R^2}\begin{bmatrix} 0 & 0 & y \\ 0 & 0 & x \\ y & x & 0 \end{bmatrix} + \begin{bmatrix} 0 & 0 & \tau \\ 0 & 0 & \tau \\ \tau & \tau & 0 \end{bmatrix}. \qquad (4.2)$$

The force per unit length on the dislocation was then calculated from the Peach-Koehler formula [16],

$$F_i = -\varepsilon_{ijk}\xi_j\sigma_{kl}b_l, \qquad (4.3)$$

where ε_{ijk} is the permutation tensor. The force on each dislocation was calculated by substituting Eq. (4.2) into Eq. (4.3). The glide force on each dislocation was found by taking the dot product of these forces with the slip directions $[0\,1\,0]$ and $[1\,0\,0]$, for dislocations *A* and *B*, respectively, using

$$F_{A,glide} = -\frac{\mu b y}{2\pi R^2} - \tau b \qquad (4.4a) \quad \text{and} \quad F_{B,glide} = -\frac{\mu b x}{2\pi R^2} - \tau b. \qquad (4.4b)$$

That is, dislocation *A* was confined to move in the *y* direction (force due to applied stress acts down in Fig 4.1) and dislocation *B* was confined to move in the *x* direction (force due to applied stress acts to left in Fig. 4.1). The interaction stress is, of course, always attractive.

A glide force on a dislocation will not necessarily cause the dislocation to move. In bulk materials the glide force must exceed the force required to overcome the Peierls barrier. In thin films, which are the subject of this study, the glide force must exceed a thickness dependent critical force $\tau_c b$, which is dependent on the channeling stress τ_c [3]. The magnitude of the difference between the glide force and the critical force is termed the excess glide force F_{ge}, following [17]. In this model, F_{ge} and the dislocation velocity *v* were related by a mobility *M* using a mobility law $v = MF_{ge}$. In the case where the magnitude of the glide force is less than the magnitude of the critical force, the dislocation remains stationary. Given this mobility law and that v_A and v_B represent

dy/dt and *dx/dt*, respectively, the system of equations describing the motion of the dislocations is given by

$$\frac{d\hat{x}}{d\tilde{t}} = \begin{cases} \left\{\left|\frac{-1}{2\pi}\frac{\hat{x}}{\hat{R}^2} - \frac{\tau}{\mu}\right| - \frac{\tau_c}{\mu}\right\} sign\left(\frac{-1}{2\pi}\frac{\hat{x}}{\hat{R}^2} - \frac{\tau}{\mu}\right), & \left|\frac{-1}{2\pi}\frac{\hat{x}}{\hat{R}^2} - \frac{\tau}{\mu}\right| > \frac{\tau_c}{\mu} \\ 0 \quad , \quad \left|\frac{-1}{2\pi}\frac{\hat{x}}{\hat{R}^2} - \frac{\tau}{\mu}\right| < \frac{\tau_c}{\mu} \end{cases}$$

$$\frac{d\hat{y}}{d\tilde{t}} = \begin{cases} \left\{\left|\frac{-1}{2\pi}\frac{\hat{y}}{\hat{R}^2} - \frac{\tau}{\mu}\right| - \frac{\tau_c}{\mu}\right\} sign\left(\frac{-1}{2\pi}\frac{\hat{y}}{\hat{R}^2} - \frac{\tau}{\mu}\right), & \left|\frac{-1}{2\pi}\frac{\hat{y}}{\hat{R}^2} - \frac{\tau}{\mu}\right| > \frac{\tau_c}{\mu} \\ 0 \quad , \quad \left|\frac{-1}{2\pi}\frac{\hat{y}}{\hat{R}^2} - \frac{\tau}{\mu}\right| < \frac{\tau_c}{\mu} \end{cases} \quad ,(4.5)$$

where *t* is time and $\hat{x} = \frac{x}{b} \quad \hat{y} = \frac{y}{b} \quad \hat{R} = \sqrt{\hat{x}^2 + \hat{y}^2} \quad \tilde{t} = \frac{t}{t_0} \quad t_0 = \frac{1}{M\mu}$

Equations (4.5) were solved using a Runge-Kutta technique following [18]. The time step *h* in this solution was adaptive such that the time step decreased as the rate of approach of the dislocations increased and increased with increasing distance between dislocations. This approach reduced computation time when the dislocations were initially far from each other and prevented spurious results from occurring when the dislocations were close with high velocities. In the implementation of this solution, *h* was initially set to $h = 0.01$ and thereafter was prescribed to be

$$h_n = \alpha \hat{R}_{n-1}\left(\frac{\tilde{t}_{n-1} - \tilde{t}_{n-2}}{\hat{R}_{n-1} - \hat{R}_{n-2}}\right), \quad (4.6)$$

where *t* is time, *n* corresponds to the time step number, and $\alpha = 0.005$ for the solutions reported here. The value of α was converged such that lower values (smaller time steps) did not yield different cross-sectional areas.

The focus of this work was to determine the capture cross-section of a thread such that it would interact with another thread within this area; in this case the interaction leads to annihilation of both threads. Thus, the initial conditions that lead to an interaction are of interest. The distance from the thread to the boundary of its capture

cross-section was calculated at four degree increments around the thread. This allowed the shape of the capture cross-section to be determined. The accuracy of the distance along any given trajectory was ± 5%. The threads were allowed to move until either the distance between the dislocations was less than one Burgers vector or the dislocation velocities began to increase in a direction away from interaction, i.e. $d^2R/dt^2 > 0$. Once the boundary of the cross-section was determined, the cross-sectional area A was calculated as

$$A = \frac{\pi}{90}\sum_{i=1}^{90} r_i^2 \ . \qquad (4.7)$$

4.3 Results

The features of the capture cross-section boundary can be divided into two regimes with fundamentally different behaviors: (1) applied stress less than the channeling stress and (2) applied stress greater than the channeling stress. These are illustrated in Figure 4.2, which shows the capture cross-section, with dislocation B at the origin, for applied film stresses ranging from 0.0001μ to 0.011μ for a thread in a film with channeling stress τ_{ch} = 0.01μ. Figure 4.2b is an enlargement of the region around the origin in Fig. 4.2a so that the cross-sections at very low stress can be seen.

With no applied stress, the threads will come together to form a junction only if the stress exerted by one thread on the other exceeds the channeling stress. Thus, the capture cross-section must be symmetric about the x- and y-axes. Any applied stress causes asymmetry in the capture cross-section. The asymmetry arises because the applied stress drives the two dislocations in fixed directions, while the interaction stress drives the dislocations towards each other at all stress levels, hence an increase in cross-sectional area in only one quadrant. This asymmetry increases with increasing stress, as illustrated in Fig. 4.2b. The solid curve shows the nearly symmetric capture

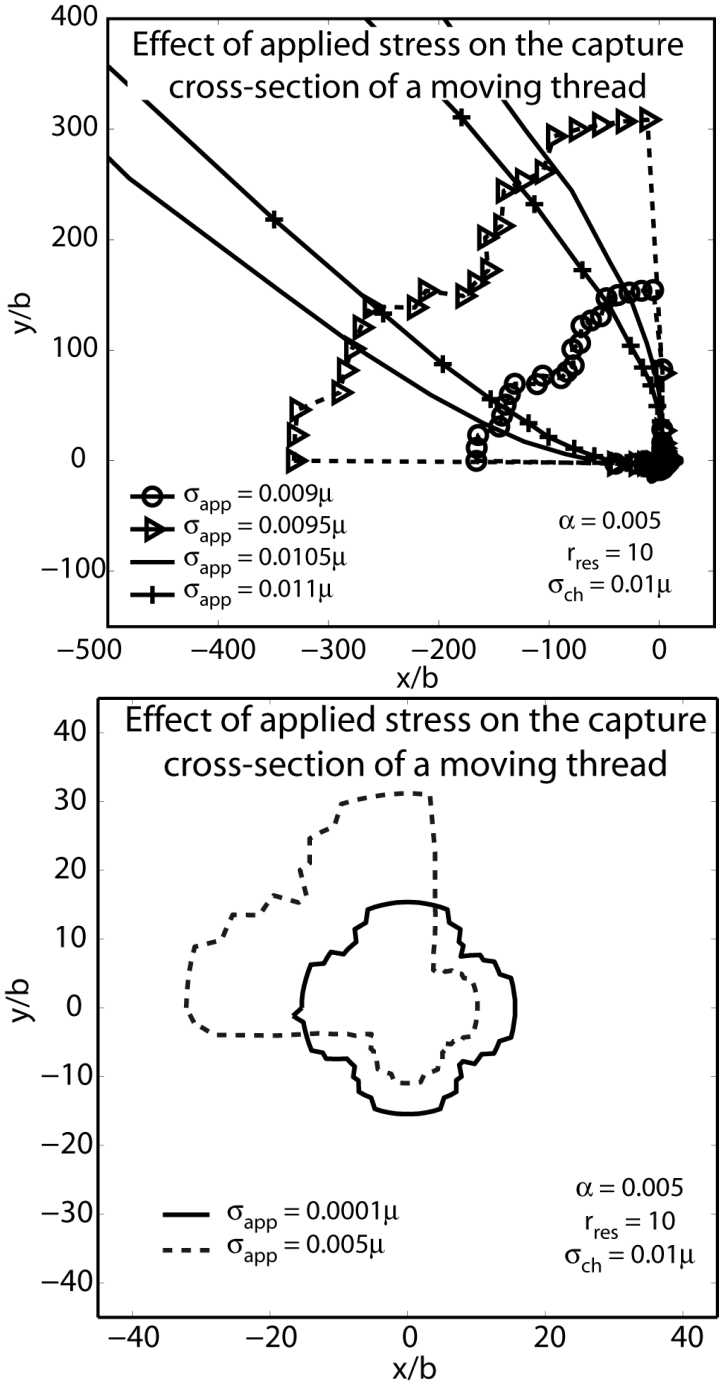

Figure 4.2. (a) Boundary of the capture cross-section for different applied stresses with dislocation B at the origin. The channeling stress is 0.01μ. (b) A zoom of the capture cross-section from (a) to better illustrate the capture cross-section at low applied stresses.

cross-section at a very low stress and the dashed curve shows the cross-section at an applied stress of half the channeling stress. The dashed curves in Fig. 4a show the capture cross-section at stresses just below the channeling stress. Note that the cross-sectional area has increased substantially. When the applied stress is below the channeling stress, interaction will occur when the other thread is close enough to supply the additional stress needed to exceed the channeling stress. Near the channeling stress, the additional stress required to move the thread is very low, so the dislocations can be far apart and still draw each other together to annihilate. In fact, in the limit as the applied stress approaches the channeling stress, the threads can be arbitrarily far apart and will still annihilate. Thus, when the applied stress is below the channeling stress, increasing the applied stress increases the area of the capture cross-section.

When the applied stress exceeds the channeling stress, the threads do not require interaction with any other thread to move; they are already moving on the trajectory determined by their glide plane. Figure 4.2a shows the shape of the capture cross-section with increasing applied stress above the channeling stress (solid curves). Of course, if the threads start out equidistant from their point of intersection along the positive x and y axes, they will interact under any applied biaxial stress thus the capture cross section extends to infinity at 135˚. However, for any other initial position of threads, the interaction stresses between the threads must at some point become more important than the applied stress in order for the threads to interact. As the applied stress increases, the region in which this can occur becomes smaller. Thus, the capture cross-section appears as a band at 135° that narrows with increasing applied stress.

Perhaps the most dramatic illustration of these results is shown in Fig. 4.3. The area of the capture cross-section scaled by the channeling stress squared is plotted as a

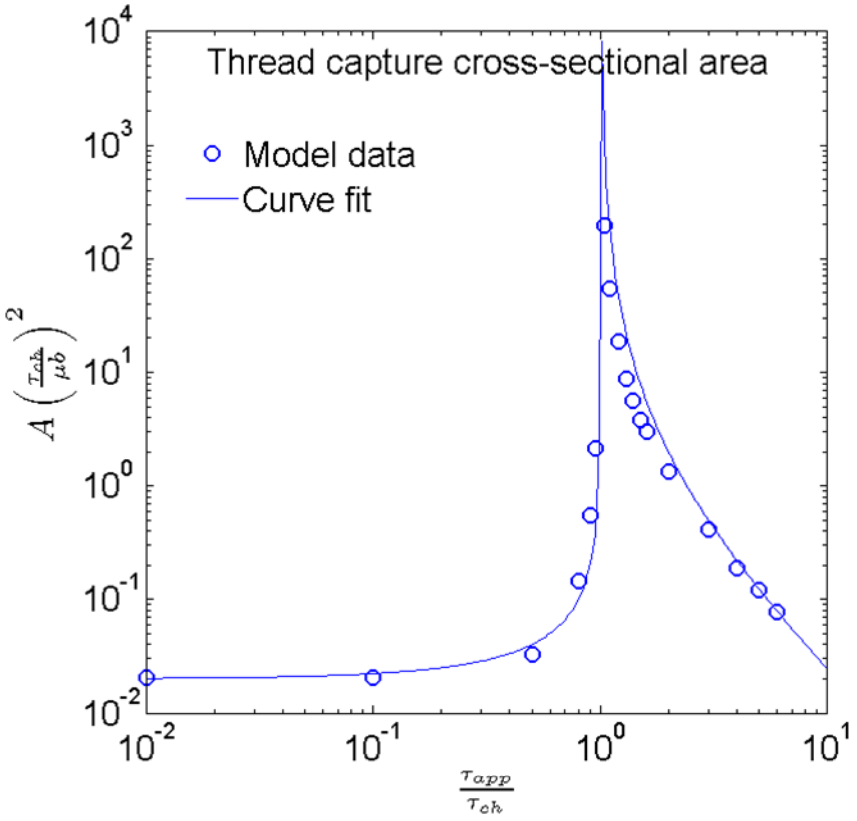

Figure 4.3. Cross-sectional area variation with applied stress. The area of the capture cross- section increases to infinity as the applied stress increases from very low loading to the channeling stress.

function of stress normalized by the channeling stress. All of the applied stresses and channeling stresses (corresponding to different film thicknesses) values fall on the same curve if plotted in this manner. The curve fit plotted is given by

$$A\left(\frac{\tau_{ch}}{\mu b}\right)^2 = \begin{cases} \dfrac{\chi_1}{1-\dfrac{\tau}{\tau_{ch}}}, & \tau < \tau_{ch} \\ \dfrac{\chi_2}{\left(\dfrac{\tau}{\tau_{ch}}-1\right)^2}, & \tau > \tau_{ch} \end{cases}, \tag{4.8}$$

where χ_1 and χ_2 are taken to be 0.02 and 2, respectively, for the curve fit shown in Fig. 4.3. The striking result here is that the area of the capture cross-section increases by nearly five orders of magnitude as the applied stress approaches the channeling stress.

4.4 Discussion

The results show that the capture cross section depends strongly on the applied stress. The dramatic increase in the area of the capture cross-section as the stress in the film approaches the channeling stress has several important implications for film strength. First, because the capture cross-section of a thread is very large near the channeling stress, we expect threads to interact most frequently when film stresses are near the channeling stress—in fact, interactions between threads may be the most dominant in this stress regime. Although the Burgers vectors of the dislocations in this model could only cause annihilation, the observed trend should hold for junction formation between threads as well. This result is consistent with results from three-dimensional DDD simulations that showed that thread-thread interactions were the most frequent when local stresses were near the channeling stress [4]. Second, the size of the capture cross-section is proportional to the inverse of the square of the

channeling stress, or roughly with the square of the film thickness. Thus, for films with equal numbers of threads, our model predicts that the fraction of threads stopped by thread-thread interactions should decrease as film thickness decreases. This means that fewer annihilations will occur and more threads will remain in the film to relax stresses as applied strain is increased. However, the decrease in the number of thread-thread interactions with decreasing film thickness cannot be easily linked to strain hardening because the misfits play an increasing role in stopping threads as film thickness decreases [19].

While this model is expected to give qualitatively correct results for the dependence of the capture cross section as a function of applied stress, it cannot fully describe film behavior because it does not consider interaction with misfit dislocations in the path of the threads. Of course, if one thread stops in an interaction with a misfit before it reaches the other thread, then the two threads will never interact. Fluctuations in the stress field may also change the apparent capture cross-section observed in simulations or real films. If a thread passes through a region of stress lower than the channeling stress, the thread will stop even if the average film stress is above the channeling stress. Thus, the capture cross-sections calculated here do not necessarily correspond to the exact in situ capture-cross section of threads in all films. Nevertheless, the calculations provided here provide a framework for determining the relative likelihood of interactions between threads based on film thickness and applied stress.

4.5 Conclusions

We have presented an analytical model to calculate the capture-cross section of a thread gliding in response to an applied stress, such that another thread with opposite

Burgers vector on an intersecting path will annihilate with the thread when it is inside this capture cross-section. This model is expected to accurately represent the qualitative behavior of real threading dislocations in thin films. For applied stresses below the channeling stress, the size of the capture cross-section increases with the applied stress. For applied stresses above the channeling stress, the size of the capture cross section decreases with the inverse of the square of the applied stress. When the applied stress is equal to the channeling stress, the size of the capture cross-section diverges. This behavior of the capture cross-section of a thread in response to applied film stresses is a critical element in understanding the link between local dislocation behavior and macroscopic film relaxation.

REFERENCES

[1] Baker SP. Plastic deformation and strength of materials in small dimensions. Mater. Sci. Eng. A 2001;319-321:16.

[2] Freund LB. The Stability of a Dislocation Threading a Strained Layer on a Substrate. J. Appl. Mech. 1987;54:553.

[3] Nix WD. Mechanical properties of thin films. Metall. Trans. A 1989;20:2217.

[4] Fertig RS, Pant P, Schwarz KW, Baker SP. Dislocation dynamics simulations of dislocation interactions and stresses in thin films. In preparation 2008.

[5] Essmann U, Mughrabi H. Annihilation of Dislocations During Tensile and Cyclic Deformation and Limits of Dislocation Densities. Philos. Mag. A 1979;40:731.

[6] Kusov AA, Vladimirov VI. The Theory of Dynamic Annihilation of Dislocations. Physica Status Solidi B-Basic Research 1986;138:135.

[7] Dodson BW. Dislocation Filtering - Why It Works, When It Doesnt. J. Electron. Mater. 1990;19:503.

[8] Beltz GE, Chang M, Speck JS, Pompe W, Romanov AE. Computer simulation of threading dislocation density reduction in heteroepitaxial layers. Philos. Mag. A 1997;76:807.

[9] Romanov AE, Pompe W, Beltz G, Speck JS. Modeling of threading dislocation density reduction in heteroepitaxial layers .2. Effective dislocation kinetics. Physica Status Solidi B-Basic Research 1997;199:33.

[10] Romanov AE, Pompe W, Beltz G, Speck JS. Modeling of threading dislocation density reduction in heteroepitaxial layers .1. Geometry and crystallography. Physica Status Solidi B-Basic Research 1996;198:599.

[11] Romanov AE, Pompe W, Beltz GE, Speck JS. An approach to threading dislocation "reaction kinetics". Appl. Phys. Lett. 1996;69:3342.

[12] Romanov AE, Pompe W, Mathis S, Beltz GE, Speck JS. Threading dislocation reduction in strained layers. J. Appl. Phys. 1999;85:182.

[13] Speck JS, Brewer MA, Beltz G, Romanov AE, Pompe W. Scaling laws for the reduction of threading dislocation densities in homogeneous buffer layers. J. Appl. Phys. 1996;80:3808.

[14] Fertig RS, Pant P, Schwarz KW, Baker SP. Dislocation dynamics simulations of dislocation interactions and stresses in thin films. Submitted to Acta Materialia 2009.

[15] Beltz GE, Chang M, Eardley MA, Pompe W, Romanov AE, Speck JS. A theoretical model for threading dislocation reduction during selective area growth. Mater. Sci. Eng. A-Struct. Mater. Prop. Microstruct. Process. 1997;234:794.

[16] Hirth JP, Lothe J. Theory of Dislocations. New York: John Wiley and Sons, Inc., 1982.

[17] Freund LB, Hull R. On the Dodson-Tsao excess stress for glide of a threading dislocation in a strained epitaxial layer. J. Appl. Phys. 1992;71:2054.

[18] Boyce WE, DiPrima RC. Elementary Differential Equations and Boundary Value Problems. New York: John Wiley & Sons, Inc., 1997.

[19] Pant P, Schwarz KW, Baker SP. Dislocation interactions in thin FCC metal films. Acta Mater. 2003;51:3243.

CHAPTER 5
THREADING DISLOCATION INTERACTIONS IN AN INHOMOGENEOUS STRESS FIELD: A STATISTICAL MODEL

Ray S. Fertig and Shefford P. Baker

Department of Materials Science and Engineering, Cornell University, Ithaca, NY 14853

ABSTRACT - A statistical model is presented to characterize the influence of stress field inhomogeneity on the probability of interactions between threading dislocations in thin films. Any degree of stress field inhomogeneity is shown to increase the likelihood of interactions between threading dislocations. However, below a critical level, the effect of stress inhomogeneity is negligible while above this level a dramatic effect is observed. The approach taken is applicable to any system of interacting particles with spatially dependent velocities.

5.1 Introduction

The behavior of dislocations in thin films has been a subject of study for several decades [1-4]. One area of focus has been the role of dislocation-dislocation interactions on mechanical behavior, specifically their role in strain hardening [5, 6]. The most stable dislocation-dislocation interactions at high stress have been shown to be interactions between two threading dislocations (threads) [7, 8], which extend through the thickness of a film. Computational [9-11] and experimental [12-14] results have shown that these interactions occur frequently, even though interactions between threads seem intuitively unlikely [15, 16] from a simple consideration of thread

density. Recent dislocation dynamics simulations results have suggested that the primary reason for the unexpectedly high rate of occurrence of thread-thread interactions is the presence of inhomogeneous stresses in the film [17]. Inhomogeneous stresses have been postulated theoretically [18] and observed experimentally [19, 20] in films, but their effect on thread-thread interactions has not been studied. In this study, we propose an analytical model to examine the effect of spatial inhomogeneities in the stress field of a thin film on the likelihood of thread-thread interactions, in order to obtain a more rigorous understanding of thin film mechanical behavior. The results are shown to be consistent with simulation results and a general trend is established: inhomogeneities in the stress field in a thin film *always* increase the likelihood of a thread-thread interaction. The model presented here is general to any system with interacting particles with velocities that have a fixed spatial dependence.

5.2 Statistical Model

In the model presented here, we assume that *M* threads move through a film divided up into *N* bins of equal size (Fig. 5.1), with a discrete stress associated with each bin. For simplicity, the inclination of a thread on its slip plane is ignored so that each thread can be represented by a single point in the *x*-*y* plane, as shown in Fig. 5.1. Because dislocations in thin films are constrained by the thickness of the film, there exists a critical resolved shear stress τ_c, below which a thread will not move [3, 21]. If the resolved shear stress τ on the thread exceeds τ_c, we assume that the thread moves with a velocity that is related to the excess stress $\tau_{exc} = \tau - \tau_c$ [4]. We assign a normalized excess stress $s_i = \frac{\tau_{exc,i}}{\tau_c}$ to each bin *i* such that $\sum_{i=1}^{N} s_i = N \int_{-\infty}^{\infty} sQ(s)ds$, where

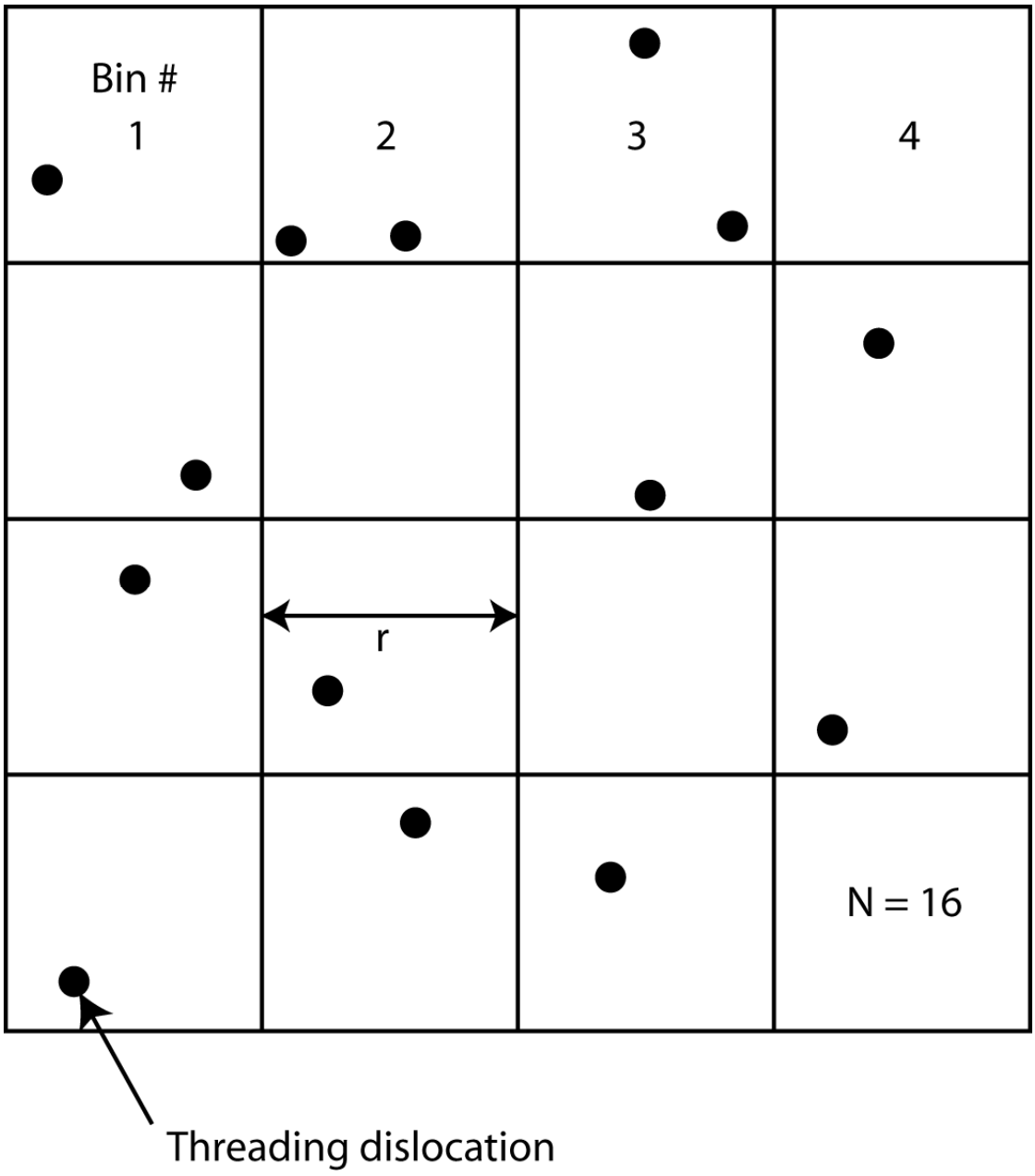

Figure 5.1. Plan view schematic of film divided into equally sized bins. Each bin has a particular shear stress associated with it. Threading dislocations, indicated by filled circles, are distributed throughout the film in a way that depends on the stress distribution.

Q(s) is some probability density function that describes the distribution of film stresses. We assume that any thread in bin *i* moves with velocity $v_i = \beta s_i^n$ [4], where β is the thread mobility and *n* is the stress exponent.

As threads move through the film, they spend time $t_i = (r/\beta)s_i^{-n}$ in each bin, where *r* is the width of a bin. The probability p_i that a single dislocation will be in a particular bin *i* at a given time is then just the fraction of time spent in bin *i* relative to the time required to move through all the bins,

$$p_i = \frac{t_i}{\sum_{j=1}^{N} t_j} = \frac{s_i^{-n}}{\sum_{j=1}^{N} s_j^{-n}} = \frac{1}{N s_i^n \left\langle s^{-n} \right\rangle}, \tag{5.1}$$

where the notation $\left\langle s^{-n} \right\rangle$ indicates the average value of s^{-n}. Because s^{-1} diverges as *s* approaches zero we introduce a cutoff parameter, *c*, such that $s \geq c$ in every bin. Physically, *c* sets a lower limit on thread velocity. The average value in Eq. (5.1) can be easily obtained from the probability density function *Q(s)*,

$$\left\langle s^{-n} \right\rangle = \int_c^{\infty} Q(s) s^{-n} ds . \tag{5.2}$$

Eq. (5.1) describes a Bernoulli distribution for each bin, thus the probability $P_{k,i}$ that *k* out of *M* threads are in bin *i* is written as

$$P_{k,i} = \frac{M!}{k!(M-k)!} p_i^k (1-p_i)^{M-k} . \tag{5.3}$$

Because the focus of this study is the effect of stress inhomogeneity on the likelihood of a thread-thread interaction, we require the width *r* of each bin to be equal to an interaction radius, such that any two threads in the same bin will interact. The probability of a thread-thread interaction occurring in any bin *i* is then

$$P_{\text{int},i} = \sum_{k=2}^{M} P_{k,i} . \tag{5.4}$$

Significant simplifications can be made to Eqs. (5.3) and (5.4) by considering only the case where $p_i << 1$, such that the likelihood of two threads being in a single bin is low and the likelihood of three or more threads can be neglected. This requires

that the number of threads relative to the number of bins be small, $M/N << 1$. Since $\rho_{TD} = M/A$ and $r = \sqrt{A/N}$, where ρ_{TD} is the thread density and A is the film area, we have

$$M/N = \rho_{TD} r^2 . \tag{5.5}$$

Thus, an equivalent requirement is $\rho_{TD} r^2 << 1$. Recent analytic results have shown that $r \sim 100b$ [22], so $M/N << 1$ is satisfied for all $\rho_{TD} << 10^{-4} b^{-2}$. For higher dislocation densities, the occurrence of more than two threads in the same bin cannot be neglected. However, even at higher thread densities, the qualitative conclusions presented here will be unaffected, since the factors that facilitate interactions between two threads will also facilitate interactions between multiple threads.

Substituting Eq. (5.3) into Eq. (5.4) and neglecting occurrences of more than two dislocations per bin, yields

$$P_{\text{int},i} \approx P_{2,i} = \frac{M(M-1)}{2} p_i^2 (1-p_i)^{M-2} . \tag{5.6}$$

For the case $p_i << 1$, the exponential term in Eq. (5.6) can be replaced with the first term of a Taylor series

$$P_{\text{int},i} \approx \frac{M(M-1)}{2} p_i^2 (1-(M-2)p_i) . \tag{5.7}$$

Substituting Eq. (5.1) into Eq. (5.7) and assuming that $M >> 1$, gives

$$P_{\text{int},i} \approx \frac{M^2}{2N^2} \left(\frac{s_i^{-2n}}{\langle s^{-n} \rangle^2} - \frac{M}{N} \frac{s_i^{-3n}}{\langle s^{-n} \rangle^3} \right). \tag{5.8}$$

The number of interactions ϕ is then determined by taking the average of $P_{int,i}$ over i bins and multiplying by N,

$$\phi = N \langle P_{\text{int}} \rangle = \frac{M^2}{2N} \left(\frac{\langle s^{-2n} \rangle}{\langle s^{-n} \rangle^2} - \frac{M}{N} \frac{\langle s^{-3n} \rangle}{\langle s^{-n} \rangle^3} \right). \tag{5.9}$$

Multiplying ϕ by two threads per interaction and dividing by M gives the fraction of threads f involved in a thread-thread interaction, which can be written, using Eq. (5.5), as

$$f = \rho_{TD} r^2 \left(\frac{\left\langle s^{-2n} \right\rangle}{\left\langle s^{-n} \right\rangle^2} - \rho_{TD} r^2 \frac{\left\langle s^{-3n} \right\rangle}{\left\langle s^{-n} \right\rangle^3} \right). \tag{5.10}$$

The fraction of interacting threads in a homogeneous field f_h, where $\left\langle s^{-2n} \right\rangle = \left\langle s^{-n} \right\rangle^2$, is then given by $f_h = \rho_{TD} r^2 \left(1 - \rho_{TD} r^2\right)$.

In order to examine the effect of stress inhomogeneity on f in Eq. (5.10), a distribution $Q(s)$ must be constructed. It has been shown via discrete dislocation dynamics simulations [17] that the resolved shear stresses in a film are well characterized by a normal distribution. Thus, the stresses used in this study are assumed to be normally distributed following

$$F(s) = \frac{1}{\sigma\sqrt{2\pi}} \exp\left(-\frac{1}{2} \left(\frac{s-\mu}{\sigma} \right)^2 \right), \tag{5.11}$$

where μ and σ are the mean value and standard deviation of s, respectively. Because only the values of s between the cutoff stress c and infinity are allowed, the distribution in Eq. (5.11) is truncated below c and normalized such that the integral over the new probability density function $Q(s)$ is unity,

$$Q(s) = \begin{cases} \left[\int_c^\infty F(s) ds \right]^{-1} F(s), & s \geq c \\ 0, & s < c \end{cases}. \tag{5.12}$$

5.3 Results and discussion

After constructing this probability density function, f is determined from Eq. (5.10), using $Q(s)$ as in Eq. (5.2) to solve for the necessary averages. We examined the

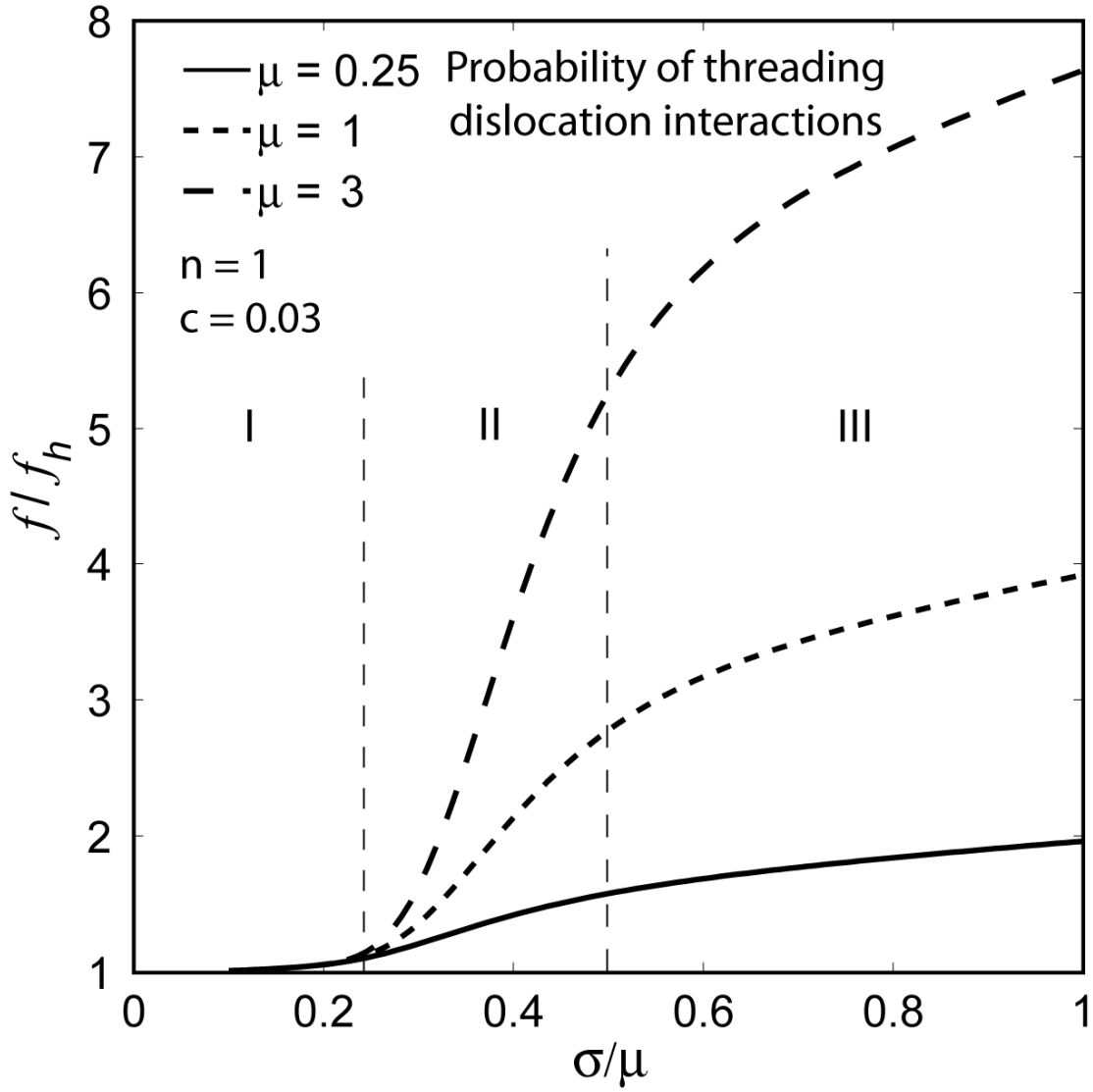

Figure 5.2. Normalized probability of interactions between threading dislocations versus the coefficient of variation (standard deviation/mean) of the stress distribution. For all $\sigma/\mu \geq 0.25$, $f/f_h > 1$, *which indicates any inhomogeneity increases the likelihood of thread-thread interactions*

effect of varying σ, μ, n, and c on the fraction of interacting threads f normalized by f_h. Fig. 5.2 shows the effect of varying μ and σ on f/f_h, where c and n are held constant at 0.03 and 1, respectively. The data are plotted as a function of the coefficient of variation, σ/μ, which represents the degree of inhomogeneity in the stress field. A general observation is that f/f_h is greater than unity for all values of σ and μ, which indicates that stress inhomogeneity *always* increases the likelihood of thread-thread interactions from that of a homogeneous stress field. Furthermore, any increase in inhomogeneity continues to increase the likelihood of interaction. The curves can be divided up into three regions relatively independent of μ. The first is from $\sigma/\mu = 0$ to $\sigma/\mu \approx 0.25$, where increases in σ/μ increase the likelihood of interaction only slightly. The second region is from $\sigma/\mu \approx 0.25$ to $\sigma/\mu \approx 0.5$, where a rapid increase in interaction likelihood is observed for a relatively small increase in σ/μ. The threshold value of $\sigma/\mu \approx 0.25$ is unexpected and represents a remarkable change in the influence of stress inhomogeneity. In the third region, $\sigma/\mu > 0.5$, the interaction likelihood continues to increase, but at a decreasing rate. This is expected since f/f_h is bounded by $1/f_h$. The values of $\rho_{TD}r^2$ were also varied (not shown) and it was observed that the curves displayed in Fig. 2 were essentially unchanged for different values of $\rho_{TD}r^2 << 1$.

The effect of the stress exponent n is illustrated in Fig. 5.3a, where μ and c are held constant at 1.0 and 0.03, respectively. Here n is shown to scale the effect of stress inhomogeneity, which increases with increasing n. The qualitative trends for $n = 1/2$ and 3/2, however, are the same as for $n = 1$: inhomogeneous stress facilitates thread-thread interactions, especially for $\sigma/\mu > 0.25$. The primary effect of changing n is a drastic change in the effect of inhomogeneous stresses for $\sigma / \mu > 0.25$, where an increase in n results in a substantial increase in interaction likelihood. Below this threshold value, the effect of changing n is much less pronounced. These results

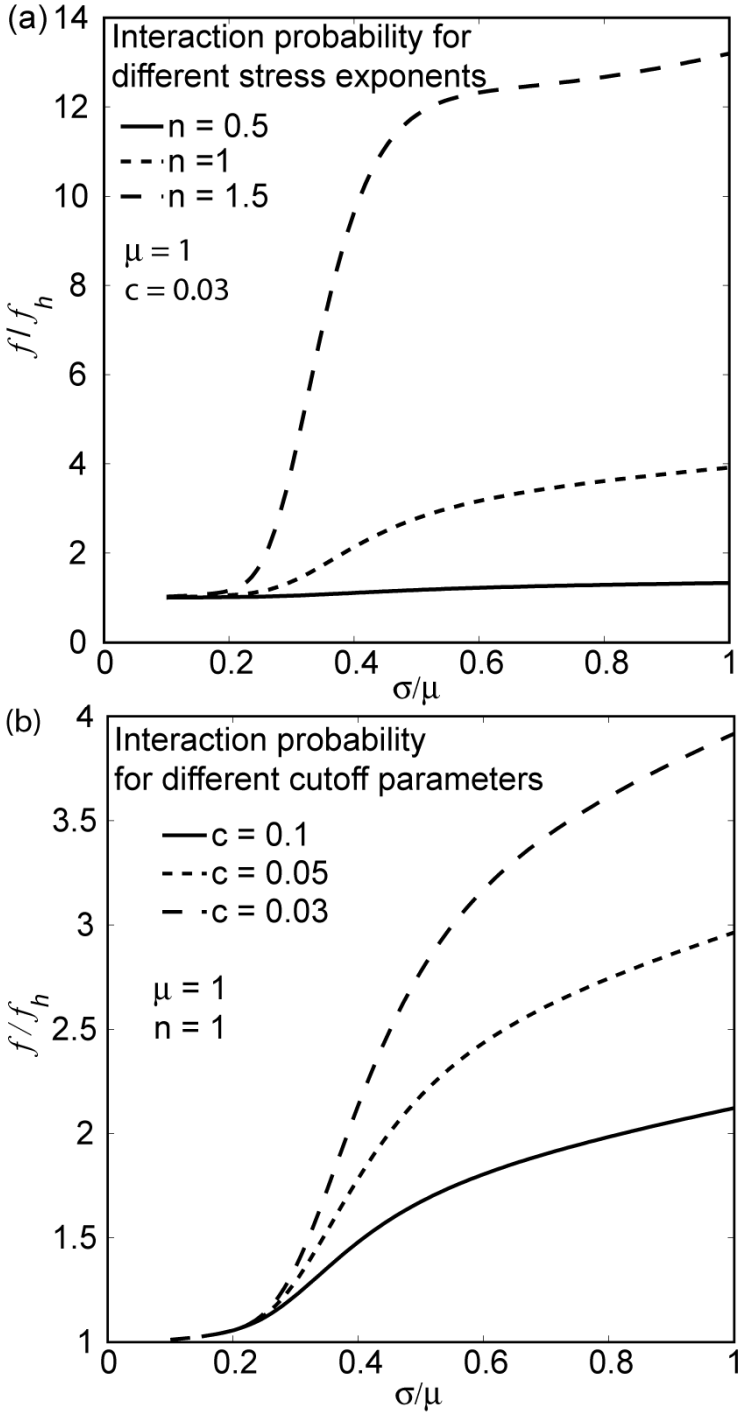

Figure 5.3. Normalized probability of interactions between threading dislocations versus the coefficient of variation (standard deviation/mean) of the stress distribution for different (a) stress exponents n and (b) cutoff parameters c. Note that neither n nor c qualitatively affects the results.

indicate that precise understanding of the relationship between the force on a thread and thread velocity is critical for determining the frequency with which thread-thread interactions occur and, consequently, for developing accurate strain hardening models. Fig. 5.3b shows the effect of changing the cutoff parameter c, for $\mu = 1$ and $n = 1$. As was observed when n was varied, the variation of c does not change the qualitative results observed in Fig. 5.2. Decreasing c has the effect of increasing the likelihood of interaction due to the fact that lower dislocation velocities are allowed with lower values of c. Again, the effects of changing c are confined predominantly to the region $\sigma / \mu > 0.25$.

Several comments regarding the applicability of this model to real films are warranted. In order for Eq. (5.1) to precisely describe the probability of a thread being in bin i, the thread must sample every bin. If a film with some inhomogeneous stress field is initially seeded randomly with threads, the thread locations would be uncorrelated to the stresses and the corresponding fraction of threads that would interact would be characterized by f_h. In this case, Eq. (5.1) becomes more precise as the threads move through an increasing number of bins, spending more time in low stress bins and less time in high stress bins. Thus, for a particular instant in time, the likelihood of interactions in a real film will have lower and upper bounds f_h and f, respectively. A second difference is that in this model, threads are assumed to be able to move into any bin, but in real films threads are confined to move on their slip planes. This difference does not invalidate the qualitative results provided that stresses in the real film do not vary systematically in space, *e.g.* one edge of the film is at high stress and another edge is at low stress. If the film stresses in a real film are such that a thread moving along a slip plane samples stresses that satisfy a probability density function $Q(s)$, the probability in Eq. (5.1) will still be valid. Therefore the probability of interaction, as calculated from Eq. (5.8), is valid in a real film if a sufficient number

of threads are traveling on intersecting paths. Finally, the stresses are continuous and correlated in real films, but in the model proposed here they are discrete and random. Because the stresses in the model were only used to get a distribution of velocities, we do not believe this assumption introduces significant qualitative differences between real films and model films.

Regardless of the precise description of the stress field, two features of Eq. (5.10) are notable. First, the fraction of threads that interact is expected to vary linearly with the thread density. Second, a parabolic dependence of thread-thread interactions on interaction radius is expected. The interaction radius has been shown to be inversely proportional to the stress [22] for positive excess stress, so higher μ would decrease r and result in a lower f. However, as long as $\rho_{TD} r^2 << 1$, changes in r have only a negligible effects on the normalized f/f_h shown in Fig. 5.2.

The prediction that inhomogeneous stresses increase the likelihood of thread-thread interactions is consistent with recent dislocation dynamics simulations of passivated single crystal thin films [17]. In these simulations, the stress field was such that σ/μ was always greater than the threshold value of $\sigma/\mu \approx 0.25$ during relaxation. Thus the proposed model would predict a much higher number of thread-thread interactions than expected from a basic thread density calculation. In the simulations, the *majority* of threads were immobilized by thread-thread interactions rather than by interactions with misfit dislocations at the interface, which is surprising given the high density of misfit dislocations relative to threads. However, consistent with the analytical model developed here, the thread-thread interactions were also observed to occur nearly exclusively in regions of low film stress.

In summary, the model presented here can be used to examine the effect of stress inhomogeneity on the likelihood of thread-thread interactions in a thin film. The primary result is that the probability of thread-thread interactions is *always* greater in

an inhomogeneous field than in a homogeneous field. It was shown that the fraction of interacting threads should be proportional to the thread density and to the square of the interaction radius, which has been related elsewhere [22] to the mean stress. A threshold value of the coefficient of variation of the shear stress $\sigma/\mu \approx 0.25$ was found such that, below this value, the influence of the stress inhomogeneity and stress exponent on the fraction of interacting threads is low. Above this critical value, the effects of the stress inhomogeneity are striking, with the probability of thread-thread interactions becoming significantly greater than in a homogeneous field. Finally, a strong sensitivity to the stress exponent was shown, which demonstrates the need for precise understanding of stress-velocity relationship in films. We would like to point out that the approach presented here is not limited to dislocations in films. Rather, it is applicable to any system with interacting objects that move with a velocity related by a power law to a spatially inhomogeneous field.

This work was funded by the National Science Foundation Contract No. DMR-0311848. R. F. thanks S. Hicks for his useful discussion on the statistical aspects of this problem.

REFERENCES

[1] F. C. Frank and J. H. van der Merwe, Proc. R. Soc. A **198**, 205 (1949).

[2] J. W. Matthews and A. E. Blakeslee, J. Cryst. Growth **27**, 118 (1974).

[3] W. D. Nix, Metall. Trans. A **20A**, 2217 (1989).

[4] L. B. Freund and S. Suresh, *Thin Film Materials: Stress, Defect Formation and Surface Evolution* (Cambridge University Press, Cambridge, United Kingdom, 2003).

[5] L. B. Freund, J. Appl. Phys. **68**, 2073 (1990).

[6] W. D. Nix, Scripta Mater. **39**, 545 (1998).

[7] K. W. Schwarz, J. Appl. Phys. **85**, 120 (1999).

[8] P. Pant, K. W. Schwarz, and S. P. Baker, Acta Mater. **51**, 3243 (2003).

[9] G. E. Beltz, M. Chang, J. S. Speck, W. Pompe*, et al.*, Philos. Mag. A **76**, 807 (1997).

[10] K. W. Schwarz, Phys. Rev. Lett. **91**, 145503 (2003).

[11] P. Pant, K. W. Schwarz, and S. P. Baker, Unpublished (2006).

[12] B. W. Dodson, J. Electron. Mater. **19**, 503 (1990).

[13] F. K. LeGoues, Phys. Rev. Lett. **72**, 876 (1994).

[14] E. A. Fitzgerald, M. T. Currie, S. B. Samavedam, T. A. Langdo*, et al.*, Phys. Status Solidi A **171**, 227 (1999).

[15] R. Hull, J. C. Bean, R. E. Leibenguth, and D. J. Werder, J. Appl. Phys. **65**, 4723 (1989).

[16] M. J. Matragrano, D. G. Ast, G. P. Watson, and J. R. Shealy, J. Appl. Phys. **79**, 776 (1996).

[17] R. S. Fertig, P. Pant, K. W. Schwarz, and S. P. Baker, Unpublished (2006).

[18] U. Jain, S. C. Jain, A. Atkinson, J. Nijs*, et al.*, J. Appl. Phys. **73**, 1773 (1993).

[19] M. A. Phillips, R. Spolenak, N. Tamura, W. L. Brown*, et al.*, Microelec. Engr. **75**, 117 (2004).

[20] T. J. Balk, G. Dehm, and E. Arzt, Acta Mater. **51**, 4471 (2003).

[21] L. B. Freund, J. Appl. Mech. **54**, 553 (1987).

[22] R. S. Fertig and S. P. Baker, Unpublished (2006).

CHAPTER 6
MULTISCALE MODELING OF THIN FILMS: LINKING DISLOCATION DYNAMICS WITH MACROSCOPIC MECHANICAL BEHAVIOR

Ray S. Fertig, III[1] and Shefford P. Baker[2]

[1]*Firehole Technologies, Inc.; 210 South 3rd Street; Laramie, WY 82070, USA*

[2]*Department of Materials Science and Engineering, Cornell University; Ithaca, NY 14853, USA*

ABSTRACT - The difficulty in linking macroscopic mechanical behavior of thin films with dislocation-level behavior has hampered multiscale modeling efforts in thin films for many years. Previous research has suggested that knowledge of particular dislocation interactions cannot be readily translated into knowledge of film strength. But in this work, we present a method to unite dislocation dynamics with macroscopic mechanical behavior of thin films. We use dislocation dynamics simulations to statistically characterize the relationship between stress evolution and the behavior of dislocations in films, including specific interactions and interaction strengths. Our novel method applies the knowledge obtained from the simulations to predict not only macroscopic mechanical behavior, but also the types of dislocation interactions that occur, as well as the distribution of stresses.

6.1 Introduction

The behavior of dislocations in films has been a topic of experimental and analytical study for more than half a century [1-4], with extensive computational study

for the past fifteen years [5-10]. But despite these efforts, the link between, say, the strength of a particular type of dislocation interaction and the global mechanical behavior of a film has not been uncovered. This inability to link behavior of individual dislocations with macroscopic film behavior stems from several difficulties: (1) the multitude of types of dislocation interactions and their varied strengths, (2) the difficulty comparing experimental observations obtained by electron microscopy with macroscopic stress-strain behavior of the same film, (3) the immense computational resources required to perform detailed three-dimensional simulations of many interacting dislocations, and (4) the uncertainty of the effect of grain boundaries and interfaces on dislocation mobility, nucleation, and annihilation. Recently, however, we have developed a methodology to overcome some of these challenges in the case of passivated films on rigid substrates.

The methodology that we present here is the result of much study of dislocations in thin films via large-scale three-dimensional dislocation dynamics simulations [11, 12]. A review of these results and their relationship to other work in the field is published elsewhere [13]. The picture of dislocation behavior that emerges is described here as a way of summarizing our previous conclusions and laying the foundation for the model developed below. In any film with some supply of threading dislocations (threads), the threads will propagate through the film, as shown in Figure 1, when the applied stress σ_{app} in the film at the location of the thread is greater than a thickness-dependent critical stress called the channeling stress σ_{ch} [14]. As the thread moves through the film, it deposits misfit dislocations (misfits) at the film/substrate and film/passivation interfaces. These misfits relax the macroscopic strain, but cause a local stress fluctuation near the misfit. This means that as the misfit structure develops, an inhomogeneous stress field develops with it. The thread stops moving when either the local stress on the thread is less than the channeling stress or the thread interacts

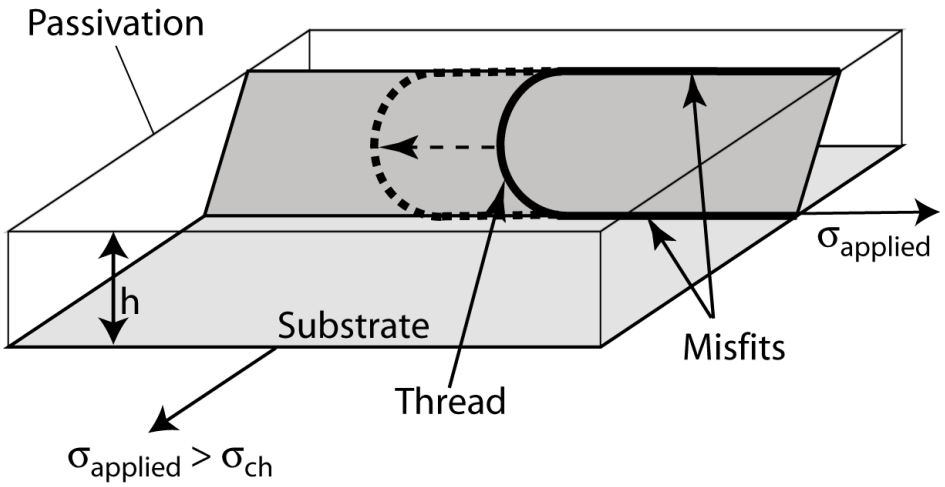

Figure 6.1. A schematic of a threading dislocation (thread) gliding through a film depositing misfit dislocations at the film/substrate and film/passivation interfaces.

with another thread or misfit at a location where the local stress on the interacting thread is less than the strength of the dislocation interaction. Our simulations have shown that the former is sufficiently rare so that *threads can be considered to stop simply when they interact with another dislocation and the local stress felt by the interacting thread is less than the strength of the interaction.*

We can further distinguish between two fundamentally different modes of thread interactions: thread-thread interactions and thread-misfit interactions. Our dislocation dynamics simulations showed that thread junctions and thread annihilations were the primary thread-thread interactions responsible for stopping threads. The strength of these interactions is almost always higher than any stress in the film at any time [8, 13]. Thus, in our model we assume that *any* thread-thread interaction will stop the involved threads from further propagation through the film, regardless of where they occur in the film. (However, these interactions typically do occur in regions of low stress, but this is a result of varying thread velocities in the film and increasing size of the capture cross-section of the thread, not as a result of the strength of the interaction.)

Interactions between threads and misfits are relatively weak, with strengths only between about $\tau_{TM} = 1.0\,\tau_{ch}$ to $\tau_{TM} = 1.3\,\tau_{ch}$ [8]. Thus, as the film stress increases above these values, a local stress level below the average stress is required for the interaction to stop the thread. In our model, we assume that a thread-misfit interaction will stop a thread when it encounters *any* local region of stress lower than the interaction strength of a thread-misfit interaction. This is reasonable because the regions of low stress tend to be heavily populated by misfits. Implicitly, we are assuming that all thread-misfit interactions have the same strength. However, as we will show, selecting a single nominal value for the thread-misfit strength gives film strengths within ~10% of using either the upper or lower bound on thread-misfit interaction strengths.

This paper outlines the development of a model for dislocation-mediated film relaxation and strength based on fundamental behavior of individual dislocations. We have already outlined a simple picture of film relaxation. In the next section we develop the equations for the model. This is done by reducing the problem of film relaxation to the problem of quantifying the distance a thread travels before stopping in a thread-misfit interaction and the distance a thread travels before stopping in a thread-thread interaction during some increment of thread motion. Following the development of the model, we compare model results with results from dislocation dynamics simulations. We also examine the effects of local stress inhomogeneities on film stresses, as an example of the utility of the analytical model, and show that stress inhomogeneity significantly increases strain hardening of a film.

6.2 Strain hardening model

We begin constructing a strain hardening model in a manner similar to the model proposed by Freund [15]. The total strain ε in the film is simply the sum of the applied strain ε_{app} and the strain relaxed by the dislocations ε_P. The strain relaxation rate due to the glide of threading dislocations $\dot{\varepsilon}_P$ is given by the simple equation

$$\dot{\varepsilon}_P = -\alpha \rho_T b v , \tag{6.1}$$

where α is a geometric factor that depends on the slip system of interest, the existence of a passivation layer, and the orientation of the film; ρ_T is the mobile thread density; b is the Burgers vector; and v is the average velocity of the mobile threads. For this model we assume an average velocity that is proportional to the difference between the film stress and the channeling stress, a quantity termed excess stress τ_x.

$$v = M \tau_x , \tag{6.2}$$

where M is the dislocation mobility. The excess stress can be written as

$$\tau_x = \mu\left(\varepsilon_{app} - \varepsilon_{ch} + \varepsilon_P\right), \tag{6.3}$$

where ε_{ch} is the channeling strain. Substituting Equations (6.2) and (6.3) into (6.1) yields the governing differential equation for plastic strain relaxation.

$$d\varepsilon_P = -\alpha M \mu b \rho_T(t)\left(\varepsilon_{app} - \varepsilon_{ch} + \varepsilon_P\right)dt \tag{6.4}$$

Equation (6.4) is a simple, general equation that describes macroscopic film relaxation by dislocations in all films. All of the microscale behavior is contained in the term for mobile thread density. The difficulty in equation (6.4) is determining how the density of mobile threads varies in time. Thus, we see that the crucial questions that must be answered in order for this model to be useful are: What stops threads? And how far do the travel before stopping?

To answer these questions, we begin by considering the potential contributions to the change in mobile threading density. Mobile thread density can increase by nucleation of new dislocations $d\rho_{nuc}$ or by previously stopped threads breaking free from an immobilizing interaction $d\rho_{brk}$. The mobile thread density decreases by threads stopping in thread-thread interactions $d\rho_{TT}$ or by threads stopping in thread-misfit interactions $d\rho_{TM}$. Thus, the total change in mobile threads can be written as

$$d\rho_T = d\rho_{nuc} + d\rho_{brk} - d\rho_{TT} - d\rho_{TM}\ . \tag{6.5}$$

For the sketch here we will neglect the contribution due to nucleation, as this was not simulated in our dislocation dynamics simulations. For the purposes of illustration, we model the case of a constant applied strain; thus $d\rho_{brk}$ is negligible. We note, however, that if a constant strain rate were modeled, $d\rho_{brk}$ could play a significant role. Thus, Eq. (6.5) is reduced to

$$d\rho_T = -d\rho_{TT} - d\rho_{TM}\ . \tag{6.6}$$

The density of mobile threads stopped by thread-thread interactions after moving some distance dx is approximately

$$d\rho_{TT} = \frac{C_1 \rho_T dx}{\lambda_{TT}}, \tag{6.7}$$

where C_1 is a constant of order unity and λ_{TT} is the average distance that a thread travels before interacting with another thread. Via simple geometric arguments

$$\lambda_{TT} = \frac{C_2}{2r\rho_T}, \tag{6.8}$$

where C_2 is a constant of order unity and r is the average radius of a capture cross-section. The capture cross-section around a thread is defined such that any other thread inside this cross-section that can interact to form a junction or annihilate with the thread *will* form this interaction. Substituting Eq. (6.8) into (6.7) and using the fact that $dx = vdt$ gives the change in thread density due to thread-thread interactions in some time dt

$$d\rho_{TT} = 2\beta r v \rho_T^2 dt, \tag{6.9}$$

where β is a constant of order unity.

The rate of TM interactions can be approximated in a manner similar to the thread-thread interactions,

$$d\rho_{TM} = \frac{\gamma \rho_T dx}{\lambda_{TM}}, \tag{6.10}$$

where λ_{TM} is the average distance traveled by a thread before stopping in a thread-misfit interaction. This is just the distance between regions of stress lower than the average thread-misfit interaction strength. Unlike the case of thread-thread interactions, λ_{TM} is not dependent on the thread density. Thus, we can write the change in thread density due to blocking by misfits in some time dt as

$$d\rho_{TM} = \frac{\gamma \rho_T v}{\lambda_{TM}} dt, \tag{6.11}$$

where γ is a constant of order unity. Substituting Eqs. (6.9) and (6.11) into Eq. (6.6) yields

$$\frac{d\rho_T}{dt} = -v\left(2\beta r \rho_T^2 + \frac{\gamma}{\lambda_{TM}} \rho_T\right). \tag{6.12}$$

Equation (6.12) describes the microscale behavior of the film using fundamental quantities about individual dislocation behavior and local film stress. The difficultly in solving Eq. (6.12) is that r is dependent on local film stress; and λ_{TM} is dependent on average film stress, the magnitude of the stress fluctuations, and the strength of a thread-misfit interaction. Below, we summarize previous work in which all of these quantities were extensively studied using three-dimensional dislocation dynamics simulations [12].

Using an analytical model, we showed that the relationship of the capture cross-section A of a thread is related to the excess stress by

$$A\left(\frac{\tau_{ch}}{\mu b}\right)^2 = \begin{cases} \chi_1\left(\dfrac{-\tau_{ch}}{\tau_x}\right), & \tau_x < 0 \\ \chi_2\left(\dfrac{\tau_{ch}}{\tau_x}\right)^2, & \tau_x \geq 0 \end{cases}, \tag{6.13}$$

where $\chi_1 \sim 0.02$ and $\chi_2 \sim 2$ for the film modeled here. For the purposes of relaxation at a constant strain, we assume that the excess stress is always greater than or equal to zero. If we assume a circular capture cross-section, the interaction radius is

$$r(\tau_x) = \sqrt{2}\,\frac{\mu b}{\tau_x}. \tag{6.14}$$

Using dislocation dynamics simulations we showed that the average distance traveled by a thread before interacting with a misfit was simply a function of the difference between thread-misfit interaction strength τ_{TM} and a measure of the low stress regions $\left(\tau_x + \tau_{ch} - \hat{\tau}\right)$,

$$\lambda_{TM} = \frac{1}{\phi}\exp\left[-\eta\left(\frac{\tau_{TM} - \left(\tau_x + \tau_{ch} - \hat{\tau}\right)}{\tau_{ch}}\right)\right], \tag{6.15}$$

where ϕ and η are constants, and $\hat{\tau}$ is the standard deviation of the resolved shear stress on a slip plane. For the 200 nm film we simulated, $1/\phi =$ 508 nm and $\eta \sim 2.763$ [12].

Having defined the functional forms for λ_{TM} and r, we can rewrite Eq. (6.12) using Eqs. (6.2), (6.14), and (6.15) to give

$$\frac{d\rho_T}{dt} = -M\tau_x\left(2\beta\sqrt{2}\,\frac{\mu b}{\tau_x}\,\rho_T^2 + \gamma\phi\exp\left[\eta\left(\frac{\tau_{TM} - \left(\tau_x + \tau_{ch} - \hat{\tau}\right)}{\tau_{ch}}\right)\right]\rho_T\right), \tag{6.16}$$

Simplifying Eq. (6.16) yields

$$\frac{d\rho_T}{dt} = -M\left(2\beta\sqrt{2}\mu b\rho_T^2 + \tau_x\gamma\phi\exp\left[\eta\left(\frac{\tau_{TM} - \tau_x + \hat{\tau}}{\tau_{ch}} - 1\right)\right]\rho_T\right). \tag{6.17}$$

Equation (6.17) coupled with Eq. (6.4) describes film relaxation using both microscale and macroscale quantities. The solution of this system and it's comparison with simulation results is presented in the following section.

6.3 Comparison of the analytical model with dislocation dynamics simulation results

We now compare the analytical model developed above with the results from dislocation dynamics simulations [11]. To evaluate the analytical model, we use a simple forward-integration scheme to solve Eqs. (6.4) and (6.17) simultaneously, using Eq. (6.3) to relate the strains to the excess stress. For the purpose of comparison, we use same material parameters as the simulation: M = 1 m/MPa-s, μ = 42 GPa, b = 0.255 nm, and τ_{ch} = 72.8 MPa. From the simulation results we were able to calculate ϕ = 1/(508 nm) and η = 2.763. The geometric parameter $\alpha = 2/\sqrt{6}$ was used to model a (001) passivated fcc film with threads moving only on slip systems that can relax an applied biaxial stress.

In the dislocation dynamics simulation, loading was performed via five strain increments, with dislocations allowed to relax each increment until all dislocations had stopped moving. The applied strain in the analytical model was held constant and allowed to relax at the same strain intervals as the simulation:

$\varepsilon_{app} = 1.3, 1.8, 2.3, 2.8, \text{and } 3.3\frac{\tau_{ch}}{\mu}$. In the simulation, dislocation loops were randomly seeded on each of the eight active slip planes that relax a biaxial stress in a (001) film; each loop contributed two threads. To account for this initial density in our model, the initial thread density for the first strain increment was $\rho_{T,0} = 8.75 \times 10^{12}$ m^{-2}, which corresponds to 140 threads in a 16 μm^2 film and gives an initial plastic strain of $\varepsilon_{P0} = -1.2281 \times 10^{-4}$. As discussed above, the increment in strain may cause some dislocations to break free. We do not currently have a functional form for this, so the change in mobile thread density for each jump in strain was assumed to be the same as the simulations. Also, to further match the dislocation dynamics simulations, the standard deviation of stress $\hat{\tau}$ at the end of each interval of the simulations was applied for the entire increment in the model.

Given the simplifications and assumptions in analytical model, its agreement with the results from the dislocation dynamics simulations is remarkable. These results are shown in Figure 6.2. The stresses for the analytical model are presented as equivalent biaxial stresses, where the equivalent biaxial stress σ_{biax} is related to the resolved shear stress $\sigma_{biax} = \tau_{RSS}\sqrt{6}$ in the case of an (001) fcc film. The open squares correspond to the dislocation dynamics simulation results. The solid curve gives results of the analytical model for thread-misfit strength of $1.15\tau_{ch}$. The dashed and dotted curves show model results for the extreme values of thread-misfit interaction strength of $1.0\tau_{ch}$ and $1.3\tau_{ch}$, respectively. The solid curve with open circles shows the model prediction of the film stress when the stress inhomogeneity is taken to be zero. As was

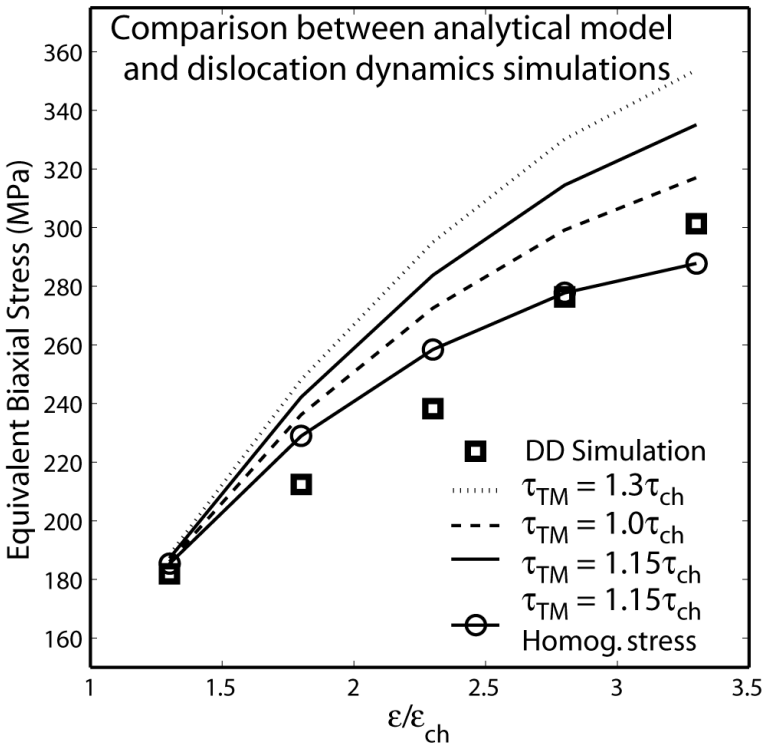

Figure 6.2. Comparison between the analytical model presented in Eqs. (6.4) & (6.16) with the results of dislocation dynamics simulations (open squares). The analytical model results for thread-misfit interaction strength of $1.15\,\tau_{ch}$, $1.3\,\tau_{ch}$ and $1.0\,\tau_{ch}$, are shown by the solid, dotted, and dashed curves, respectively. The solid curve with open circles represents the predicted film stress for thread-misfit interaction strength of $1.15\,\tau_{ch}$ when stress inhomogeneity is set to zero in the model.

mentioned above, the film stress difference using either extreme value for the thread-misfit strength and using the nominal value is less than ~10%, so using a single value to characterize thread-misfit strength appears warranted.

Perhaps the most striking result from studying the analytical model is the significance of stress inhomogeneity. We have qualitatively argued that stress inhomogeneity plays a large role in film stress, but have been unable to quantify its effect prior to developing this model [13]. For a thread-misfit strength of $1.15t_{ch}$, including realistic inhomogeneous stresses shows a strengthening of about 160 MPa. But modeling the film as one with only homogeneous stresses shows a strengthening of about 100 MPa. Thus, stress inhomogeneity accounts for about 40% of the strengthening that was observed in the simulations.

Although our model is in good agreement with the dislocation dynamics simulations, the agreement is not exact. Several features of the dislocation dynamics simulations could not be modeled using this model. First, the relationship between 1-D relaxation and 3-D relaxation that was used for the model assumed that the dislocations were evenly divided among all active slip systems, which was not the case in the dislocation dynamics simulations. Second, the stress inhomogeneity in the model is taken to be constant throughout each relaxation increment. In the dislocation dynamics simulations, this value varied throughout the relaxation. Finally, we assumed that threads always stopped when they encountered low stress regions less than some chosen interaction strength. It would be possible in the dislocation dynamics simulation for there not to be an available misfit to interact with, so that the thread could move farther and cause more film relaxation. Despite these shortcomings, however, the analytical model captures the major features of dislocation-mediated relaxation in a film.

The impact of our results cannot be overstated: we have constructed a model for film stress based on individual dislocation behavior and pairwise interactions that is in remarkable agreement with three-dimensional dislocation dynamics simulations that took roughly 100,000,000 times longer to calculate. This is critical, since the dislocation dynamic simulations cannot be run to strains much higher than shown here without an extreme increase in the already high computational burden due to the number of misfit dislocations that exist in the model. The strain hardening rates are also in good agreement with the simulation results and the quantitative values of the stresses are also close. In addition, the analytical model gives us a way to evaluate the contributions of stress inhomogeneity and different types of dislocation interactions to the film stress. We also point out that most experimental measurements (e.g. [16, 17]) of the stress-strain behavior of single-crystal films show a stress plateau similar to the one predicted by the analytical model, most easily seen in the case with homogeneous stresses. We expect this to occur in the dislocation dynamics simulations but cannot run them to high enough strains.

The analytical model presented in this paper contains several simplifying assumptions that could be enhanced to increase its level of sophistication. First, the relationship between the density of misfit dislocations ρ_{TM} and the stress inhomogeneity $\hat{\tau}$ in the film needs to be determined so that this relationship does not have to be extracted from dislocation dynamics simulations. Second, the model could be extended to incorporate different amounts of plastic strain from different slip systems; this could be accomplished by extending these 1-D equations to a full 3-D tensor representation. Third, the velocity of the thread of the thread varies as it moves through the film because of stress fluctuations. We have shown that this causes threads to concentrate in regions of low stress [13]; this concentration is ignored in the model except through arbitrarily increasing β. Finally, in order to extend the model to include

complex load histories, the functional form for breaking interactions $\rho_{brk}(t)$ to create mobile threads needs to be determined. And if nucleation during loading plays a significant role in creating mobile threads, the its functional form must also be determined $\rho_{nuc}(t)$. Despite these additional features for modeling varied loadings, the analytical model presented here represents a significant step toward developing a model to link the microscopic behavior of dislocations with the macroscopic behavior of a film.

REFERENCES

[1] Frank FC, van der Merwe JH. One-Dimensional Dislocations. II. Misfitting Monolayers and Oriented Overgrowth. Proceedings of the Royal Society of London. Series A, Mathematical and Physical Sciences 1949;198:216.

[2] Matthews JW, Blakeslee AE. Defects in epitaxial multilayers. I. Misfit dislocations. Journal of Crystal Growth 1974;27:118.

[3] Freund LB. The Stability of a Dislocation Threading a Strained Layer on a Substrate. J. Appl. Mech. 1987;54:553.

[4] Nix WD. Mechanical properties of thin films. Metall. Trans. A 1989;20:2217.

[5] Schwarz KW, Tersoff J. Interaction of threading and misfit dislocations in a strained epitaxial layer. Appl. Phys. Lett. 1996;69:1220.

[6] Schwarz KW. Simulation of dislocations on the mesoscopic scale. I. Methods and examples. J. Appl. Phys. 1999;85:108.

[7] Nicola L, Van der Giessen E, Needleman A. 2D dislocation dynamics in thin metal layers. Mater. Sci. Eng. A-Struct. Mater. Prop. Microstruct. Process. 2001;309:274.

[8] Pant P, Schwarz KW, Baker SP. Dislocation interactions in thin FCC metal films. Acta Mater. 2003;51:3243.

[9] Quek SS, Xiang Y, Zhang YW, Srolovitz DJ, Lu C. Level set simulation of dislocation dynamics in thin films. Acta Mater. 2006;54:2371.

[10] Quek SS, Wu Z, Zhang Y-W, Xiang Y, Srolovitz DJ. Dislocation junctions as barriers to threading dislocation migration. Appl. Phys. Lett. 2007;90:011905.

[11] Fertig RS, Pant P, Schwarz KW, Baker SP. Dislocation dynamics simulations of dislocation interactions and stresses in thin films. Submitted to Acta Materialia 2009.

[12] Fertig RS. Dislocations and Strength in Thin Films: Simulations and Modeling. PhD Dissertation. Ithaca, NY: Cornell University, 2008.

[13] Fertig RS, Baker SP. Simulation of dislocations and strength in thin films: A review. Prog. Mater. Sci. 2009;54:874.

[14] Nix WD. Yielding and strain hardening of thin metal films on substrates. Scr. Mater. 1998;39:545.

[15] Freund LB, Suresh S. Thin Film Materials: Stress, Defect Formation and Surface Evolution. Cambridge, United Kingdom: Cambridge University Press, 2003.

[16] Dehm G, Inkson BJ, Balk TJ, Wagner T, Arzt E. Influence of film/substrate interface structure on plasticity in metal thin films. Dislocations and Deformation Mechanisms in Thin Films and Small Structures Symposium, 17-19 April 2001. San Franciso, CA, USA: Mater. Res. Soc, 2001. p.2.

[17] Dehm G, Balk TJ, Edongue H, Arzt E. Small-scale plasticity in thin Cu and Al films. Microelec. Engr. 2003;70:412.

CHAPTER 7
SUMMARY AND FUTURE WORK

7.1 Summary

In this thesis, three-dimensional discrete dislocation dynamics simulations were used as a tool to train our intuition about dislocation behavior in films. Specifically, we discovered that both TT and TM interactions play important roles in film relaxation and that they act in a fundamentally different ways. In general, because TT interactions are strong, they *permanently* stop threads, preventing them from relieving strain at higher strain levels. On the other hand, because TM interactions are weak the threads involved in these interactions can easily break free at higher strain levels to relax the applied strain. Stress inhomogeneity plays a crucial role in both of these interactions, albeit in different ways. Stress inhomogeneity concentrates threads in regions of low stress, making the likelihood of TT interactions greater than would be predicted based solely on the thread density alone. In addition, the capture cross-section of the thread is highest in these low stress regions, which further increases the likelihood of a TT interaction. We also observed that TM interactions played a significant role in stopping threads even when the average film stress was higher than the TM interaction strength. Because the stresses were inhomogeneous, even when the average film stresses exceed the TM interaction strength there were still regions in the film where the stresses were low enough that a TM interaction could stop the thread. In fact, the low stress regions were likely to contain a high density of misfits, so that the TM interaction was likely. Our results suggested that a reasonable approximation of the distance that a thread traveled before being stopped by a misfit was simply the

distance between regions of stress lower than the TM interaction strength. Thus, the simulations suggested a link for a more general analytical model.

The effect of film stresses on the capture cross-section of two threads at different film stresses was calculated using an analytical model. This capture cross-section is directly related to the likelihood of TT interactions. The results revealed that the area of the capture cross-section increases by many orders of magnitude when the film stress is near the channeling stress. Our results also allowed us to determine a functional form for the area of this cross-section for implementation in an analytical strain hardening model.

The quantitative effect of film stresses on the location of threads in the film was examined via a statistical model. We specifically looked at if and how much stress inhomogeneity concentrated threads in a film. We discovered that stress inhomogeneity could cause threads to concentrate such that the apparent density of threads, as seen by other threads, was an order of magnitude greater than the film-averaged density.

Finally, we used our results from the DD simulations and the analytical models to construct a strain hardening model from fundamental dislocation behavior. This model was able to account for varying degrees of TT and TM interactions as well as the effects of different thread densities. Ultimately, this model was a proof-of-concept that such a model is possible. The additional parameters that are needed to make it rigorously applicable to a variety of films were also identified, and are discussed below.

7.2 Future work

This thesis has demonstrated the feasibility of constructing a model for strain hardening in films from well-known dislocation behavior. We developed the model specifically for the single-crystal films that were simulated using DDD techniques. However, several features of film relaxation need to be quantified to make this model more rigorous and robust. These areas are discussed in the first subsection below. The extensions of the model that would be required to capture the behavior of polycrystalline films are outlined in the second subsection.

7.2.1 Considerations for single-crystal strain-hardening

The analytical model presented in Chapter 6 required three simplifications that must be addressed before an analytical model can be developed that completely describes single-crystal film deformation based on dislocation behavior: dislocation nucleation, breaking of interactions, and evolution of stress inhomogeneity. We assumed that dislocations are not nucleated during deformation, in both the simulations and the analytical model. However, it is possible that nucleation occurs during deformation, at least in some films. We distinguish between nucleation of two types: nucleation from the dislocation structure and nucleation from other defects. For nucleation from a pre-existing dislocation structure, such as a Frank-Read source or a spiral source, three-dimensional dislocation dynamics simulations may well provide insight into nucleation behavior. However, for dislocation nucleation facilitated by grain boundaries, interfaces, or point defects, atomistic simulations need to be coupled with experimental findings in order to understand the critical parameters for

nucleation. In-situ transmission electron microscopy studies (e.g. [1, 2]) have began to shed some light on this problem, but much work remains.

In order to compare the analytical strain hardening model with the DDD simulations, the number of mobile threads determined by the simulation was used for the calculation in the analytical model. This is because the relation between the number of threads that break free of their TM interaction and magnitude of the strain increment is not known. This relation will obviously be some function of the interaction strength, but it is complicated by the fact that threads don't stop just anywhere in the film; they stop in regions of low stress. Consequently, knowledge of how fast these regions of low stress approach the strength of a TM interaction is critical. In other words, we need to know how stress inhomogeneity evolves.

In the analytical model presented in Chapter 6, we assumed that the stress inhomogeneity, as measured by the standard deviation, was a constant value of $0.35\,\tau_{ch}$. In reality this value will increase with increasing misfit density. Understanding the development of stress inhomogeneity will be a two step process. The first step is to relate the distribution of misfit dislocations with stress inhomogeneity in the film. The second step is to determine how the misfit spacing evolves. For example, regions in the film with low misfit density will, in general, have high stresses that will strongly drive threads or nucleate new ones. Thus, regions with low misfit density are more likely to have a increase in density during evolution than a region with already high density. This will tend to equalize the misfit spacing. But, owing to the statistical nature of dislocation motion, the misfit spacing never will be equalized. Describing this behavior in a realistic manner will be a challenge apart from knowledge of nucleation behavior.

7.2.2 Considerations for polycrystalline films

In order to develop a strain hardening model that is general to all films, the effect of grain boundaries must be considered. The principles outlined in Chapter 6 and in Section 7.2.1 are still valid for polycrystalline films, but they must be augmented for grain boundaries. Grain boundaries are known to contribute to stress inhomogeneity (e.g. [3, 4]) because elastic property discontinuities are exist because the grains have different orientations, which will affect the motion of threads as described above. In addition, grain boundaries can block, absorb, transmit, and nucleate dislocations [5, 6]. These effects can be best studied experimentally or using atomistic simulations. Using these studies, a set of rules for dislocation grain boundary interaction can be developed for implementation in a three-dimensional DDD simulation. In order to capture the effect of stress inhomogeneity created by the grain boundary, the DDD simulation will likely need to be simultaneously coupled with a finite element model to account for the stress interactions. Thus, incorporating the effects of grain boundaries into a model of strain-hardening constructed from fundamental dislocation behavior is likely the most difficult roadblock to overcome on the way to a bottom-up strain hardening model.

REFERENCES

[1] Owusu-Boahen K, King AH. The early stages of plastic yielding in polycrystalline gold thin films. Acta Mater. 2001;49:237.

[2] Legros M, Dehm G, Keller-Flaig RM, Arzt E, Hemker KJ, Suresh S. Dynamic observation of Al thin films plastically strained in a TEM. Mater. Sci. Eng. A-Struct. Mater. Prop. Microstruct. Process. 2001;309:463.

[3] Balk TJ, Dehm G, Arzt E. Parallel glide: Unexpected dislocation motion parallel to the substrate in ultrathin copper films. Acta Mater. 2003;51:4471.

[4] Phillips MA, Spolenak R, Tamura N, Brown WL, MacDowell AA, Celestre RS, Padmore HA, Batterman BW, Arzt E, Patel JR. X-ray microdiffraction: local stress distributions in polycrystalline and epitaxial thin films. Microelec. Engr. 2004;75:117.

[5] de Koning M, Miller R, Bulatov VV, Abraham FF. Modelling grain-boundary resistance in intergranular dislocation slip transmission. Philos. Mag. A 2002;82:2511.

[6] de Koning M, Kurtz RJ, Bulatov VV, Henager CH, Hoagland RG, Cai W, Nomura M. Modeling of dislocation-grain boundary interactions in FCC metals. Journal of Nuclear Materials 2003;323:281.